

---

## The Agulhas Current retroflexion

The southern termination of the Agulhas Current is unique for a western boundary current in this respect that it takes place at the meridional extremity of the adjacent continent. This is unlike the continental constraints to which the comparable Gulf Stream, the Kuroshio or the Brazil Currents are subject. Since the African continent separates the Atlantic and Indian basins, the Agulhas Current, at its termination, is also the only western boundary current that lies on the border between two subtropical gyres. This creates unusual conditions for inter-ocean exchanges of water masses, energy and biota between these two gyres with a range of implications for the global oceanic circulation and for biogeographical patterns. Temporal changes in the magnitude of this exchange process may therefore have implications for global water circulation in the ocean and, if such changes are sufficiently large and of sufficient duration, may influence global climate.

Furthermore, the nature of the termination of the Agulhas Current – described below – allows warm tropical and subtropical surface water to remain in the region for a considerably longer time than in comparable western boundary currents. The thus enhanced flux of heat<sup>98,147</sup> and moisture to the atmosphere has a marked effect on the overlying atmosphere<sup>496</sup> of the region. Not unexpectedly, statistical investigations<sup>136,497</sup> have demonstrated that this ocean region has a strong influence on rainfall patterns over southern Africa. Results from ocean–atmosphere models<sup>139</sup> are largely consistent with this view. However, there is consensus that it is the inter-ocean exchanges of water that have the most profound climatic consequences.

The interchange processes that occur in the ocean regions south of Africa are therefore of considerable oceanographic interest and have wide implications. The behaviour of the Agulhas Current must naturally play an important role in these processes. The kinematic nature of the Agulhas Current, once it has passed the southern tip of the African continental shelf, is quite exceptional for a western boundary current. The current turns back on itself in a tight loop, called the Agulhas

Current Retroflexion, with most of its waters contained in this swift recurvature before they flow back into the South Indian Ocean. The nature and dynamics of this peculiar behaviour have received considerable research attention over the past three decades and are now fairly well understood. This growth in knowledge represents one of the major advances in global oceanography of this period.

Upon closer examination, the scale and the dynamics of the processes in the Agulhas Current retroflexion are seen to be of truly monumental proportions<sup>813</sup>. A water mass with an estimated flux of 12 000 cubic kilometre per day, i.e. about 1400 times that of the Amazon River, moving at a rate of 150 km/day, is turned around in a loop with a diameter of about only 400 km to flow directly in the opposite direction. As could be expected, this configuration is highly unstable and global observations of hydrographic, sea surface temperatures and sea surface height have demonstrated that this region is the most intensely variable to be found in the world ocean. The high contrasts in horizontal gradients for a number of ocean variables found here make this area eminently amenable to observation, but the rapid changes that occur severely limit the applicability of a number of standard hydrographic measurement techniques that cannot be used in a quasi-synoptic fashion.

Notwithstanding these serious limitations to observational strategies, brought about by the attributes of the current dynamics itself, much has been learnt about the nature of the Agulhas Current retroflexion.

### The nature of the Agulhas retroflexion

No matter what oceanographic data with a global distribution are used, the extremely high variability south of Africa is always apparent. This result, using modern satellite data<sup>261</sup>, has to some extent been adumbrated by analyses of the global<sup>363</sup> and regional<sup>498</sup> distribution of eddy kinetic energy from ships' drift (Figure 4.1) as well as of hydrographic data<sup>499</sup>. Standard deviations of the detrended dynamic height relative to 1000 decibar

## Using drifting buoys in the Agulhas Current

After the application of satellite remote sensing, the use of satellite telemetered, drifting buoys has probably contributed most to the rapid increase in knowledge about the Agulhas Current system over the past two decades.

The deployment of drifters in the Agulhas Current was pioneered by Christo Stavropoulos of the CSIR (Council for Scientific and Industrial Research) in Durban, South Africa, when a spar buoy with subsurface drogue was launched 280 km south-east of Durban and tracked successfully by the French Eole satellite for 89 days in 1973<sup>411</sup> (see Figure 7.2). A similar buoy was moored for 315 days on the Mozambique Plateau<sup>521</sup> using the Nimbus VI satellite for positioning and data relaying. With the assistance of the National Aeronautical and Space Administration (NASA, USA) the CSIR subsequently constructed another nine buoys, placed in the Agulhas Current<sup>350,374</sup> and followed over distances of more than 14 000 km. Having booked this substantial success, an additional eight buoys, from the CSIR, NOAA and the National Centre of Atmospheric Research of the US, were then deployed from the South African Antarctic research vessel *RSA* to the south of Africa<sup>522</sup>. Apart from gaining valuable new information on the Agulhas Current system with these Lagrangian drifters that complemented existing hydrographic concepts<sup>92,349</sup>, these experiments also demonstrated the longevity, robustness and positional accuracy of these drifters, in particular in the extreme wave and weather conditions of the Southern Ocean.

This South African technical information was effectively used to persuade the international meteorological community and funding agencies that a major endeavour to cover the ocean in the southern hemisphere with drifting meteorological buoys, for a period of at least one year, was technically feasible. It was hoped thus to provide a high-resolution meteorological data set that did not suffer from the large gaps in global coverage due to the small number of weather stations, restricted to land, in the southern hemisphere<sup>523</sup>.

This experiment, the First Global GARP Experiment (FGGE, GARP: Global Atmospheric Research Programme), took place from October 1978 to July 1979 with 301 buoys being launched<sup>524</sup>. Twenty-three South African buoys formed part of this international effort<sup>525</sup>. Since South Africa was considered a political pariah at the time, South African participation was not acknowledged in any official FGGE documents, the origin of its buoys usually being designated as "Other"!

The use of the FGGE buoys in the Agulhas Current region has been scientifically very profitable. The role of the East Madagascar Current<sup>80,308</sup>, topographic control on the Agulhas Current<sup>130</sup> and the eddy kinetic energy over the wider system<sup>311,346</sup> have all been addressed. Pioneering work in combining drifter tracks with contemporaneous satellite imagery in the thermal infrared<sup>526</sup> has established somewhat of a trend for subsequent investigations<sup>65,458</sup>.

The South African Weather Bureau has continued to deploy drifting weather buoys in the South Atlantic<sup>527</sup> on an annual basis, but a substantial proportion of these have been undrogued and are of less use for studying ocean currents. Some more sophisticated buoys have been deployed in the Agulhas Current itself<sup>366</sup>, but only on a limited, experimental basis.

The utility of drifters for studying the Agulhas Current is continuing. The possibility of placing subsurface floats to follow specific water masses<sup>253-54</sup> has been realised through a large international programme called KAPEX (Cape of Good Hope Experiment) and has presented many important new results and concepts. The onset of Argo profiling floats<sup>825</sup> is revolutionising the manner in which deep hydrographic information is becoming available. By 2003 more than 80 per cent of such data worldwide came from Argo floats and this percentage is bound to increase. This will make an enormous difference to the study of the South West Indian Ocean in future, but will probably not lessen the need for dedicated research cruises.

show that the region of the Agulhas retroflection has the highest mesoscale variability of any region in the Southern Ocean. A structure function analysis for the Agulhas Current system itself, based on a quasi-synoptic set of cruises<sup>414</sup>, has furthermore shown that, within this system, the retroflection component has by far the most intense variability on all spatial scales. A totally independent result could be produced by analysing the Lagrangian movements of surface drifters.

Four separate studies to determine the advective surface flow in the southern hemisphere, by using the trajectories of the large number of satellite-reporting drifters during the years 1978 to 1979 (see box), have been completed<sup>310-11,346</sup>. Up to 300 drifting buoys were placed south of 20° S and in the area of interest more than 2000 hourly measurements were made. Only in the Agulhas retroflection region was a total kinetic energy

per unit mass exceeding 4000 cm<sup>2</sup>/s<sup>2</sup> found<sup>310</sup>. This extreme is also found for the eddy kinetic energy, the variations being most prominent for fluctuations with periods of months.

The distribution of higher-frequency eddy kinetic energy, i.e. with periods of days and weeks, also show an extreme south of Africa, but distributed in a zonal tongue, from the Agulhas retroflection eastwards<sup>310</sup>. This suggests a dynamical process with longer periods confined to the Agulhas retroflection region. Analysis of current meter records in the Agulhas retroflection by Schmitz and Luyten<sup>500</sup> shows that the normalised frequency distributions of eddy kinetic energy in this region are comparatively depth-independent, peaked at the mesoscale and are the most energetic found in the ocean to date (Figure 6.1). This comparison includes the Gulf Stream and Kuroshio systems. Records from

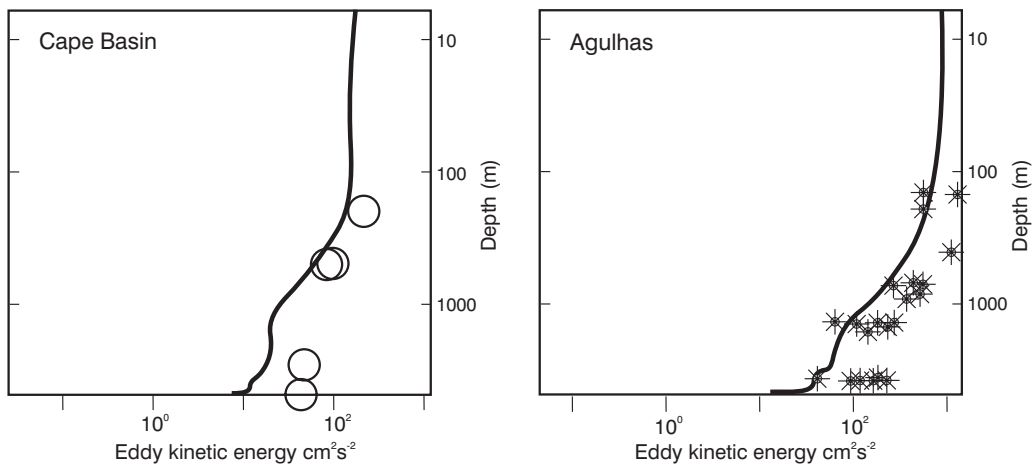


**Figure 6.1.** The vertical distribution of eddy kinetic energy from current meter records in the Cape Basin (circles) and in the Agulhas Current (stars) compared to calculated profiles from a numerical model<sup>509</sup> for the region, all for the period 1993–1996.

current meter moorings in the Cape Basin and in the Agulhas Current retroflection in general give higher values for the eddy kinetic energy, but with a similar depth distribution.

#### Sea surface temperatures

Variability in current behaviour can also be gauged from short-term variations in sea surface temperatures, par-

ticularly in regions where high horizontal gradients in the sea surface temperatures are known to be present. Such analyses<sup>130,418</sup> show very high values for the Agulhas retroflection, but also a tongue of high variability extending eastwards (Figure 6.3). This tongue is probably a function of meanders in the Subtropical Convergence<sup>131</sup> and eddy-shedding processes associated with the Agulhas Return Current<sup>63</sup>. This is suggested by a compendium of the locations of thermal fronts in the region over

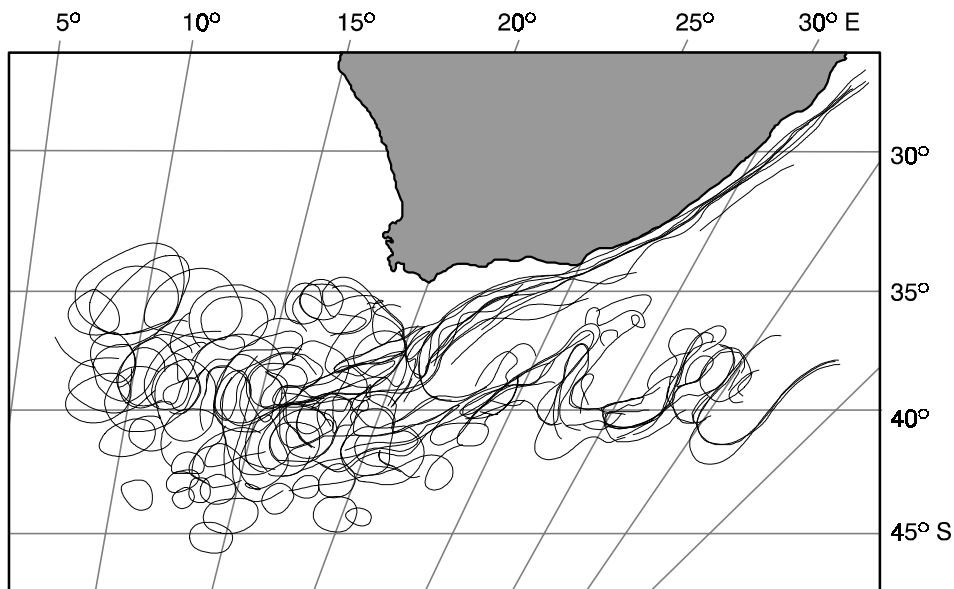


**Figure 6.2.** Superimposed thermal borders of the southern Agulhas Current, Agulhas retroflection and Agulhas Return Current, for a period of one year<sup>91</sup>. These data are from declouded images in the thermal infrared from the METEOSAT II satellite. The most distinct one for every 12-day period was used. The stability of the Agulhas Current (particularly of its northern part), the relative stability of the Agulhas Return Current and the severe instability and eddy shedding processes of the Agulhas retroflection are all very apparent.

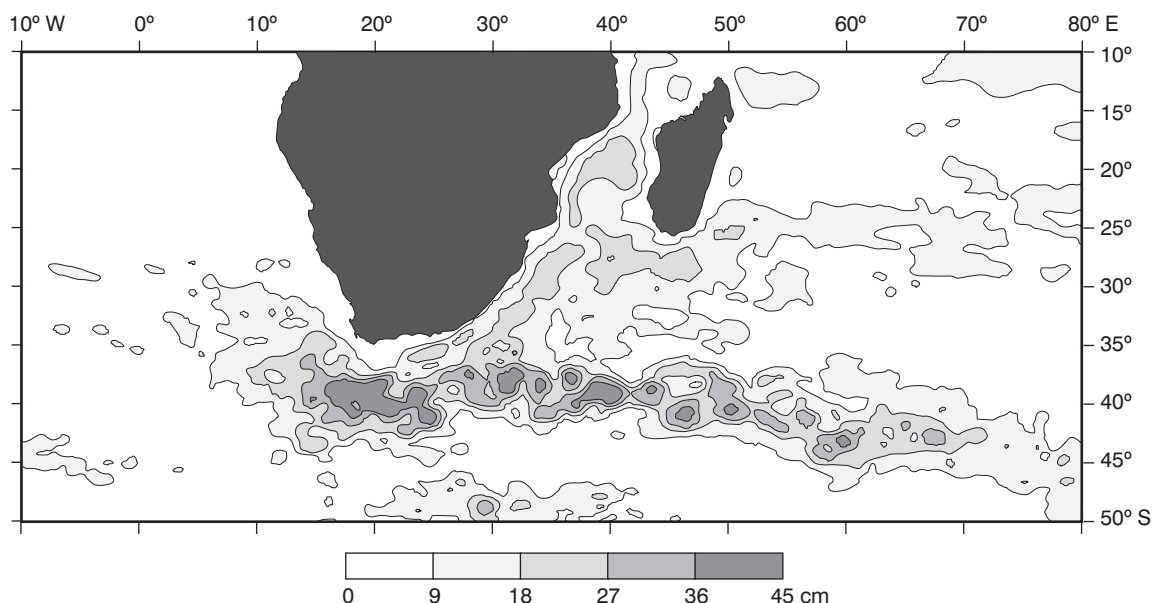


**Figure 6.3.** Sea surface variability south of Africa for the period 1992–1998. The altimetric data were from the TOPEX/Poseidon satellite. High levels of variability associated with the Agulhas retroflexion are particularly prominent. (See also Figure 3.14.)

a period of a full year (Figure 6.2). Eddies, and rings, are seen to be present predominantly around the retroflexion region while, downstream, movement in the location of the Subtropical Convergence is probably responsible for most variability there. General variability in sea surface temperatures presents instructive circumstantial data but tells one little about the ocean processes responsible for the variability. Satellite altimetry can potentially do this.

Preliminary analyses of altimetric data have suggested that the Agulhas retroflexion is a region of very high sea level variability<sup>305</sup> with the presence of large vortices<sup>501</sup>. The first definitive study of global mesoscale variability based on altimeter data from the SEASAT satellite, by Cheney et al.<sup>183</sup>, has confirmed all that had been suggested before with perhaps less reliable data. Not only does the Agulhas Current retroflexion represent a large region of high mesoscale variability, in its core the values are higher than anywhere else on the globe. This is amply demonstrated in Figure 6.3.

Similar investigations using subsequent altimetric measurements by other satellites have substantially confirmed these results<sup>501</sup>, although the area of high variability and its intensity naturally differ slightly between different periods. At least one study<sup>269</sup> has suggested that there is a seasonal cycle to the variability at the Agulhas Retroflexion and that this cycle extends about 30 per cent from the mean. It has a maximum in the austral summer and a minimum during the austral winter, consistent with previous results that were based

on another satellite<sup>502</sup>. Based on only slightly more than three full years of data, these interesting results still need to be verified more robustly.

### Modelling

Last but by no means least, global, eddy-resolving circulation models<sup>273,277</sup> also successfully simulate this region of particularly high mesoscale variability. Where eddy kinetic energy from the Geosat altimeter data exceeds  $1000 \text{ cm}^2/\text{s}^2$  in the Agulhas retroflexion region, it has been found to be only larger than  $500 \text{ cm}^2/\text{s}^2$  in a model<sup>503</sup>, although the present models do simulate the area of higher variability adequately. Eddy kinetic energy has for instance been modelled<sup>762</sup> with a fair degree of success (Figure 6.1) in a primitive equation model with a  $1/3^\circ \times 1/3^\circ$  spatial resolution.

Modelling has also been used extensively in an attempt to understand why the Agulhas Current retroflexes and why it does so at this particular location<sup>469,580,583</sup>. It has been shown<sup>580</sup> that the geographic distribution of the wind stress curls is crucial to the behaviour of the termination of the Agulhas Current. Since the line of zero wind stress curl lies well south of the poleward termination of the African continent, the current is a free inertial jet beyond this point and in a purely barotropic model with realistic values for lateral friction will move into the South Atlantic Ocean<sup>580</sup>. Otherwise, the increasing negative relative vorticity of the Agulhas Current overshoot will eventually lead to

## Origin of the term and concept *retroflection*

A review of the historical development of concepts on the circulation directly south of Africa<sup>14,285</sup> shows that two flow paradigms have been prominent since the earliest times. The first holds that all of the Agulhas Current's waters flows into the South Atlantic Ocean; the second the opposite, namely that none of it goes westward, but that all is returned to the Indian Ocean. Over the past 150 years these two concepts have battled for supremacy.

It is instructive to note that a recurvature of a major part of the Agulhas Current is inherent to the current portrayal put forward by James Rennell as early as 1832<sup>7</sup>. Subsequent studies<sup>504</sup> that made use of sea surface temperatures<sup>780</sup> as well as ships' drift, undertaken particularly in the Netherlands<sup>10,505</sup> in the 1850s, strongly supported this concept. In fact, in some of these Dutch publications<sup>780</sup> it is explicitly stated that the previous concept of the Agulhas Current rounding the Cape of Good Hope and moving northward in the South Atlantic Ocean is without any doubt wrong. The major work on this subject by K.F.R. Andrau was subsequently seldom referred to directly, more-or-less lost to science, and portrayals of a bifurcation in the Agulhas Current – some water going east, some west – became more fashionable<sup>24,281,284</sup> (Figure 3.1). The quality, quantity and geographic distribution of the data available at the time were such that both interpretations could logically be sustained simultaneously, even when combinations of hydrographic data first allowed a portrayal of the whole water column by Dietrich in 1935<sup>40</sup>. Even he considered the coastal upwelling system along the west coast of southern



Nils D. Bang

Africa as representing an Atlantic branch of the Agulhas Current<sup>42</sup>. As late as 1972, Darbyshire<sup>506</sup> still concluded, quite emphatically, that no true return current existed for the Agulhas for three of his four surveys<sup>215</sup>.

A comprehensive, quasi-synoptic and detailed set of cruises covering the full Agulhas system<sup>92</sup> was undertaken for the first time only in 1969. When the data from this project were being analysed by Nils Bang<sup>90,444</sup> in the early 1970s, he was particularly struck by the discontinuous nature of the flow, with a host of fronts and mesoscale features. Bang evidently struggled with the interpretation of these data, suggesting a number of alternative explanations for the current's disposition<sup>90</sup>. Searching for a suitably descrip-

tive term that would convey the impression of a dynamic flexing activity instead of a static, geometrically stable process, he came across the term "retroreflect", commonly used to describe the turning back on itself of the mammalian gut<sup>14</sup>.

This excellent verbal portrayal of the flow regime, suggested by the new data, established a novel conceptual framework for all data gathered before and since. The catchy descriptive terminology aided the acceptance of the recurvature concept by a wider community, particularly once it became clear that all succeeding information fitted it well.

The concept of the Agulhas' retroflection, as well as the new nomenclature, is now firmly entrenched, the term *retroflection* being widely employed in oceanography to describe the behaviour of a number of other currents, such as, for instance, the Brazil Current<sup>507,687</sup>.

an eastward turning<sup>581</sup> in both barotropic and baroclinic configurations. Retroflection can also be brought about by increasing the large horizontal friction<sup>582</sup>. Lesser horizontal friction will lead to strongly variable flow. Some<sup>583</sup> have tried to show that under certain circumstances time-dependant phenomena, such as ring shedding, are essential to the existence of a retroflection. To study the requirements for a steady retroflection regime, an investigation has been carried out<sup>778</sup> by modifying the wind forcing, the bottom topography, the lateral friction and the layer depth in a model with steady barotropic flows. It has been found that steady retroflection regimes can be created under a number of conditions, for instance with large friction or with dominant inertial effects when friction values are low. Instabilities in this barotropic steady flow<sup>741</sup> may produce inter-monthly and inter-annual variability. Nevertheless, in

this barotropic model the frequency of ring formation is set by the physics of the large-scale instabilities and the rectification processes due to these instabilities decrease the degree of retroflection of the mean state. More about wind-driven and other modelling is to be found below under the rubric of the dynamics of the Agulhas retroflection.

### *Direct measurements*

Although the nature of the variability in this retroflection region, as well as its approximate geographic extent, may be estimated from the abovementioned data, only few continuous measurements, such as current observations, have been made here to date. One deployment of current meter moorings, spaced over the full southern Agulhas Current and Agulhas retroflection

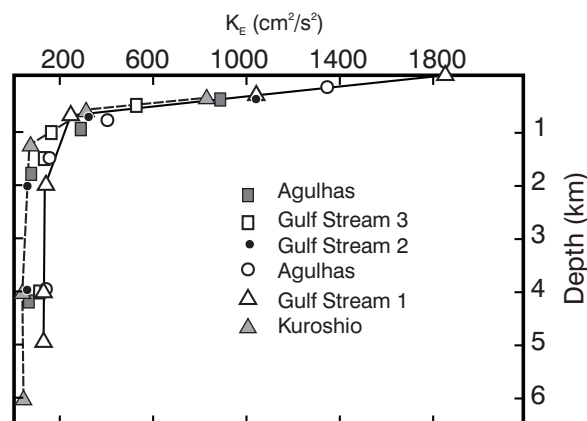


**Figure 6.4.** The vertical distribution of the current kinetic energy for representative components of the Agulhas Current retroflection<sup>509</sup>, a summary of the available data at 55° W longitude (east of the New England seamounts, Gulf Stream 1), a mooring located at 68° W (west of the New England seamounts, Gulf Stream 2), one placed at the New England seamounts (Gulf Stream 3) and the Kuroshio<sup>510</sup>. The energy of the Agulhas Current is high, compared to the other western boundary currents, at all depths.

region<sup>508</sup>, has presented data that give some indications of the nature of the current variability. These results may profitably be compared to those found in similar western boundary currents<sup>509</sup> (Figure 6.4).

It shows that the kinetic energy distribution of the currents is very similar, so that in this respect the Agulhas Current is not exceptional. Differences in kinetic energy below 1000 m are mostly due to the dissimilar location of a current meter mooring relative to the current system it was supposed to monitor. Differences between the western boundary currents are of the same order as the differences found between different parts of the same current system (Figure 6.4). The spatial distribution of kinetic energy amongst the different western boundary currents also is very similar, peaking at the mesoscale<sup>509</sup>.

There is therefore abundant proof, from a number of totally independent data sets, for the very high mesoscale variability of the Agulhas Current retroflection, implying some continuous process resulting in substantial changes in current structure and position of the main flow elements.

### *Current predilection*

The first description of the southern termination of the Agulhas Current that combined hydrographic data from a number of different deep-sea cruises has already been presented by Dietrich in 1935<sup>40</sup>. It shows a substantial part of the transport, but by no means all<sup>42</sup>, flowing back into the South Indian Ocean in a recurvature of the current to the south-west of Cape Agulhas. An analy-

sis of widely spaced hydrographic stations in the region in the early 1960s was the first to demonstrate unequivocally the presence along the Subtropical Convergence of intense eddies<sup>511</sup>, and the analysis of the combined data set collected for the International Indian Ocean Expedition (see box) allowed for contouring that also showed some intense eddies here<sup>75</sup>. However, it was only once a full oceanographic project, consisting of three simultaneous research cruises with closely spaced stations over the full region, had been completed that the true nature of the terminal region of the western-most extent of the Agulhas Current became clear<sup>90,444</sup> (Figure 6.5).

In Figure 6.5 the characteristic disposition of the Agulhas Current, based on these data, is demonstrated quite admirably. Having passed by the southern tip of the Agulhas Bank, at about 19° E, the current turns abruptly south carrying its water as far as the 42° S parallel before moving in a north-easterly direction. The neck of the retroflection proper was only about 180 km wide. On this occasion the Agulhas Current, under the influence of a Natal Pulse, was even closer to the Agulhas Return Current in the vicinity of Port Elizabeth, but this is an unusual configuration. It is nonetheless of considerable importance, since this close juxtaposition of opposing currents may occasionally bring about an upstream retroflection here<sup>64,412</sup>. South-east of Cape Town (Figure 6.5) a large, anti-cyclonic eddy is evident in the hydrographic data. The volume transport in this feature relative to 1100 m has been estimated<sup>92</sup> to have been  $15 \times 10^6 \text{ m}^3/\text{s}$ , while that of the Agulhas Current itself was  $40 \times 10^6 \text{ m}^3/\text{s}$ .

## Studying the Agulhas system with large observational programmes

Progress in the understanding of the extended Agulhas system has come about mainly in two ways: by local efforts with a limited geographical scale and by large, usually international, programmes on a much more extensive scale. Investigations using the R.V. *Meiring Naudé* from the CSIR (Council for Scientific and Industrial Research, South Africa) in Durban<sup>317</sup> formed a key component of the former. This is described in an inset of Chapter 4. One of the most important international programmes that stimulated oceanographic research in the region for many years to come, was the International Indian Ocean Expedition<sup>224</sup> of the 1960s. Its effect is described in an inset to Chapter 2. But there have been a number of other sea-going programmes since that have had a decisive influence on the development of our understanding of this current system.

The ARC (Agulhas Retroflection Cruise) took place in 1983 from the US research vessel *Knorr*. Initiated by Dr Arnold Gordon of the then Lamont-Doherty Geological Observatory, it included a number of South African and Dutch participants. It aimed at understanding



Arnold L. Gordon

the inter-ocean exchange of waters at the Agulhas termination<sup>65</sup> and consisted of one of the most extensive cruises in this region up to that time. Many of the results it achieved were seminal<sup>61,458</sup>. It was followed in 1987 by the South African SCARC<sup>787</sup> (Subtropical Convergence and Agulhas Retroflection Cruise) from the R.V. *SA Agulhas*. This multi-disciplinary cruise was one of the first to use satellite remote sensing to guide its sea-going programme<sup>456</sup> and investigated seven Agulhas rings and eddies. It successfully documented one of the most extensive leakages of Subantarctic water<sup>528</sup> across the Subtropical Convergence. These single-cruise projects were followed by a number of multi-cruise programmes.

The BEST (Benguela Sources and Transports) was a collaborative programme<sup>535</sup> involving the Woods Hole Oceanographic Institution, the National Oceanic and Atmospheric Administration of the US and the (then) South African Sea Fisheries Research Institute and took place from 1992 to 1993. Its prime aim was to establish the flux of Agulhas water in the South East Atlantic Ocean by the judicious combination of bottom mounted instruments, hydrographic observations and satellite remote sensing. It successfully established that most of

the flow in this region was due to Agulhas rings<sup>536</sup> and not the Benguela Current. The geographically largest and most elaborate research programme in the Agulhas system to date has been the KAPEX (Cape of Good Hope Experiment)<sup>677,678,650</sup> undertaken by a number of German, US and South African organizations from 1997 to 1999. It covered the Agulhas system from Durban on the east coast of South Africa to beyond the Walvis Ridge in the South Atlantic Ocean. During the programme a number of sound sources were placed in the region and a large number of RAFOS floats launched to pass through this international array. The results of this highly successful programme filled a special issue<sup>627</sup> of the journal *Deep-Sea Research II*.

A subsequent multi-disciplinary, Dutch-South African programme initiated by Professor Will de Ruijter of Utrecht University consisted of two observational parts: the MARE (Mixing in Agulhas Rings Experiment)<sup>658</sup> and the ACSEX (Agulhas Current Sources Experiment)<sup>650</sup>.



Will P.M. de Ruijter

The MARE was carried out over a period of one year on three cruises at six-month intervals, starting in 1999. It aimed at studying the slow demise of one particular ring over this period. The ACSEX was carried out during four cruises on the Dutch research vessel *Pelagia* in the Mozambique Channel and in the region south of Madagascar. It has shown that no coherent Mozambique Current exists, but that the flow in the Mozambique Channel is characterized by the regular formation of eddies that subsequently drift poleward<sup>728</sup>. It has been continued by LOCO (Long Term Ocean Climate Observations) in which a current mooring array continues to monitor the flow through the narrows of the Mozambique Channel.

In later years, the ACE (Agulhas Current Experiment)<sup>788</sup> was funded by the UK to study the fluxes of the Agulhas Current by placing a number of current meter moorings across the current at Port Edward, off South Africa's east coast. It has presented the most accurate estimate of this flux to date and in the process discovered an Agulhas undercurrent<sup>368</sup>. The ASTTEX (Agulhas-South Atlantic Thermohaline Transport Experiment) consists of a similar set of moorings in the South East Atlantic that builds on the results of BEST and will try to quantify the flux of Agulhas water in the Cape Basin.

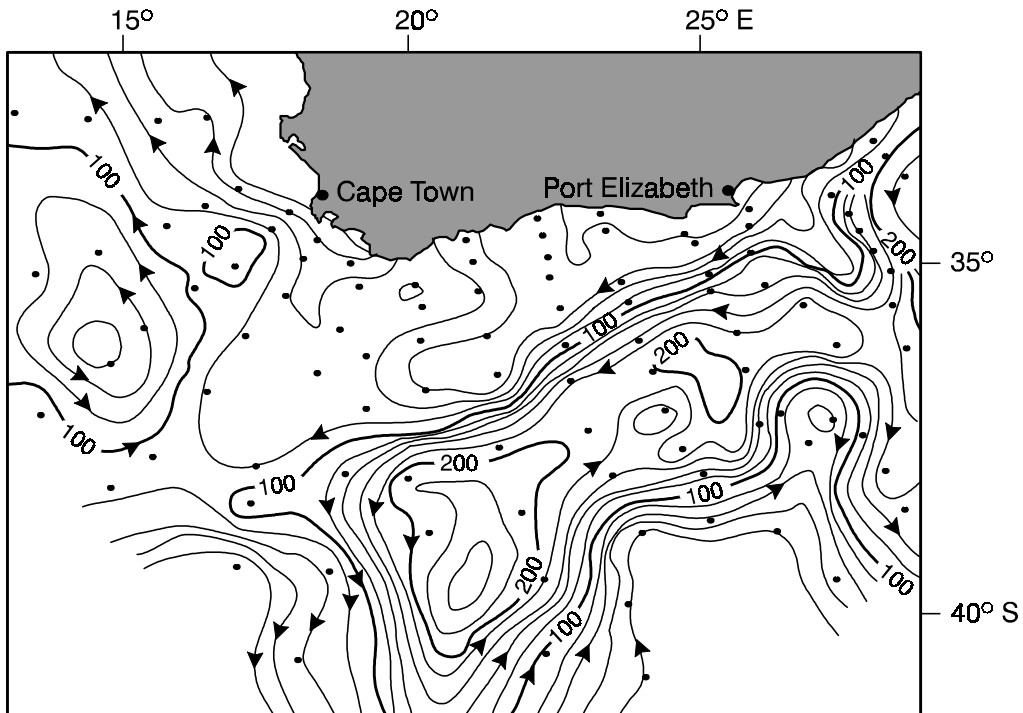


**Figure 6.5.** The Agulhas retroflexion as evident in hydrographic measurements collected in March 1969. Shown here is the depth of the sigma-t 25.80 surface<sup>91</sup>. Dots represent hydrographic stations; arrows inferred directions of movement. The concentration of isobaths identifies the core of the Agulhas and of the Agulhas Return Current. Closer inspection also shows a Natal Pulse off Port Elizabeth (viz. Figure 5.15) and an Agulhas ring west of Cape Town.

### *Retroflexion inconstancy*

As might be expected from the multifarious results pertaining to the current's variability (viz. Figure 6.2) this is by no means the only configuration of the Agulhas retroflexion. Satellite imagery, particularly in the thermal infrared<sup>59</sup>, has shown it in a number of positions<sup>91</sup>. It has in fact been demonstrated that the Agulhas retroflexion loop, or its products, may extend continuously as far as 10° E, i.e. outside the Agulhas Basin (viz. Figure 1.2) and well into the Cape Basin<sup>512</sup> west of the Agulhas Plateau. This demonstrates that the Heezen Ridge, which separates these two basins at about 5° E, seems to have no, or limited, restraining effect on the Agulhas retroflexion loop.

A representative thermal infrared image from the NOAA 9 satellite for the Agulhas retroflexion is given in Figure 6.6. The question arises how representative this one image might be and how much it truly tells one about the movement of water through the system. Using satellite imagery for 623 days it has been shown that the average diameter of the retroflexion loop is 341 km (standard deviation 72 km), that anti-cyclonic shear-edge features to its north are 307 km ( $\pm 89$  km) and eddies to its north-west (viz. Figure 6.5) 324 km ( $\pm 7$  km)<sup>414</sup>.

Based on about 1000 useful images, the maximum easterly position of the retroflexion has been shown to lie at 20°30' E longitude, the westerly position at 9°40' E<sup>91</sup>. In general the Agulhas retroflexion seems to lie between 20° E and 15° E, with no preferred locations, as has been surmised previously<sup>59</sup>. Although the range of these features is relatively large, it does demonstrate some consistency in the occurrence and characteristics of these features. Comparing these surface temperature portrayals with the tracks of some drifters has shown that there exists a close and reliable correspondence between them.

A drifting buoy that became entrained in the Agulhas Current south of Port Elizabeth<sup>350</sup> clearly circumscribed a tight retroflexion loop at about 15° E longitude before drifting eastwards (viz. Figure 7.3). Other buoys have done the same<sup>513</sup>. Buoys passing through the retroflexion show advective rates of more than 1 m/s, very similar to those observed in the Agulhas Current itself. Comparing<sup>349</sup> the main features of all the available drift tracks with the main features of the retroflexion, as evident in the results of hydrographic measurements, demonstrates that the portrayals of the nature of the retroflexion in satellite imagery are very accurate ones of the water movement through the region. What can

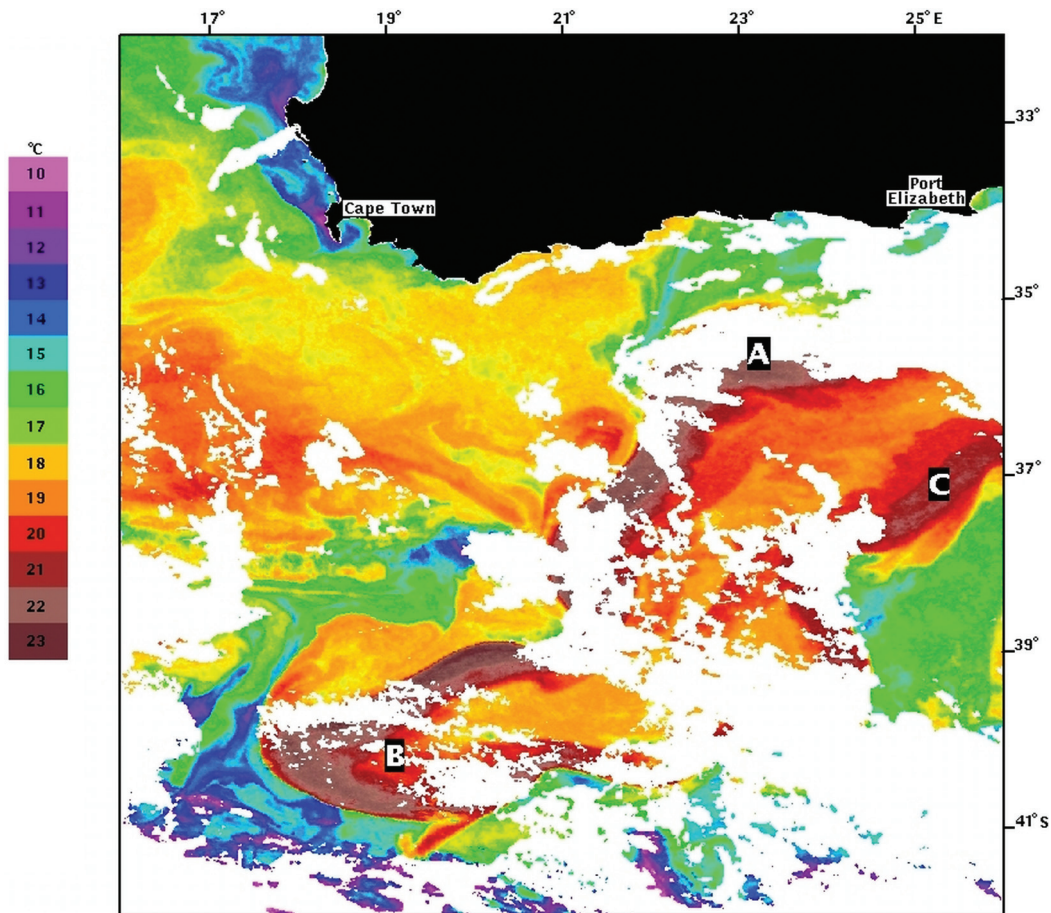


**Figure 6.6.** The Agulhas retroflexion<sup>91</sup> region south of Africa manifested in the sea surface temperatures. This thermal infrared image is from the NOAA series of satellites for 13 November 1985. Red–yellow hues indicate warmer water, black the land and white the clouds. **A** denotes the southern Agulhas Current, **B** the western extent of the retroflexion loop and **C** the Agulhas Return Current. Note the cold upwelled water off Cape Town, the cold Subantarctic Surface water at the westernmost extremity of the retroflexion loop and the cold coastal water being advected along the Agulhas Bank from the vicinity of Port Elizabeth by the Agulhas Current.

these images then tell us about the transient comportment of the retroflexion?

#### *Temporal behaviour*

First, they show<sup>91</sup> that the Agulhas retroflexion loop normally protrudes farther and farther westwards into the South Atlantic Ocean with time (Figure 6.7). The mean rate of this progradation is about 10 km/day. Sometimes during this process the Agulhas Current and Agulhas Return Current amalgamate, somewhat upstream of the furthest extent of the loop, and a separate, independently circulating annulus of Agulhas water, an Agulhas ring, is formed. This process was first identified in satellite imagery<sup>60</sup>, although the possibility of such a process of loop occlusion had been hypothesised before<sup>444,511</sup>, based on the same mechanism

already observed in the Gulf Stream at the time<sup>514–15</sup>. Could a major meander in the incipient Agulhas Current trigger or force the occlusion of a ring? Such a meander could be a Natal Pulse<sup>62</sup> that had travelled this far downstream intact. This would constitute a mechanism very different from that found acting in ring shedding events in the Gulf Stream system.

An analysis of the downstream progression of Natal Pulses, using satellite altimetry that had been validated by thermal infrared information<sup>401</sup>, has shown that nearly all ring shedding events at the Agulhas retroflexion are preceded by the appearance of a Natal Pulse at the Natal Bight, with a lag time of 165 days (Figure 6.8). All the Natal Pulses investigated as part of this particular study proceeded downstream at the previously estimated<sup>62</sup> speeds of about 20 km/day, up to the latitude of Port Elizabeth. Downstream of here their

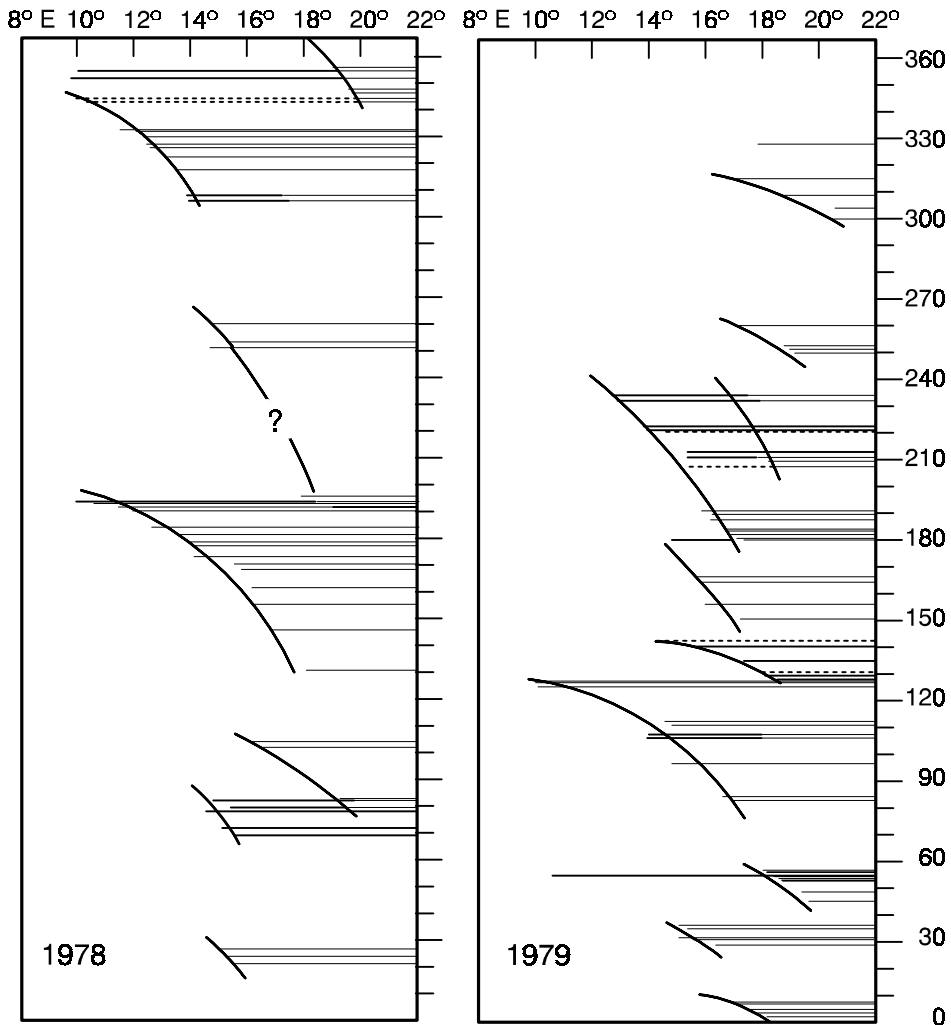


**Figure 6.7.** The zonal location of the westernmost limit of the Agulhas Current retroflexion from thermal infrared imagery from the METEOSAT satellite for 1978 and 1979<sup>91</sup>. Peaks indicate the furthest extent of each progradation event as the Agulhas retroflexion loop has pushed into the South Atlantic Ocean. Dotted lines represent less reliable results.

progression slowed to about 5 km/day. This is indicated by the increased slopes of their distance-made-good lines in Figure 6.8 beyond a distance of 800 km from Durban. On these Natal Pulses reaching the retroflexion region, a ring was shed in each case.

For this study, extending over more than a year, at least one ring was formed without the intervention of a Natal Pulse. It has therefore been assumed<sup>401,516</sup> that rings will form spontaneously when the retroflexion loop has been extended sufficiently, but that the incidence of a Natal Pulse will precipitate such an event. Thus ring shedding may be forced by the Natal Pulse itself or by it interacting with meanders on the Agulhas Return Current<sup>401</sup>. Since the Natal Pulse itself may be triggered by eddies coming from elsewhere<sup>653</sup> this means that the control for the frequency of ring shed-

ding may reside in other parts of the Indian Ocean. It has been shown that monsoonal winds in the Indian Ocean create Kelvin waves that hit Indonesia, then propagate southward along the Indonesian coast and in turn trigger Rossby waves that propagate westward across the subtropics of the Indian Ocean. When they reach Madagascar and the Mozambique Channel they generate eddies which in turn are responsible for the eventual shedding of Agulhas rings. Others<sup>652</sup> have shown that this whole process may be dependant on ENSO cycles and the presence of the Indian Ocean dipole. Inter-annual variability originating in climate modes in the equatorial region of the Indian Ocean may therefore affect the frequency of ring shedding at the Agulhas retroflexion<sup>652</sup>.

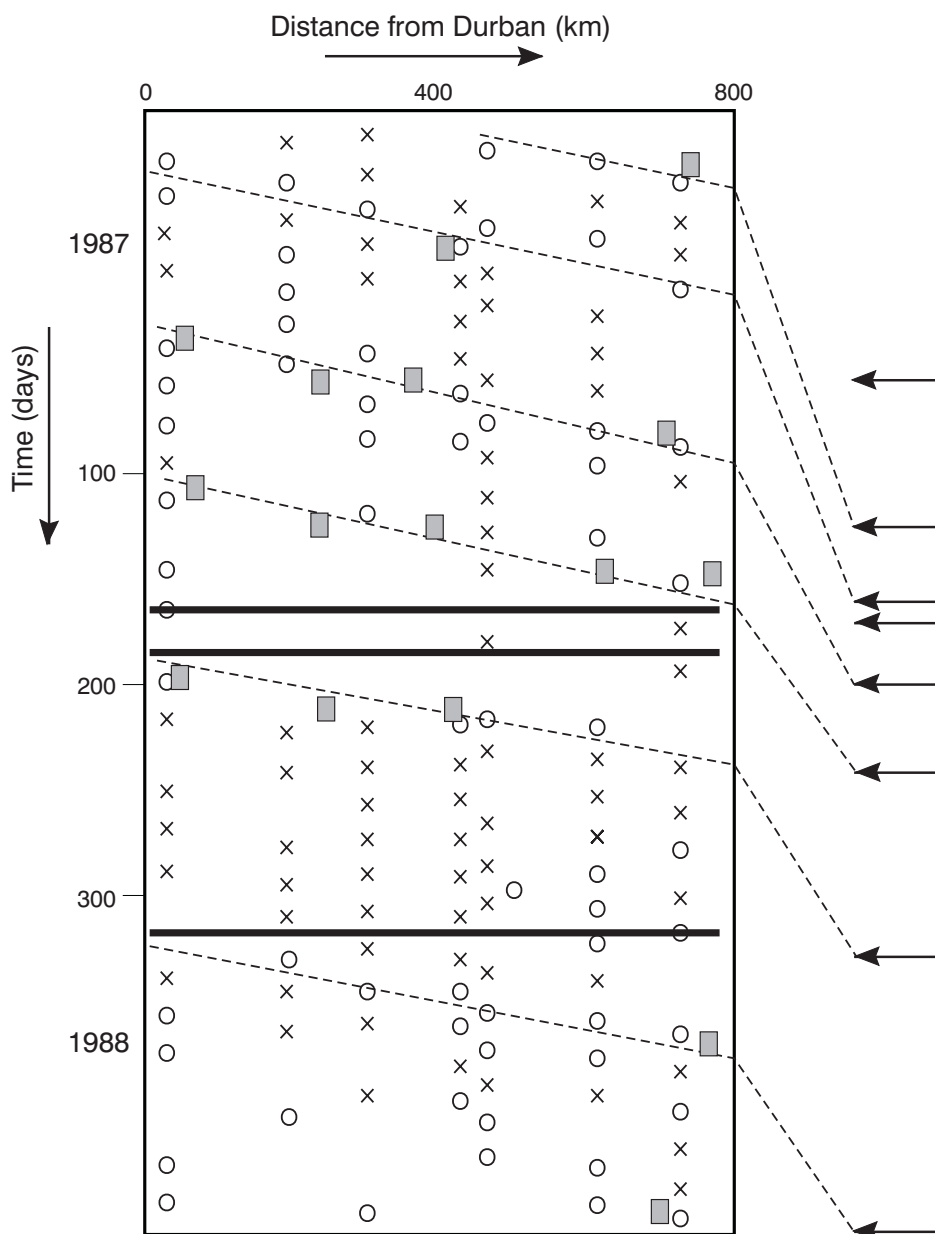


**Figure 6.8.** A space-time diagram of altimeter (Geosat) and thermal infrared (NOAA) observations along the south-east coast of South Africa starting from 1 November 1986. The ellipses denote Natal Pulses from altimetry; rectangles confirmational sightings in infrared images and crosses observations during which no Natal Pulses were evident. Dashed lines show the assumed tracks of Natal Pulses whereas arrows give observed ring shedding events. The horizontal black bars indicate a cloud-free infrared-image of the full region during which no Natal Pulses were observed. The internal coherence of these independent data sets is impressive<sup>401</sup>. They show that Natal Pulses proceed downstream at a nearly identical and uniform rate until they reach a distance of 800 km from Durban, after which they all slow down. This is along the Agulhas Bank. Shortly after they reach the retroflexion region, a ring is shed (arrows) in nearly all cases, suggesting the important role Natal Pulses play in triggering ring shedding events.

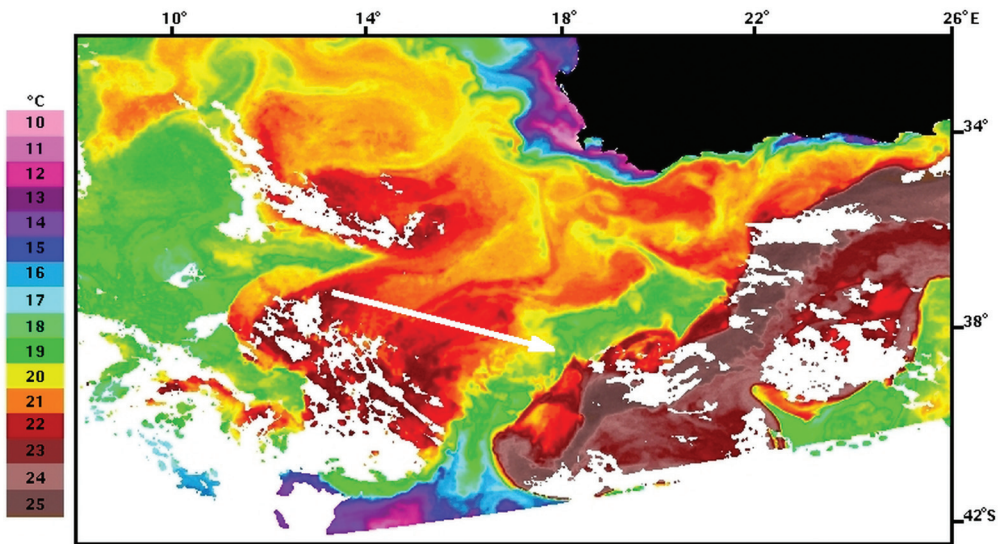


**Figure 6.9.** Northward penetration of cold Subantarctic Surface Water (blue-green) during the separation of an Agulhas ring. These thermal data are from the NOAA 14 satellite and show the characteristic development of such an event on 16 to 17 December 2000. A similar occurrence may be seen in Figure 6.6.

### *Spawning events*

Normally, each of the progradation events of the Agulhas retroflexion loop that terminates in the shedding of an Agulhas ring lasts about 40 days<sup>91</sup>. Within each event, westward penetration of the retroflexion loop shows an increasing rate of progress until abrupt ring spawning occurs. This event duration may, however, be quite variable. There seems to be no clear periodicity and for long periods there may be no spawning events at all<sup>517</sup>.

First results have suggested an annual production of six to nine rings. Other investigators have estimated only four to five ring shedding events per year<sup>74,464,518</sup>. Garzoli et al. have monitored the movement of Agulhas rings past a line of inverted echo-sounders placed along 30° S latitude in the south-eastern Atlantic Ocean<sup>519</sup> and have determined that a minimum of four to six Agulhas rings per year entered this region during the period from 1992 to 1993<sup>520</sup>. In such an extremely variable system it would be highly unlikely that the frequency of shedding events would be identical for each year, although the probable average seems to be stable, about one every two months<sup>413</sup>. This may be compared<sup>755</sup> to the shedding of rings from the southern Brazil Current that exhibits quasi-periodic ring formation roughly every 150 days and the East Australian Current with 130 days.

At least one of these events at the Agulhas retroflexion has been hydrographically observed and measured at sea<sup>61</sup>. The newly formed ring essentially retains all

the kinematic characteristics of its parental Agulhas Current, at least initially. It extends to the same depth, has the same velocity and temperature structure, but starts cooling very rapidly at the sea surface<sup>262</sup>.

### *Accompanying flows*

These ring-shedding events are accompanied by a number of significant, secondary circulations. One of these is the equatorward penetration of a cold wedge of Subantarctic Surface Water, between the newly formed ring and the new retroflexion loop (Figure 6.9). This seems to be an inherent part of the dynamics of the ring-shedding process. Usually the width of this throughflow remains relatively modest<sup>91</sup> with the cold water spreading laterally only to the north of the gap between the retroflexion loop and the newly spawned ring. However, on occasion it has been observed to be wider than 150 km<sup>512</sup>. Shannon et al.<sup>528</sup> have described an event in which such cold water extended as far north as 33° S latitude, a distance of 1000 km, and was observable at the sea surface for a period of two months. This particular intrusion covered an area of  $734 \times 10^3 \text{ km}^2$ , 5 standard deviations greater than the mean area for such intrusions established from an investigation extending over nine years<sup>657</sup>.

On this occasion temperatures of the sea surface were below 17 °C here and salinities below 34.9, and these anomalous water characteristics extended throughout the upper water column, suggesting that this represents true advection of cold water and not only an out-

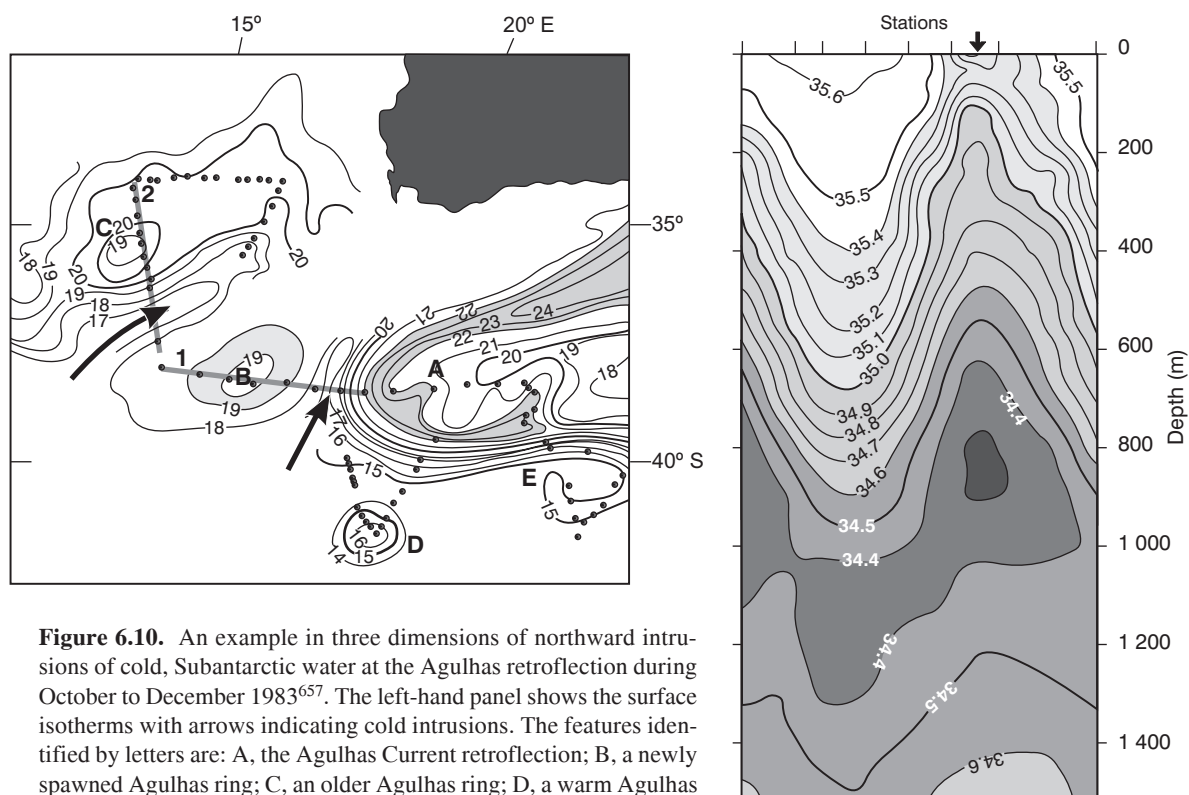


**Figure 6.10.** An example in three dimensions of northward intrusions of cold, Subantarctic water at the Agulhas retroflexion during October to December 1983<sup>657</sup>. The left-hand panel shows the surface isotherms with arrows indicating cold intrusions. The features identified by letters are: A, the Agulhas Current retroflexion; B, a newly spawned Agulhas ring; C, an older Agulhas ring; D, a warm Agulhas eddy; and E, the Agulhas Return Current. Dots indicate hydrographic stations. The hydrographic section in the right-hand panel shows a vertical salinity section along line 2. This line is indicated in the left-hand panel. It intersects two Agulhas rings and the section shows the water with lower salinity between these as well as its low salinity surface expression (arrow). Lines on top of this panel show the location of hydrographic stations.

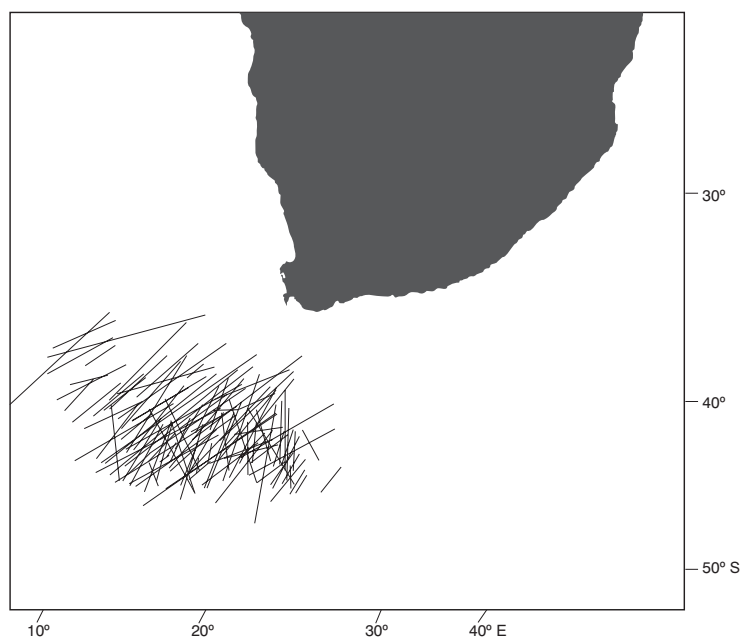


**Figure 6.11.** The geographic orientation and lengthwise dimensions of Subantarctic water intrusions at the Agulhas retroflexion for the period 1981–1990. This portrayal is based on thermal infrared observations from satellite<sup>657</sup>.

**Table 6.1.** Characteristics of the intrusions of Subantarctic Water into the Agulhas retroflection region<sup>657</sup> from thermal infrared observations by satellite.

Zonal distribution	8° E to 22° E
Meridional distribution	Subtropical Convergence ~35° S
Average number per year	5
Temporal occurrence frequency	38 per cent
One intrusion present	21 per cent of times when intrusions are present
Two intrusions present simultaneously	49 per cent of times when intrusions are present
Three intrusions present simultaneously	30 per cent of times when intrusions are present
Average length of intrusions	410(±220) km
Average width of intrusions	80(±100) km
Average surface area of intrusions	159(±118) × 10 <sup>3</sup> km <sup>2</sup>
Average duration of intrusions	28 days

cropping as suggested by some numerical<sup>529</sup> models. Other studies<sup>657</sup> have supported these conclusions and demonstrated that these wedges of cold water found between newly shed Agulhas rings and the Agulhas retroflection may extend deeper than 1500 m (Figure 6.10). On this occasion two wedges were evident at the same time. From the vertical sections across these features it is clear that these cold wedges are only weak surface expressions of a much larger body at depth.

Over a period of a decade cold wedges associated with the shedding of Agulhas rings were found to lie between 8° and 22° E, i.e. the expected zonal range for ring shedding events (Figure 6.11). Their general orientation nearly always was in a south-west/north-east direction. Intrusions are evident about 38 per cent of the time (see also Table 6.1). The recurrence of this pulse of cold water, probably carrying a collection of foreign biota, has an as yet unquantified effect on the South East Atlantic Ocean<sup>530</sup>. The converse, i.e. an unusual flux of warm Agulhas water into the South East Atlantic, has also been observed<sup>439</sup>.

In this particular instance of an enhanced flow of warm water, the configuration of Agulhas retroflection, Agulhas rings, and winds was conducive to drawing considerable amounts of surface water from the Agulhas Current retroflection, through Agulhas filaments and the like. A large ocean area off Cape Town was covered with warm surface water that was replenished from the Agulhas retroflection for an unusually long period. This exceptional culmination of a number of factors that seem to influence flow of warmer water from the Agulhas coincided with 1986 being the warmest year on record in the South East Atlantic Ocean<sup>439</sup>. But it is not only the surface waters that are influenced by the behaviour of the Agulhas retroflection. It has been demonstrated<sup>707</sup> that the deep boundary current along the west coast of southern Africa, consisting mainly of North Atlantic Deep Water (viz. Figure 2.13),

is influenced by changes in the circulation at the Agulhas retroflection. This temporal variability causes it to separate from the continental slope on some occasions and to enter the Indian Ocean in the deep return flow. The causal relationship between the behaviour of the Agulhas retroflection loop and changes to the trajectory of the deep boundary current of the South East Atlantic Ocean has not been established.

As one would expect for a region where waters from the Indian Ocean tropics, the South Atlantic gyre and the Subantarctic meet in a dynamic system of extreme variability, the water masses of the Agulhas retroflection are a true *mélange* of water types.

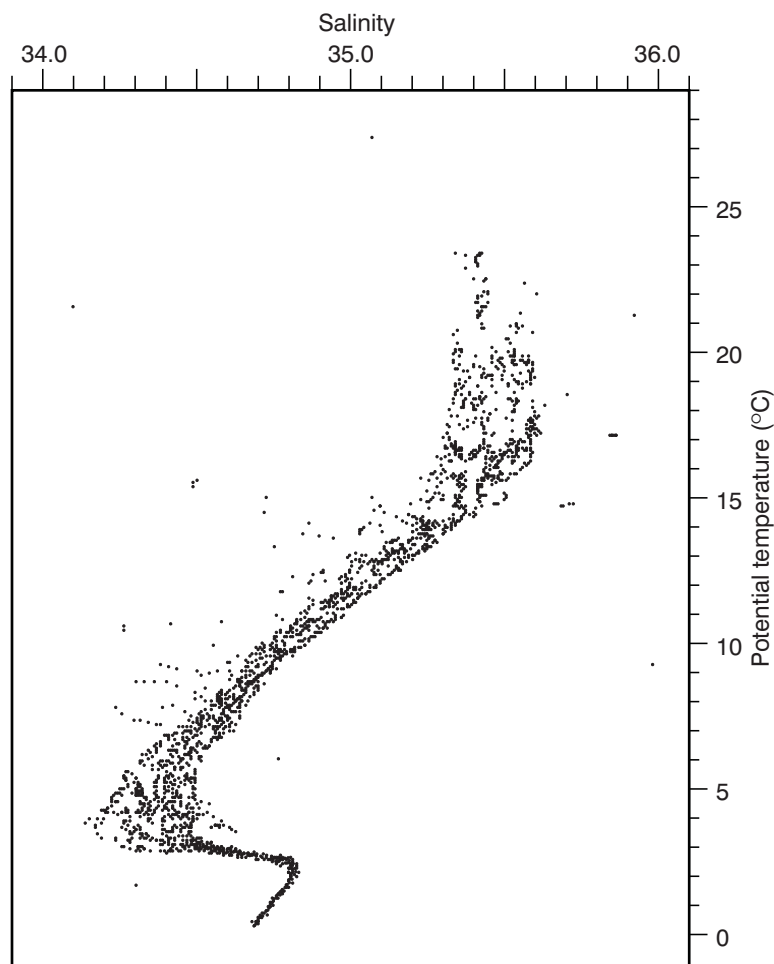
#### *Water masses*

Using all the presently available, high-quality hydrographic data of the Agulhas retroflection region, Valentine et al.<sup>236</sup> have tabulated the water types to be found here and their thermal and saline characteristics (Table 6.2, Figure 6.12).

The pictorial representation (Figure 6.12) exhibits considerable variations in the surface water warmer than 16 °C and in the Antarctic Intermediate Water. In the Central Water, between these two extremes, there is some indication of two preferred temperature–salinity relationships that represent the hydrographic characteristics of South East Atlantic and South West Indian Ocean water respectively. A precise volumetric analysis of the water masses present<sup>236</sup> shows that the warm, saline surface water of the Agulhas Current contributes relatively little to the volume of the upper 1500 m of the region. Pulses of cold Subantarctic Surface Water, with low salinities, make a distinctive, but very small overall contribution to the volume. By volume alone, the North Atlantic Deep Water is the dominant water mass, accounting for 40 per cent of the total volume.

**Table 6.2.** Thermal and saline characteristics of the principle water masses found in the Agulhas retroflection and its direct vicinity<sup>236</sup>.

	Temperature range [°C]	Salinity range [psu]
Surface Water	16.0–26.0	>35.5
Central Water		
South East Atlantic Ocean	6.0–16.0	34.5–35.5
South West Indian Ocean	8.0–15.0	34.6–35.5
Antarctic Intermediate Water		
Characteristic <i>T/S</i>	2.2	33.87
South East Atlantic	2.0–6.0	33.8–34.8
South West Indian	2.0–10.0	33.8–34.8
Deep Water		
North Atlantic Deep Water (South-east Atlantic)	1.5–4.0	34.80–35.00
Circumpolar Deep Water (South-west Indian)	0.1–2.0	34.63–34.73
Antarctic Bottom Water	–0.9–1.7	34.64–34.72

**Figure 6.12.** A scatter diagram of the potential temperature–salinity relationship of the water masses found in the Agulhas retroflection and its direct environment<sup>236</sup>. These data are all from CTD (conductivity–temperature–depth) measurements taken to the ocean bottom and represent the wide range of water masses to be found in this mixing region.

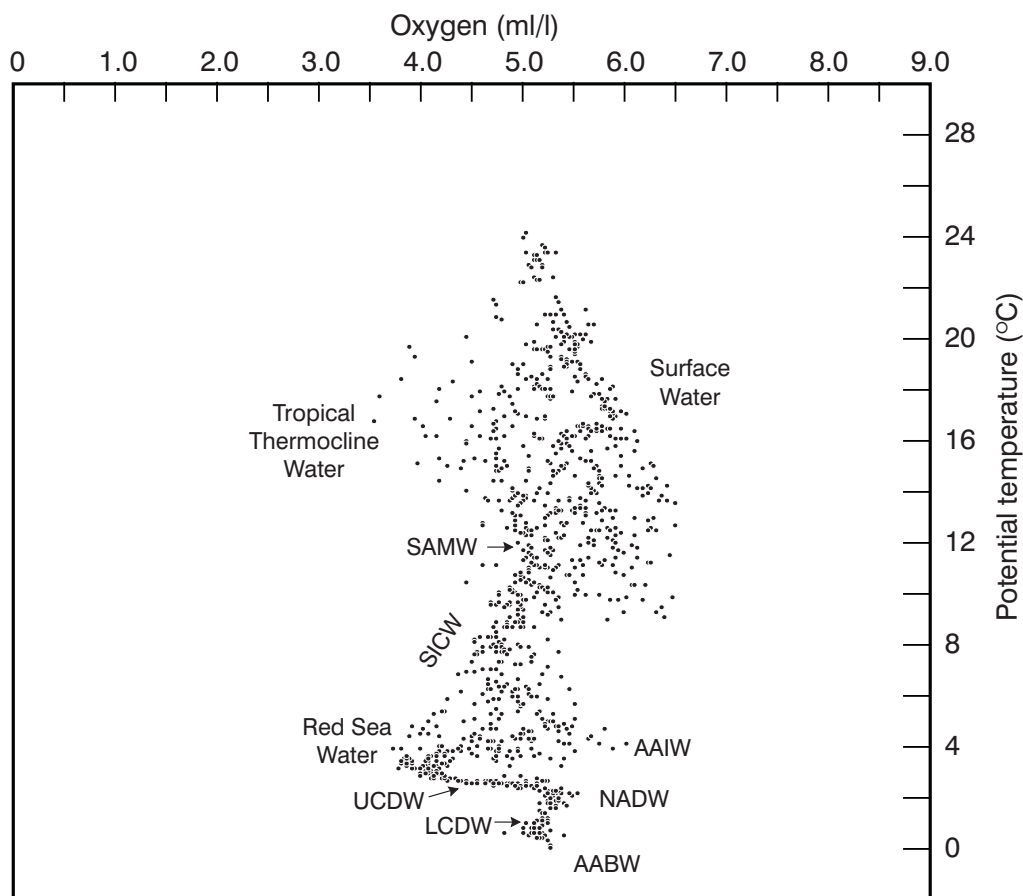


**Figure 6.13.** The potential temperature–dissolved oxygen characteristics of the water masses in the Agulhas retroflexion region<sup>230</sup>. SAMW: Subantarctic Mode Water; SICW: South Indian Central Water; AAIW: Antarctic Intermediate Water; UCDW: Upper Circumpolar Deep Water; NADW: North Atlantic Deep Water; LCDW: Lower Circumpolar Deep Water; AABW: Antarctic Bottom Water. Oxygen content is particularly valuable in distinguishing between different water masses at intermediate depths.

By comparing the temperature–salinities characteristics found in the Agulhas retroflexion (Figure 6.12) to those found in the northern Agulhas (Figure 4.15) and southern Agulhas Current (Figure 5.3), it can be seen that the two components of the surface waters of the Agulhas Current, Tropical Thermocline Water and Subtropical Surface Water, arrive in the retroflexion region fairly intact. The central and intermediate waters in the retroflexion region by contrast show many more outliers towards lower temperatures than they do farther upstream, indicating the influence of the subantarctic waters, understandably not so evident to the north. Of interest in Figure 6.13 is also the presence of Subantarctic Mode Water, made manifest by its deep oxygen maximum<sup>258</sup>. This water is introduced along the southern edge of the subtropical region and, befitting the proximity of the retroflexion to the Subtropical Convergence, is much more prominent here than in

the South Indian Ocean as a whole (viz. Figure 5.3).

Gordon et al.<sup>230</sup> have shown that the water of Indian Ocean origin introduced into the retroflexion region by the Agulhas Current is restricted to the upper 2000 m. They have also shown that a substantial, or at least a very conspicuous, remnant of Red Sea Water is carried downstream as part of the Agulhas Current flow. It is not clear whether this Red Sea Water passes through the Mozambique Channel<sup>234</sup>, or whether it comes from east of Madagascar<sup>235</sup>. Its low-oxygen characteristics are clearly seen in potential temperature–dissolved oxygen plots for the region (Figure 6.13).

#### *Shallow oxygen minimum*

Of particular relevance to an understanding of the circulation and mixing of water masses in the Agulhas retroflexion is the presence of an oxygen minimum<sup>230</sup>

found at depths of between 100 to 150 m. It is marked as Tropical Thermocline Water in Figure 6.13, and is associated with the warm surface water of the Agulhas Current. During some cruises that have intersected Agulhas rings<sup>230</sup>, this minimum was not found in older rings, suggesting that this particular water mass had been mixed out.

Water in the tropical surface layers in general has significantly lower levels of dissolved oxygen than in the subtropics<sup>84</sup>. On moving southwards, this water is overlain by Subtropical Surface Water with a higher oxygen content and underlain by the deeper oxygen maximum of Subantarctic Mode Water (Figure 6.13), thus creating a shallow oxygen minimum. This layer of

low oxygen extends to the south within the western margins of the Indian Ocean. Warren<sup>232</sup>, as was noted previously, has suggested that this particular minimum may represent the effects of biological oxygen consumption due to decaying organic matter.

Nonetheless, the layer is characteristic of the core of the Agulhas Current Water. In sequential stations carried out from west to east along an isobath of the Agulhas Bank (Figure 6.14) it can be seen that this tropical signature can be used as a valuable tracer of Agulhas Current Water<sup>531</sup>. Chapman<sup>231</sup>, by making use of all appropriate historical data, has been able to show that a layer, with a thickness of between 50 and 150 m, depleted in oxygen by about 1.1 to 1.5 ml/l occurs con-

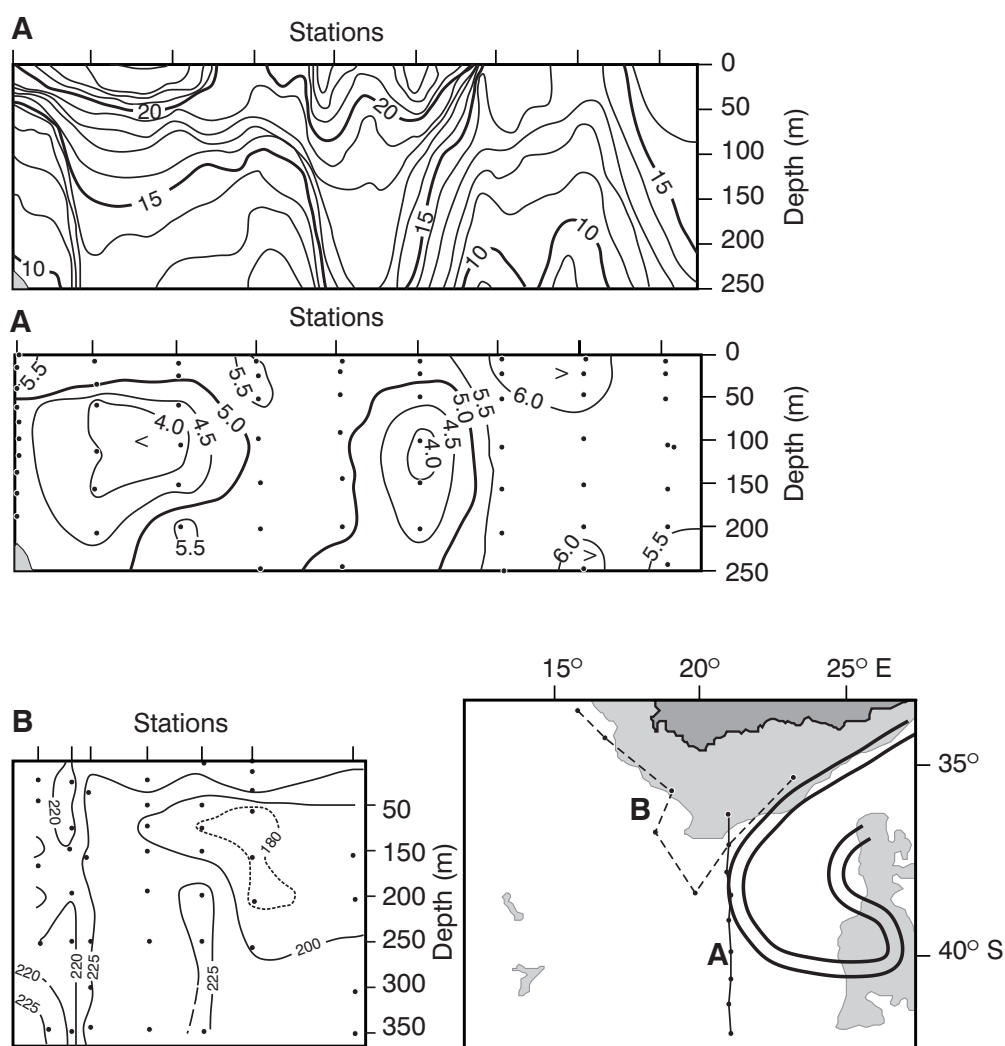


**Figure 6.14.** A temperature section (uppermost panel) and concomitant dissolved oxygen section (middle panel) across the Agulhas retroflection loop<sup>231</sup> showing the distinctive oxygen minimum layer (ml/l), centred at 100 m, that is associated with the core of the Agulhas Current. The lower panel shows an oxygen section along the southern African shelf break<sup>531</sup> ( $\mu\text{mol}/\text{m}^3$ ) demonstrating the abrupt end of this shallow oxygen minimum at the termination of the Agulhas Current. The location of the sections is shown in the map. See also Figure 6.15.

sistently at the edge of the Agulhas Current, also along its retroflection loop. It is so characteristic of Agulhas Current water that it may be used to trace water from the Agulhas Current retroflection as far north as 32° S and 10° E in the South Atlantic Ocean<sup>231</sup>.

#### *Agulhas retroflection nutrients*

A hydrographic section across the Agulhas retroflection loop (Figure 6.15) demonstrates that in this region the nutrient concentrations are usually inversely related to temperature. The lowest levels of phosphate and nitrate are thus seen to be associated with the outer rims of the loop, representing the Agulhas Current and the Agulhas Return Current. All kinematic products of the Agulhas retroflection, such as Agulhas rings, eddies and filaments, carry this signature with them. At the Subtropical Convergence the concentrations of these nutrients are much higher (Figure 6.15), Subantarctic Surface Water being characteristically higher in all nutrients except silicate. The outer edges of the Agulhas Bank are also shown to have higher levels of nutrient concentrations, probably as the result of the inshore upwelling between the Agulhas Current and the shelf slope (viz. Figures 5.2, 5.4, 5.9).

#### *Water mass modifications*

An inspection of precise temperature and salinity data from the Agulhas Current retroflection (e.g. Figure 6.12) show a number of significant outliers. Outliers in the low-salinity direction are for the greater part due to the effect of water from south of the Subtropical Convergence or from the South East Atlantic Ocean. Subantarctic water may make its presence felt by mixing processes along the lower limb of the Agulhas retroflection loop, i.e. along the confluence of the Agulhas Return Current and the Subtropical Convergence. Its major influence on the temperature–salinity characteristics of the region is probably a result of the spasmodic occurrence of wedges of subantarctic water moving northward into the region when an Agulhas ring is spawned (Figure 6.9). Within the thermocline of the Agulhas retroflection this subantarctic influence increases with depth<sup>230</sup>.

Since the high, and seasonally persistent, heat fluxes from the ocean to the atmosphere are well known for this region<sup>121,147</sup>, the possibility exists that thermohaline alterations to water above the thermocline would be evident in the water masses found here. This is indeed the case. Gordon et al.<sup>230</sup>, using a quasi-synoptic, high-quality hydrographic data set, have found that upper thermocline water in the Agulhas retroflection, upon

exposure to the colder overlying atmosphere, forms water that is anomalously salty to that of the Agulhas Current proper. Such modified water is found predominantly as thermostads within the Agulhas retroflection loop, but also in Agulhas rings<sup>230</sup>. Modifications of water masses in this region are particularly important for a number of reasons.

There is evidence that the Agulhas retroflection is a source region for Subtropical Mode Waters in the potential temperature range 17.4 °C to 17.8 °C<sup>382</sup> for the South Indian Ocean and, in a more modified form, for the South Atlantic. This exceptionally cold Subtropical Mode Water is found extensively in the eastern South Atlantic. The convective changes that bring about these modifications have been considered to be highly episodic, while there may be longer periods where the active mixing is restricted to a near-surface, wind-mixed layer<sup>382</sup>. Nevertheless, the water that has been cooled in the Agulhas retroflection is believed to be principally responsible for cooling the near-surface layers in the Indian Ocean and for ventilating thermocline and intermediate waters of the South West Indian Ocean<sup>532</sup>. Although it is considered difficult to use water mass indicators to trace water of South Indian origin in the South Atlantic, it appears possible that water altered at the Agulhas retroflection may play a determining role in the nature of the South Atlantic thermocline.

#### *Fluxes in the Agulhas retroflection*

The transport values of the Agulhas Current are known to increase downstream (Figure 6.16), but the rates of increase that have been estimated to date differ markedly, between  $2.7 \times 10^6$  m<sup>3</sup>/s per 100 km<sup>380</sup> to  $6 \times 10^6$  m<sup>3</sup>/s per 100 km<sup>230</sup>. Calculations of what this volume transport increase should be, based on the zonally integrated interior transport of the South Indian Ocean, driven by the known wind-stress curl, lie between  $9 \times 10^6$  m<sup>3</sup>/s per 100 km at 25° S to zero at 37° S<sup>534</sup>. With the adjustment of the wind stress values to more accurate ones, estimates of the volume flux of the Agulhas Current, based on the wind stress, at 37° S have been adjusted downward from  $72 \times 10^6$  m<sup>3</sup>/s<sup>534</sup> to about  $55 \times 10^6$  m<sup>3</sup>/s<sup>187</sup>. This reduces the downstream increase to  $2 \times 10^6$  m<sup>3</sup>/s per 100 km. The observed flux values as well as rates of downstream change are far in excess of those predicted by purely linear, thermohaline and wind-driven dynamics<sup>533</sup>. This has to date not been adequately explained.

The fluxes within the Agulhas retroflection itself have been calculated based on the hydrographic data collected during only a few suitable cruises.

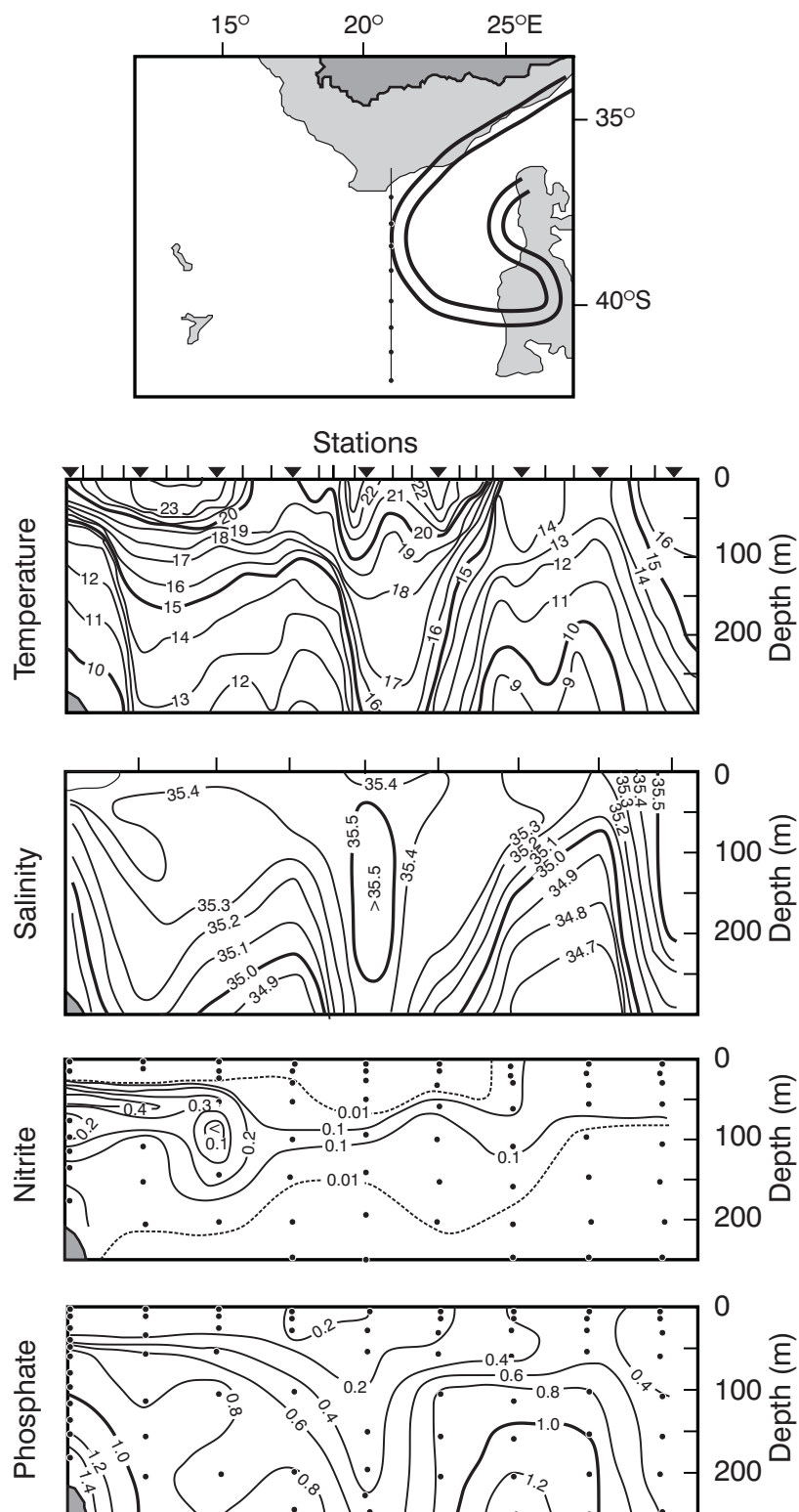


**Figure 6.15.** A hydrographic section across the Agulhas retroflection loop<sup>531</sup> showing the temperature, salinity, nitrite and phosphate ( $\mu\text{mol}/\text{m}^3$ ) for this feature. The accompanying map shows the location of the section relative to the retroflection at that time. The inverse relationship between temperature and nutrient concentration for these waters is immediately discernible. See also Figure 6.14.

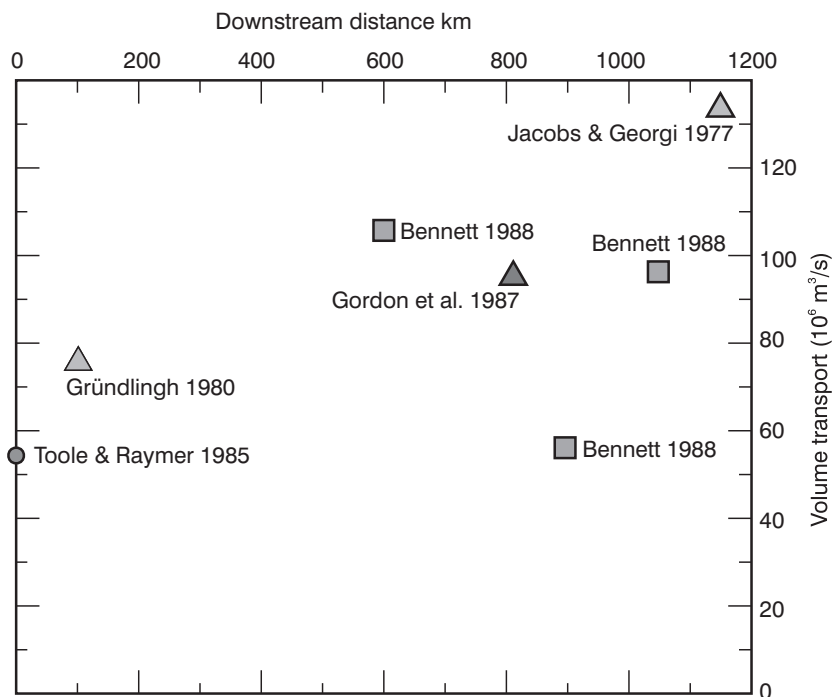


**Figure 6.16.** Volume transport values for the Agulhas Current downstream of  $30^\circ \text{S}^{533}$ . The Agulhas retroflexion lies downstream of 900 km in this figure. Individual papers referenced here by author(s) and year can be found in the Bibliography.

Gordon et al.<sup>230</sup> have estimated that  $70 \times 10^6 \text{ m}^3/\text{s}$  above 1500 m passed into the Agulhas retroflexion region through the Agulhas Current ( $95 \times 10^6 \text{ m}^3/\text{s}$  relative to the sea floor) during one particular cruise. Of this,  $10 \times 10^6 \text{ m}^3/\text{s}$  continued to flow west; the rest joined the retroflexion proper. There was a recirculation, within the loop of the Agulhas retroflexion, of  $15 \times 10^6 \text{ m}^3/\text{s}$ . About  $55 \times 10^6 \text{ m}^3/\text{s}$  left the retroflexion as the Agulhas Return Current. Early, upstream retroflexions, local recirculation and time biases in the coverage of the region during one particular cruise make it notoriously difficult to draw up a balanced budget for the water masses entering and leaving the Agulhas retroflexion region (e.g. Figure 6.16).

### Agulhas rings

The presence of intense vortices near the southern tip of Africa has been surmised<sup>46,59</sup> from or observed<sup>75,511</sup> in hydrographic data for a long time. In Figure 6.5 the dynamic topography of the Agulhas retroflexion region and vicinity clearly shows, for instance, the presence of such a substantial eddy south-west of Cape Town. It may be assumed to have been an Agulhas ring and to have had its inception in the Agulhas retroflexion. It had a characteristic diameter of about 400 km and a vol-

ume transport of 5 to  $10 \times 10^6 \text{ m}^3/\text{s}$  to 1100 decibar<sup>92</sup>. On one cruise<sup>230</sup> the spawning of such a feature has actually been observed<sup>61</sup> and the nature of a newly formed ring could be established in detail (Figure 6.17).

### Ring characteristics

First, having been recently spawned from the Agulhas Current, the surface expression of an Agulhas ring is that of a warm annulus with Agulhas Current surface water clearly distinguishable as a circular ribbon of high temperatures<sup>61</sup> with a tell-tale, subsurface oxygen minimum<sup>531</sup>. Hence the designation *Agulhas ring*. These characteristics are not seen in other mesoscale eddies cast off from the Agulhas Current<sup>458</sup>, particularly along the Subtropical Convergence<sup>63</sup>. These latter features are therefore preferably called *Agulhas eddies*. However, Agulhas rings do not retain this distinctive surface structure for a long time. Convective mixing due to severe heat loss to the atmosphere<sup>98</sup>, as well as substantial mixing due to high levels of wind stress, rapidly erases all surface contrasts between rings and their surroundings in the South East Atlantic Ocean. Before this happens to a substantial degree, surface expressions represent the dimensions of Agulhas rings quite well.

Based on more than 600 thermal infrared images

from the METEOSAT satellite, it has been established that, at the sea surface, the average diameter of an Agulhas ring is 324 km, with a standard deviation of 97 km<sup>414</sup>. An investigation on the characteristics of Agulhas rings sufficiently robust to reach the Walvis Ridge<sup>712</sup> has shown that the diameters of these features have no noticeable seasonal variations. Agulhas rings closer to Cape Town that have lost their contrasting surface expression, but that are circumscribed by encircling Agulhas filaments<sup>440</sup>, have diameters of 307 ( $\pm 89$ ) km. This apparent reduction in size may be an artefact of the Agulhas filaments partially overlying Agulhas rings<sup>92</sup>, thus making them seem smaller than they are.

Characteristics of a newly spawned ring have been observed at sea a number of times<sup>784-5</sup>. Detailed observations of a ring in March 2000<sup>785</sup> have shown that it had a maximum anomaly of sea surface height of 0.70 m, a radius of 120 km and a volume of  $38 \times 10^{12} \text{ m}^3$ . A strong azimuthal current of about 1 m/s gave this ring a kinetic energy of  $18 \times 10^{15} \text{ J}$ . The ring was strongly baroclinic, but also had a significant barotropic component. The hydrographic structure of the ring as well as

its velocity extended down to a depth of 4500 m (Figure 6.18). This is the first solid evidence that Agulhas rings extend to such depths. This does not of necessity imply that all individual rings are this deep. The Agulhas Current itself at times extends to the bottom<sup>367</sup>, but at other times is much shallower<sup>738</sup>. One would expect this therefore to be true of Agulhas rings as well. The hydrographic properties of the ring so meticulously surveyed in March 2000 differed from those of the ambient waters only at temperatures greater than 12°C. Based on a number of criteria, this specific ring has been considered a very large one<sup>785</sup>. An indication of the range of diameters to be observed is evident from Figure 6.19.

The two rings observed during a particular cruise (Figure 6.17) had different shapes and sizes. The older, more northern ring, was more nearly circular and had a diameter of about 200 km. The southern one was more elliptical with minor and major diameters of 100 km and 250 km respectively<sup>230</sup>. When ring dimensions are defined by their average diameter of maximum radial velocity, they seem smaller. Duncombe Rae<sup>127</sup> has carried out a statistical analysis of 18 rings observed in the general vicinity of Cape Town (Figure

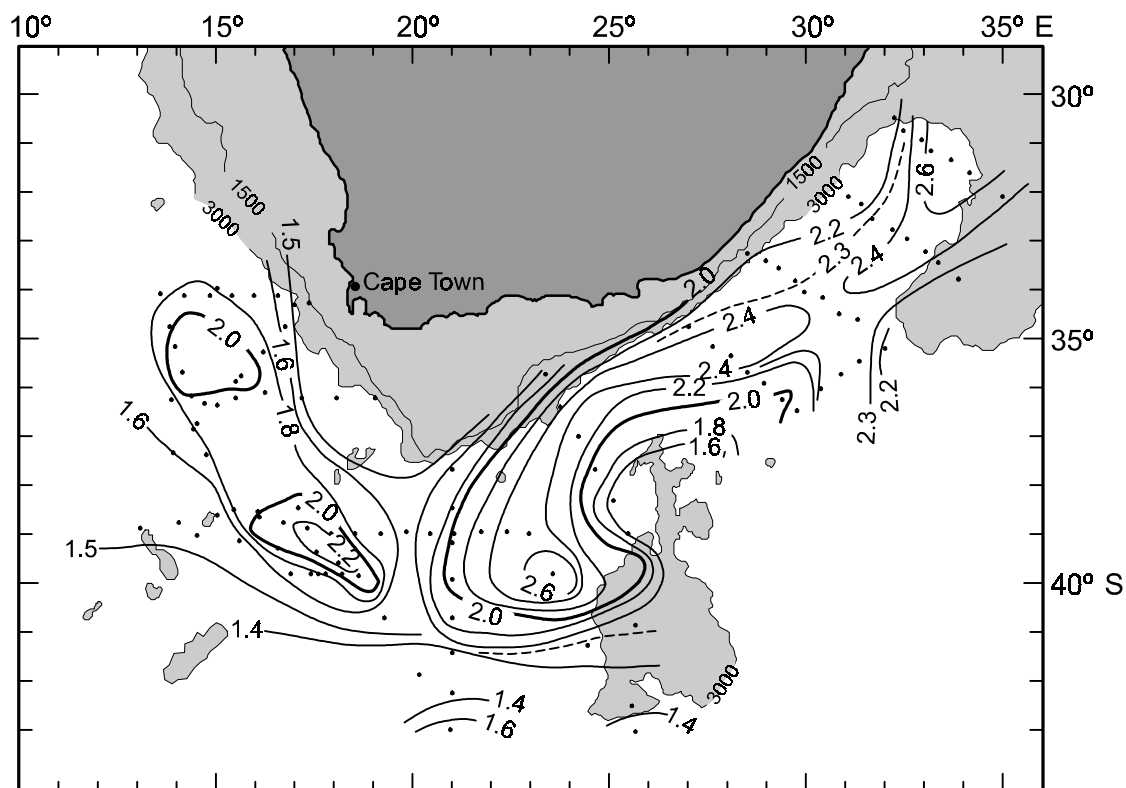


**Figure 6.17.** The dynamic height anomaly of the sea surface relative to 1500 decibar, given in dynamic metres<sup>230</sup>. The Agulhas retroflection loop is clearly circumscribed, as well as two Agulhas rings to the west of the retroflection. Regions shallower than 3000 m are indicated by shading.

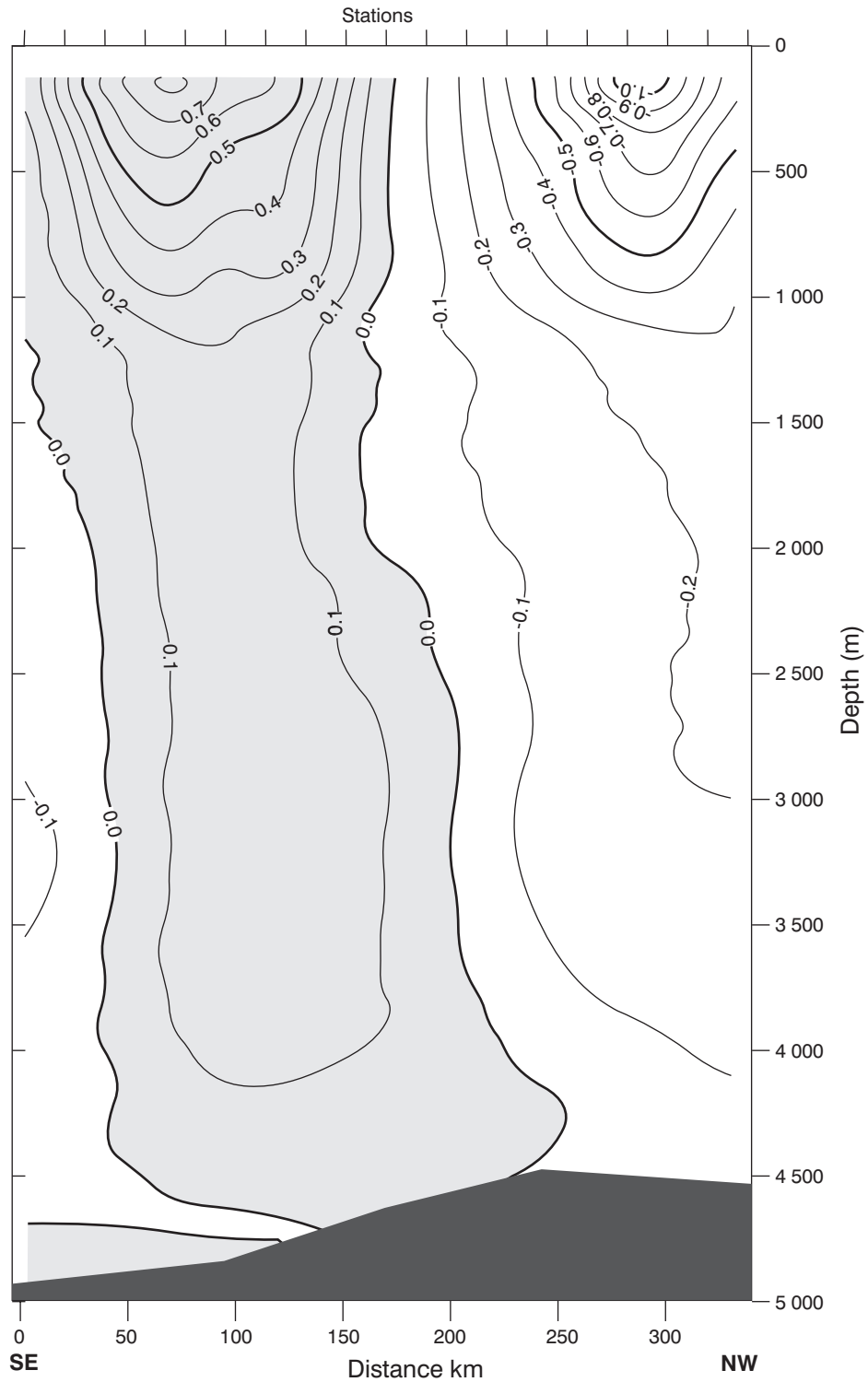


**Figure 6.18.** The full velocity structure of a relatively young Agulhas ring in the Cape Basin<sup>785</sup>. The speeds are in m/s. The shaded region indicates movement to the north-east. Speeds of slightly less than 0.1 m/s were found right down to the sea floor on this occasion.

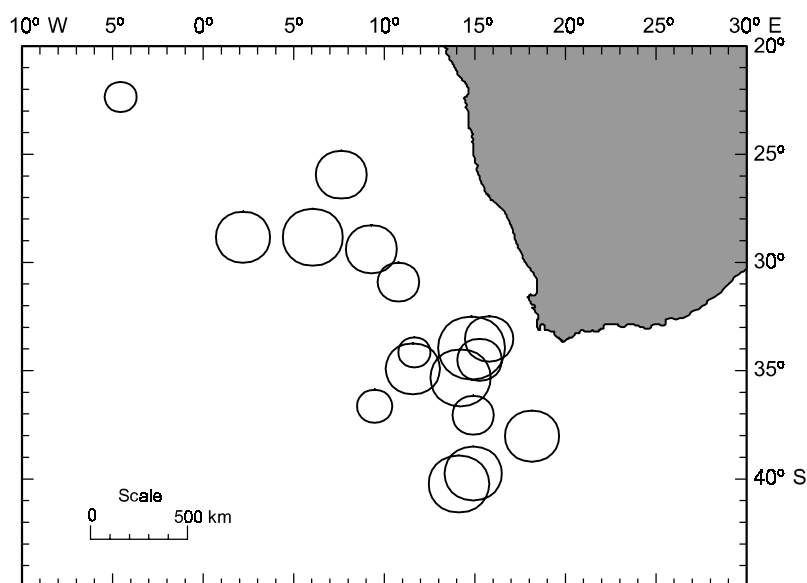


**Figure 6.19.** A compendium of Agulhas rings, their diameters and their geographical locations from eleven independent sets of hydrographic measurements<sup>127</sup> south-west of South Africa.

6.19) and, according to these hydrographic data, estimates a mean diameter of  $240(\pm 40)$  km. This is probably the most reliable assessment of the dynamic dimensions of the rings to date. The mean depth of the  $10^\circ\text{C}$  isotherm, a good proxy for the dynamic topography of these features<sup>129</sup>, is  $650(\pm 130)$  m for this set (Figure 6.19) of rings. The range of a number of variables connected to Agulhas rings is given in Table 6.3. The geographic distribution of this set of rings suggests a general north-westerly drift.

#### *Rings translating*

A subsequent survey of eddies in the Cape Basin<sup>535–7</sup>, during three major cruises, located seven eddies in the region<sup>520</sup>. Five of these were positively identified as Agulhas rings. The passage of these rings was associated with depressions in the  $10^\circ\text{C}$  isotherm lasting from 100 to 400 days at a particular spot. After the passage of a ring the thermocline appears to shallow appreciably before relaxing to the local mean depth for that temperature<sup>520</sup>, suggesting the passage of an attendant, but smaller, cyclonic eddy.

The depth to which particles are actually trapped in an eddy, and thus move with it, may depend on the ratio between the azimuthal speed and the translational speed of the eddy<sup>538</sup>. Based on the advection rates that have been observed for rings to date<sup>94,464</sup> or calculated<sup>539</sup>, it has been estimated<sup>127</sup> that the trapped depths lie between 670 m (for the highest drift speeds) and 110 m. This would imply that, although depressed isotherms

may indicate a ring depth of 4000 m or more, only intermediate and shallower waters are carried along, the rest of the signal progressing as a wave in the density field only. It still needs to be established whether this theoretical limitation on the trapped depths of Agulhas rings actually applies. Detailed modelling<sup>271</sup> has suggested that the baroclinic velocity of an Agulhas ring would exhibit an inversion at a depth of about 1250 m (Figure 6.20). There are measurements that seem to show this, but it seems that the deep velocity structure of a ring may very much be a function of its age.

#### *Ring distributions*

Using this perturbation of the temperature field to identify mesoscale features in the South Atlantic Ocean during the abovementioned three dedicated cruises has resulted in the overall distribution of eddies for the Cape Basin<sup>520</sup> given in Figure 6.21. These cruises were carried out over a 17 month period<sup>535</sup> in 1992 and 1993 to survey the region, making it a relatively synoptic survey. The distribution is not dissimilar to that portrayed in Figure 6.19. It was shown<sup>517</sup> that two to six rings co-existed in the Cape Basin at any one time. Subsequent altimetric studies<sup>465</sup> as well as investigations with floats<sup>627</sup> have largely substantiated these numbers, but shown that they may vary considerably from year to year. It has for instance been estimated<sup>628</sup> that during the KAPEX endeavour nearly 12 Agulhas rings were to be found in the south-eastern Cape Basin. The abovementioned hydrographic surveys have, how-

**Table 6.3.** A compendium of ring parameters for a number of published observations of Agulhas rings<sup>785</sup>.  $V_{\max}$  is the maximum tangential speed,  $L_{\max}$  is the radius where this maximum tangential speed is found,  $Vol_{10}$  is the volume of the ring above the 10° C isotherm, APE is the available potential energy relative to the depth of the thermocline outside the ring, KE is the kinetic energy if the ring is considered as consisting of two layers, AHA is the integrated heat excess above the 10° C isotherm (relative to a temperature profile which is representative for the surrounding water) and ASA is the integrated salinity excess above the 10° C isotherm (relative to a salinity profile which is representative for the surrounding water).

Source	Programme	Ring	$V_{\max}$ [m/s]	$L_{\max}$ [km]	$Vol_{10}$ [10 <sup>12</sup> m <sup>3</sup> ]	APE [10 <sup>15</sup> J]	KE [10 <sup>15</sup> J]	AHA [10 <sup>20</sup> J]	ASA [10 <sup>12</sup> kg]
Van Aken et al. (2003) <sup>785</sup>	MARE-1	Astrid	1.0	120	38	20	18	0.8	4.1
Van Ballegooyen et al. (1994) <sup>129</sup>	SCARC	A3		160	34			1.5	8.7
		A4		140	33			2.4	13.1
		A5		95	11			0.7	4.4
		A6		125	17			1.1	4.6
Olson and Evans (1968) <sup>94</sup>	ARC	RE	0.9	130	26	51	9		
		CTE	0.6	115	30	31	6		
Duncombe Rae et al. (1996) <sup>520</sup>	BEST 1992–1994	B1–1	0.4	85		17	2	0.2	1.2
		B2–2	0.5	65	17	11	2	0.6	3.8
		B2–3	0.3	85		7	1	0.6	3.7
		B2–4	0.3	95		23	2	0.4	1.7
McDonagh et al. (1999) <sup>542</sup>	A11	Ring 1	0.6	71	15	5	1	0.4	2.4
		Ring 2	0.8	75	24	8	3	0.2	1.4
Garzoli et al. (1999) <sup>783</sup>	KAPEX 1997	Ring 1	0.4	100	31	43	1	0.9	
		Ring 2	0.2	110	42	52		1.3	
		Ring 3	0.3	100	19	15		0.8	

ever, turned up some novel features that have not been observed here before and that are of considerable importance.

First, a number of cyclonic eddies have been found on the periphery of the retroflection region (viz. Figure 6.21). Modelling of this ocean region with high spatial resolution<sup>273</sup> has suggested the production of dipole pairs of eddies – one anti-cyclonic, the other cyclonic – at the Agulhas retroflection. It is not clear whether the cyclonic features observed during this set of cruises of 1992 and 1993 support the simultaneous shedding of eddies with opposing flow directions. For a proper understanding of the vorticity balance of the ring-spawning process as well as the long-term stability of Agulhas rings it would be of crucial importance to establish the formation mechanism for these cyclonic eddies. There are theoretical results that suggest<sup>654–5</sup> that baroclinic rings, accompanied by weaker cyclones, would inherently have a greater degree of stability.

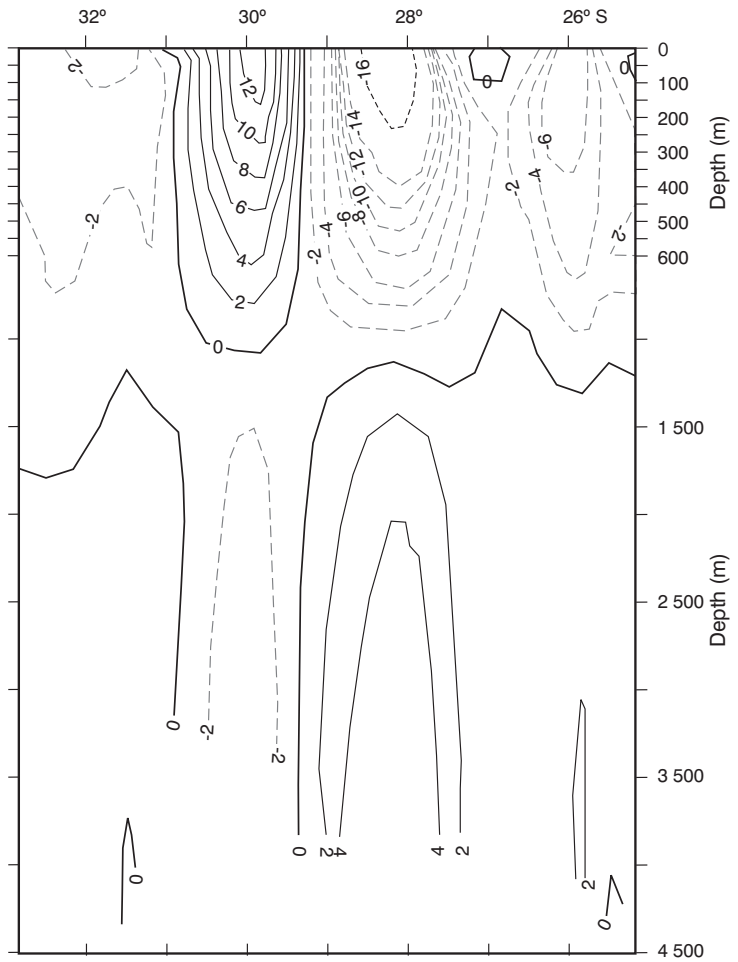
Subsequent investigations<sup>627–31</sup> have indicated a totally new and important phenomenon in this regard: independent Cape Basin cyclones. It has been demonstrated<sup>627–8</sup> that cyclones are an ubiquitous component of the circulation in this part of the South East Atlantic Ocean. They move in a south-westerly direction<sup>626,628</sup> from the edge of the African continental

shelf, crossing the average north-westerly path of Agulhas rings with advection speeds of 3–5 cm/s, very similar to those of Agulhas rings<sup>628</sup>. This phenomenon is most evident in regions surrounding the Agulhas retroflection loop and not at the retroflection itself where Agulhas rings are first formed, indicating that these cyclones do not necessarily form part of the ring-shedding process. The criss-crossing movement of Agulhas rings and cyclones is in agreement with simple theories<sup>538</sup> for vortex propagation on a  $\beta$ -plane<sup>626</sup> through a weak background flow. This crossing of the paths of cyclonic and anti-cyclonic eddies has also been observed<sup>626</sup> in other, similar ocean regions, such as the North East Pacific Ocean and the South East Indian Ocean. What are the currently known characteristics of these Cape Basin cyclones, and what role might they play in the mixing of water from Agulhas rings in this basin?

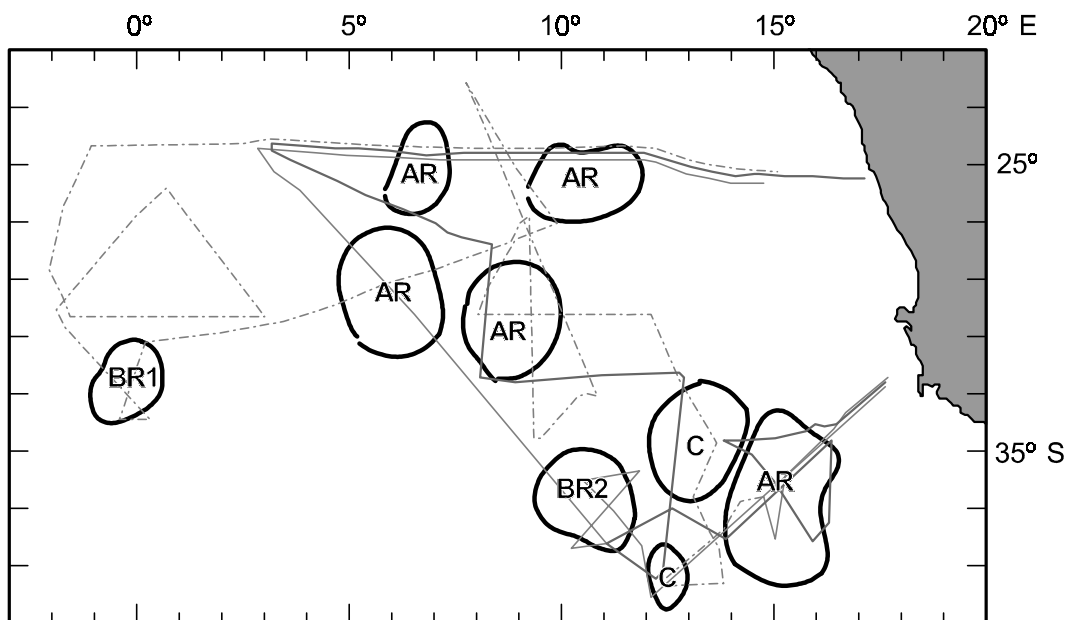
#### *Cape Basin cyclones*

It would seem that three, perhaps related, cyclone types are to be found in the Cape Basin. The first are eddies that were previously imbedded in Natal Pulses<sup>629, 632</sup>, the second lee eddies shed from the western side of the Agulhas Bank<sup>630–1</sup> and the third type cyclones shed

**Figure 6.20.** The baroclinic speed in a section across a modelled Agulhas ring<sup>271</sup>. Speeds are in cm/s with solid lines representing motion towards the reader. The model suggests that the baroclinic motion will exhibit a velocity inversion at depths greater than 1000 m, but with greatly reduced speeds.



**(Below) Figure 6.21.** Distribution of meso-scale disturbances to the depth of the 10 °C isotherm in the Cape Basin of the South Atlantic<sup>520</sup>. These locations are based on measurements undertaken during three cruises as part of the BEST series in 1992 and 1993. Thin lines denote the tracks of these cruises. Circulation features are denoted AR (Agulhas Current ring), BR (Brazil Current ring) and C (cyclonic eddy). The temperature–salinity characteristics of the postulated Brazil Current rings, denoted BR1 and BR2, are given in Figure 6.25.



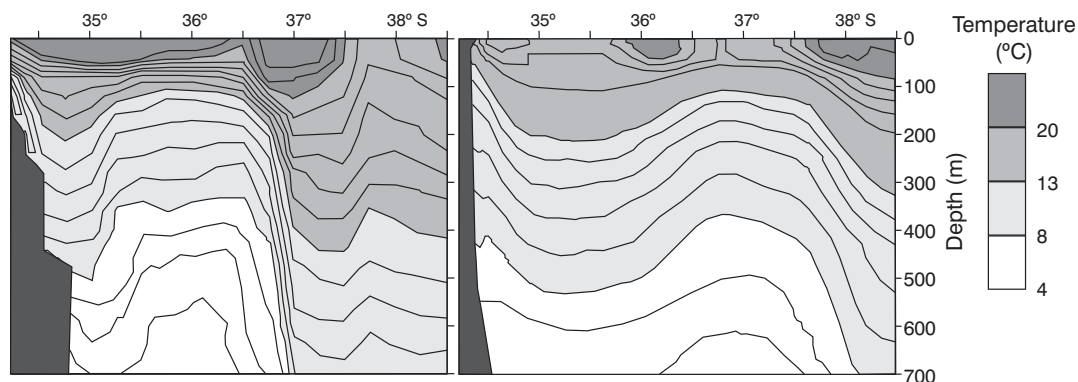


**Figure 6.22.** Vertical temperature sections across a characteristic eddy generated off the western side of the Agulhas Bank, south-west of Cape Town. The left-hand panel represent actual hydrographic observations; the right-hand panel temperature distributions simulated by a regional model<sup>630</sup>.

from the continental shelf edge of south-western Africa<sup>627–8</sup>.

The general behaviour of Natal Pulses has always suggested<sup>62,399</sup> that this special meander of the Agulhas Current has an embedded cyclone in its core (viz. Figures 4.24 and 5.15). As mentioned before, it has even been suggested that this particular cyclone originates from the lee eddy often present off Durban<sup>315, 169</sup> (viz. Figures 4.20 and 4.21), just south of the Natal Bight. More recent observations, including current meter records, float trajectories and satellite remote sensing products have demonstrated unequivocally<sup>632</sup> that the cyclone in the loop of a Natal Pulse is persistent along its trajectory and extends to the full depth of the Agulhas Current. What becomes of this well-developed cyclone once a Natal Pulse passes the tip of the Agulhas Bank south of Africa?

Studies combining RAFOS floats and satellite observations have shown<sup>629</sup> that such cyclones are shed into the South Atlantic Ocean and are sometimes instrumental in triggering the occlusion of an Agulhas ring (Figure 6.23). They may even move poleward through the gap between the newly shed Agulhas ring and the Agulhas retroflection loop. In many models<sup>763</sup> the shedding of Agulhas rings is accompanied by the formation of an accompanying cyclone. Once in the Cape Basin cyclones of this category seem to disintegrate rapidly. This behaviour of cyclones in Natal Pulses is mirrored closely by shear edge features of the southern Agulhas Current<sup>629</sup> when they move past the southern tip of the Agulhas Bank. Both these sets of cyclones may have an effect on the circulation on the western side of the Agulhas Bank.

It has been shown<sup>630</sup> that cyclonic motion is a recurrent, but not persistent, feature of the southern part of the shelf edge of the western Agulhas Bank. This motion in the lee of the bank is driven by the passing Agulhas

Current and can be quite easily modelled<sup>630–1</sup>. In such a model<sup>633</sup> leakage of vorticity from shear edge – or border – eddies along the eastern edge of the Agulhas Bank (viz. Figures 5.7 and 5.8) feeds into the lee eddy at irregular intervals enhancing it spasmodically. The modelled lee eddy bears a very strong resemblance to those measured at sea (Figure 6.22). Both in the model and in observations this lee eddy is eventually shed into the Cape Basin where it may interact vigorously<sup>628</sup> with Agulhas rings and with other cyclones. In a primitive equation model<sup>761</sup> with a spatial resolution of  $1/6^\circ \times 1/6^\circ$ , such cyclones are usually paired with Agulhas rings in dipolar or even tripolar structures<sup>760</sup>. The influence of border eddies from the eastern side of the Agulhas Bank on lee eddies as well as on the subsequent behaviour of lee eddies is shown schematically in Figure 6.23.

This figure is based on sea-surface height anomalies and on the simultaneous movement of RAFOS floats placed in two groups; the first at roughly 400 m depth, the others at an average of 800 m depth. The behaviour of both sets of floats was very similar in these cyclones, indicating their coherent depth structure. As can be seen from Figure 6.23 (first panel) floats on this occasion spent some time in border eddies on the eastern side of the Agulhas Bank. At some later stage they moved downstream and were caught up in a vigorous lee eddy (Figure 6.23, third panel). On subsequently breaking away from the shelf edge (Figure 6.23, last panel), this lee eddy crossed the Agulhas retroflection loop, cutting off an Agulhas ring in the process. The south-westward direction of drift of the lee eddy is entirely characteristic for such features; there is insufficient evidence to warrant its influence on ring shedding as equally distinctive. Of importance here is to note that the modelled<sup>631</sup> simulation, that shows vorticity being transferred from border eddies on the eastern side of the

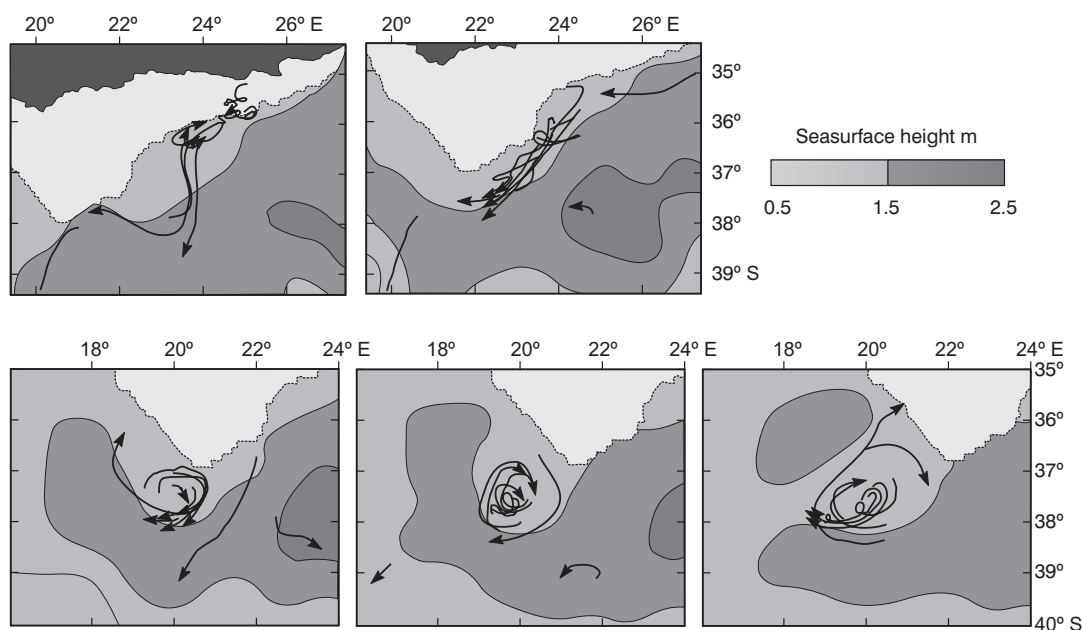


**Figure 6.23.** Evidence at depth for the role of a shear edge or border eddy in the detachment of an Agulhas ring from the Agulhas Current retroflexion<sup>629</sup>. The tracks of RAFOS floats at intermediate depths are shown in these panels relative to concurrent sea height anomalies. Arrows are given at the leading edges of each float track and show the location of the float on the day given. Anti-cyclonic motion is denoted by the grey scale and the land mass deeper than 1000 m is shown as light grey. Panels follow in the conventional sequence.

Agulhas Bank to a lee eddy on its western side, has therefore in fact been observed. However, a study during the period 1997–1999<sup>629</sup> suggested that of six cyclones identified on the landward side of the southern Agulhas Current, two dissipated at their site of formation; four propagated downstream. It therefore seems clear that not all border eddies feed the Agulhas Bank lee eddy. Of especial relevance is the role border eddies may at times play in the triggering of ring shedding events.

The last of the three types of cyclones being discussed: Natal Pulse eddies, Agulhas Bank lee eddies and Cape Basin cyclones, is the least understood. Cape Basin cyclones in most respects behave in a manner very comparable to the lee eddy described above, except that they are formed at the shelf edge equatorward of the Agulhas Bank<sup>628</sup> and therefore do not seem to be directly driven by the Agulhas Current. In general they have a diameter of 120 km, smaller therefore than Agulhas rings that have a typical diameter of 200 km. They are much weaker than Agulhas rings with which they co-exist in the Cape Basin. According to float observations at intermediate depths, Cape Basin cyclones on average exhibit kinetic energy levels 60 per cent less than Agulhas rings<sup>628</sup>. During 1997, 22 such cyclones were observed in the Cape Basin, seemingly a representative figure. The mean zonal velocity of Cape Basin cyclones westward was  $3.6(\pm 0.6)$  cm/s and

the mean poleward drift  $0.4(\pm 0.5)$  cm/s (Figure 6.24). Azimuthal speeds measured to date reach 22 cm/s. The lifetime of these cyclones is less than two to three months<sup>628</sup>, thus much shorter than that of many Agulhas rings. Because of their short lifetime and the south-westward direction of their drift, few of them are found in the northern part of the Cape Basin<sup>627</sup> and only one has to date been observed<sup>781</sup> to cross the equatorward border of this basin, the Walvis Ridge. The importance of Cape Basin cyclones lies predominantly in their presumed role in mixing of eddy and ring features within this basin.

Notwithstanding their short lifetimes, the number of cyclones in the Cape Basin at any one time would seem to exceed that of Agulhas rings by a ratio<sup>628</sup> of 3 : 2. They therefore are quantitatively an important component part of the circulation here. The periods floats, at intermediate depths, spend in these cyclones (44 days) is similar to that of floats in Agulhas rings (41 days). This short trapping period suggests that there is substantial mixing of water from within both types of features with ambient water masses. It has also been observed<sup>628</sup> that floats are frequently exchanged between Agulhas rings and Cape Basin cyclones, evidence of the entrainment and detrainment of water between these features. This implies that the presence of large numbers of cyclones in the Cape Basin substantially enhances the mixing of

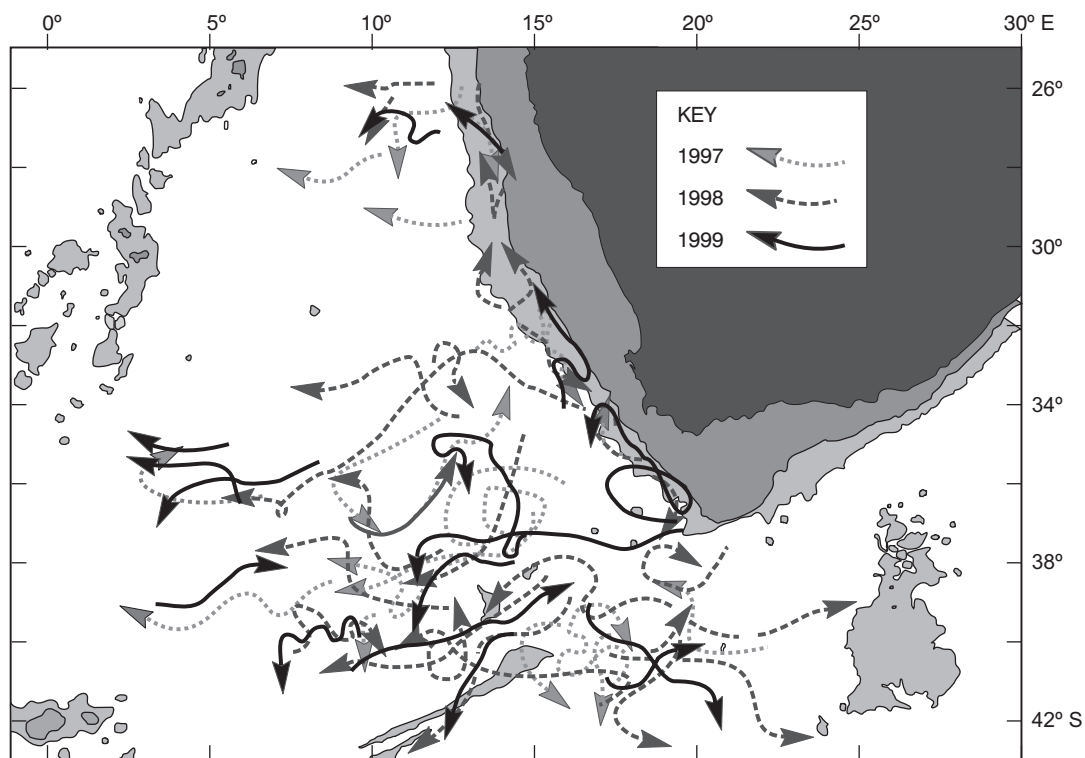


**Figure 6.24.** The tracks of cyclones in the south-eastern Atlantic Ocean for the period 1997–1999<sup>628</sup> as inferred from sea surface height anomalies. Bottom topography is described by the 1000 m and 2000 m isobaths.

water from Agulhas rings here, thus shortening their lifetime in the south-eastern part of the basin. For this reason it has whimsically been referred to by Boebel et al.<sup>628</sup> as the Cape Cauldron.

#### *Brazil rings?*

The second set of unusual, and unexpected, mesoscale features observed during cruises in the Cape Basin are eddies that have hydrographic characteristics somewhat different from those expected of standard Agulhas rings<sup>540</sup>. It has been claimed that these anti-cyclonic features have their origin at the confluence of the Brazil and Falkland Currents in the western Atlantic Ocean and are advected eastward with the high-latitude limb of the South Atlantic gyre until they reach the position shown in Figure 6.21. This somewhat startling conclusion has been based on two sets of data.

First, the potential temperature–salinity characteristics of these two particular eddies below a depth of 600 m, i.e. well away from possible atmospheric influences, is more closely comparable to that of the Brazil Current than that of the Agulhas Current. This is shown in Figure 6.25. Secondly, comparing different CFC tracers, some of which have a declining concentration

in the atmosphere, some increasing, an age for water in a feature can be calculated. From such a comparison, the age of ring BR1 (Figure 6.21) has been estimated at three years<sup>540</sup>. With a known eastward drift of 20 to 30 km/day in the southern limb of the subtropical gyre of the South Atlantic, this could place this particular ring at the Brazil Current retroflexion when it was formed. Others have come to different conclusions on the origin of these unusual rings.

It has subsequently been shown that the ring that has been claimed to have crossed the South Atlantic from the Brazil Current came from the Agulhas retroflexion where it had been spawned 16 months earlier<sup>541</sup>. This conclusion is supported by both altimetric and thermal infrared data for the region for this period. The hydrographic and kinematic nature of this anomalous ring was in all respects akin to that of neighbouring Agulhas rings, except for the higher oxygen and lower nutrient concentrations in its core. Since these are consistent with the characteristics of Subantarctic Mode Water, formed at the Subtropical Convergence in austral winter, it has been suggested<sup>542</sup> that this front is the origin of this water that may occasionally be found within the Agulhas Current. This suggestion has also been put forward by others<sup>783</sup> who have investigated a number

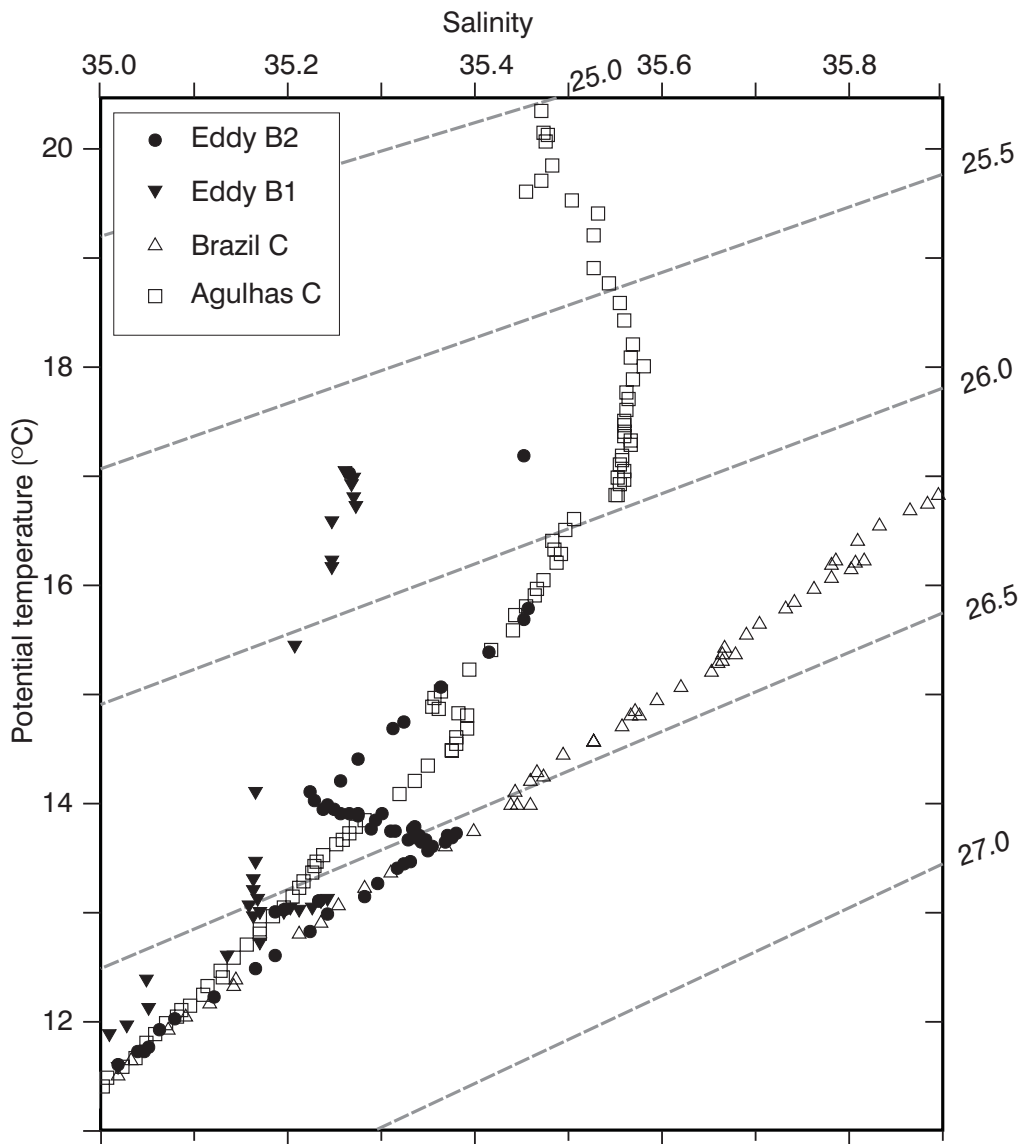


**Figure 6.25.** Temperature–salinity characteristics of two eddies (B1 and B2) observed in the South East Atlantic Ocean<sup>520</sup> that were believed to have their origin as Brazil Current rings<sup>540</sup>. Their geographic locations are shown in Figure 6.21. These temperature–salinity characteristics are juxtapositional to those distinctive of the Agulhas Current and the Brazil Current respectively.

of rings and found some with high saturations and concentrations of oxygen in a thermostat at a depth between 600 m and 1100 m. Their analysis has led to the tentative conclusion that this particular ring had incorporated a lens of water from the Subtropical Convergence by coalescing with another eddy. An entirely conclusive answer on whether Brazil rings can reach the south-eastern Atlantic has therefore not yet been given.

Nonetheless, the possibility of Brazil Current rings remaining essentially intact for what must be a considerable period must be largely dependent on the rate of

mixing between the rings and the ambient water masses. This rate of mixing is currently not known, but will most likely be a function of the speed of rotation of these features. This argument will of course also hold for Agulhas rings.

#### *Ring kinematics*

Maximum radial speeds of Agulhas rings lie between 0.29 m/s and 0.90 m/s with an average<sup>127</sup> of 0.56 m/s. The azimuthal velocity around a ring, as a function of

radius from ring centre, is very variable<sup>94</sup> (see Table 6.3) Agulhas rings do not come with a strongly constrained range of physical characteristics. The available potential energy of Agulhas rings adequately measured to date lies between 26 and  $51 \times 10^{15}$  J. Altimetric data suggest<sup>517</sup> up to  $70 \times 10^{15}$  J. The kinetic energies fall between  $2.3$  and  $8.7 \times 10^{15}$  J.

Observations of the absolute velocity field of Agulhas rings, using a sophisticated combination of acoustic Doppler current profilers, Global Positioning Systems and high-quality hydrographic data<sup>537</sup> have demonstrated that as much as 50 per cent of the total flow in the core of a mature ring is barotropic. The radius of maximum velocity in this presumed ring had shrunk to only 60 km. On the basis of some of these results Olson and Evans<sup>94</sup> and others<sup>517</sup> have concluded that Agulhas rings are the most energetic in the world and that one ring, by itself, may contribute up to 7 per cent of the annual input of energy by the wind for the entire South Atlantic basin. What does such an intense eddy look like hydrographically? This is shown in Figure 6.26.

#### *Ring hydrography*

The general vertical portrayal of this ring is characteristic of others observed in the region<sup>543</sup>. First, two warm lobes of the annulus of warm surface water are still intact. This is not represented in the salinity distributions, but is evident in the subsurface oxygen minimum that is more clearly seen on the inshore side of the ring. Secondly, phosphates are in general low, but in the extensive 16 °C to 17 °C thermostad high nitrite values are to be found (Figure 6.26). This thermostad, fully saturated with oxygen, is believed to be due to cooling and vertical convection of the Indian Ocean water in the centre of the ring<sup>65</sup> over an extended period. Heat losses in early spring of 157 W/m<sup>2</sup> for an Agulhas ring have been estimated<sup>61</sup>; 80 W/m<sup>2</sup> in autumn<sup>543</sup>. Evaporation and convection lead to increased salinities in the surface layers<sup>94</sup>. Observations of Agulhas rings much farther afield<sup>544</sup> accentuate the marked effect on their hydrographic structure of interaction with the atmosphere (Figure 6.27) shortly after they have been spawned.

These rings have been found and properly surveyed<sup>544</sup> by Arhan et al. well beyond the Walvis Ridge in the Angola Basin. One, here called R<sub>2</sub> (Figure 6.27), had a diameter of about 500 km and a core temperature of 17.1 °C. The core of its thermostad lay at a depth of 150 m. Ring R<sub>3</sub> by contrast was only 100 km in cross-section, had a core temperature of only 13.5 °C and its thermostad depth was about 400 m. This is very similar to a ring found even farther west on another cruise<sup>542</sup> and that was assumed to have come from the Brazil

Current. From satellite altimetry it could be determined that the former two vortices were the products of one ring, spawned at the Agulhas retroflection about two years earlier. This mother ring had split at the Erica Seamount. Such splitting of Agulhas rings has been inferred for the Vema Seamount as well<sup>465</sup>.

On having split at the Erica Seamount, R<sub>2</sub> moved off rapidly into the South Atlantic Ocean, whereas R<sub>3</sub> got stalled in the retroflection region for the full winter. This explains the estimated extra heat loss responsible for a much cooler thermostad in R<sub>3</sub>, its lower core salinity and considerably higher dissolved oxygen content (see Figure 6.27). These results all point to the substantial changes in the ring configuration that are driven from the sea surface. Interaction with ambient water masses will also eventually diminish such a feature until it is totally absorbed. This will influence the natural lifetime for an Agulhas ring.

#### *Ring durability*

Various estimates of the life-time of Agulhas rings have been made, covering periods from five to ten years<sup>94</sup>. Byrne et al.<sup>95</sup> have calculated the dissipation rates of some Agulhas rings based on both altimetric data and on potential energy estimates of fortuitous measurements of hydrographic anomalies in the South Atlantic that were assumed to be the remnants of Agulhas rings. They have estimated a reduction in surface elevation of rings of 85 per cent over a distance of 5000 km, roughly similar to the potential energy decline over the same distance (Figure 6.28). An e-folding distance of 2600 km<sup>362</sup> to 3000 km<sup>95</sup> seems to apply. These results imply a residence time for Agulhas rings of three to four years<sup>95</sup> in the South Atlantic Ocean.

Using a much more extensive set of sea surface height anomalies as observed by satellite altimetry, other investigators<sup>465</sup> have shown that Agulhas rings dissipate very rapidly in the Cape Basin, losing more than 50 per cent of their sea level expression within four months (Figure 6.29). What is more, more than 40 per cent of all rings thus identified never leave the southeastern Atlantic Ocean, but seem to disintegrate completely in the Cape Basin. This site-specific diffusion of the anomalous characteristics of such rings will have considerable implications for the nature and circulation of the South Atlantic Ocean. It would mean that nearly 70 per cent of the excess heat, salt and anti-cyclonic vorticity leaked from the South Indian Ocean is absorbed exclusively in this particular corner of the South Atlantic Ocean and subsequently has to make its way equatorwards by a different mechanism than being bodily carried by Agulhas rings.

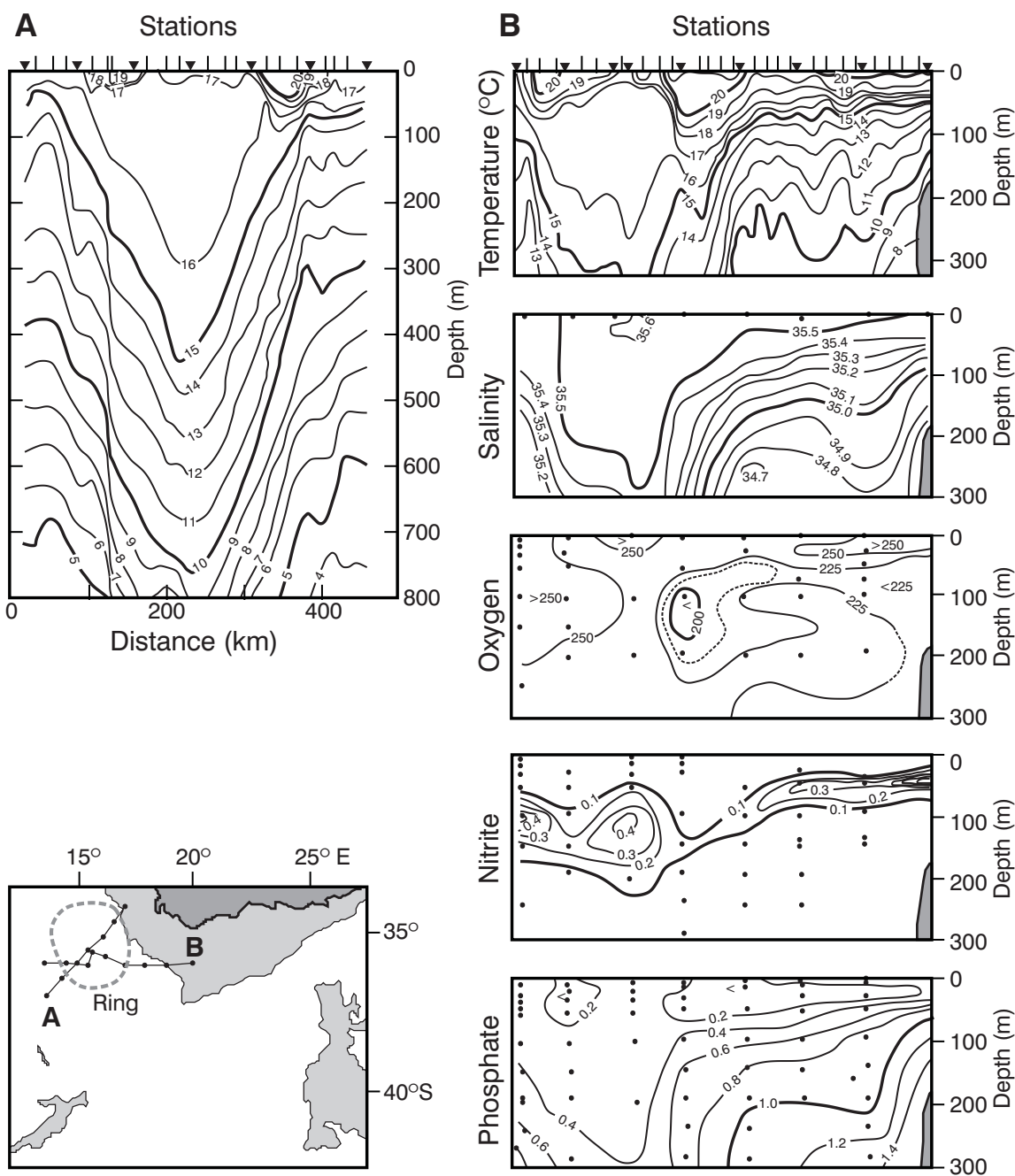


**Figure 6.26.** Two hydrographic sections across an Agulhas ring off Cape Town<sup>230,531</sup>. The locations of the ring and the sections are shown in the locational map. The hydrographic characteristics of such a ring in the upper layers are portrayed. Both nutrients and dissolved oxygen values are in  $\mu\text{mol}/\text{m}^3$ . Water depths shallower than 3000 m are shaded.

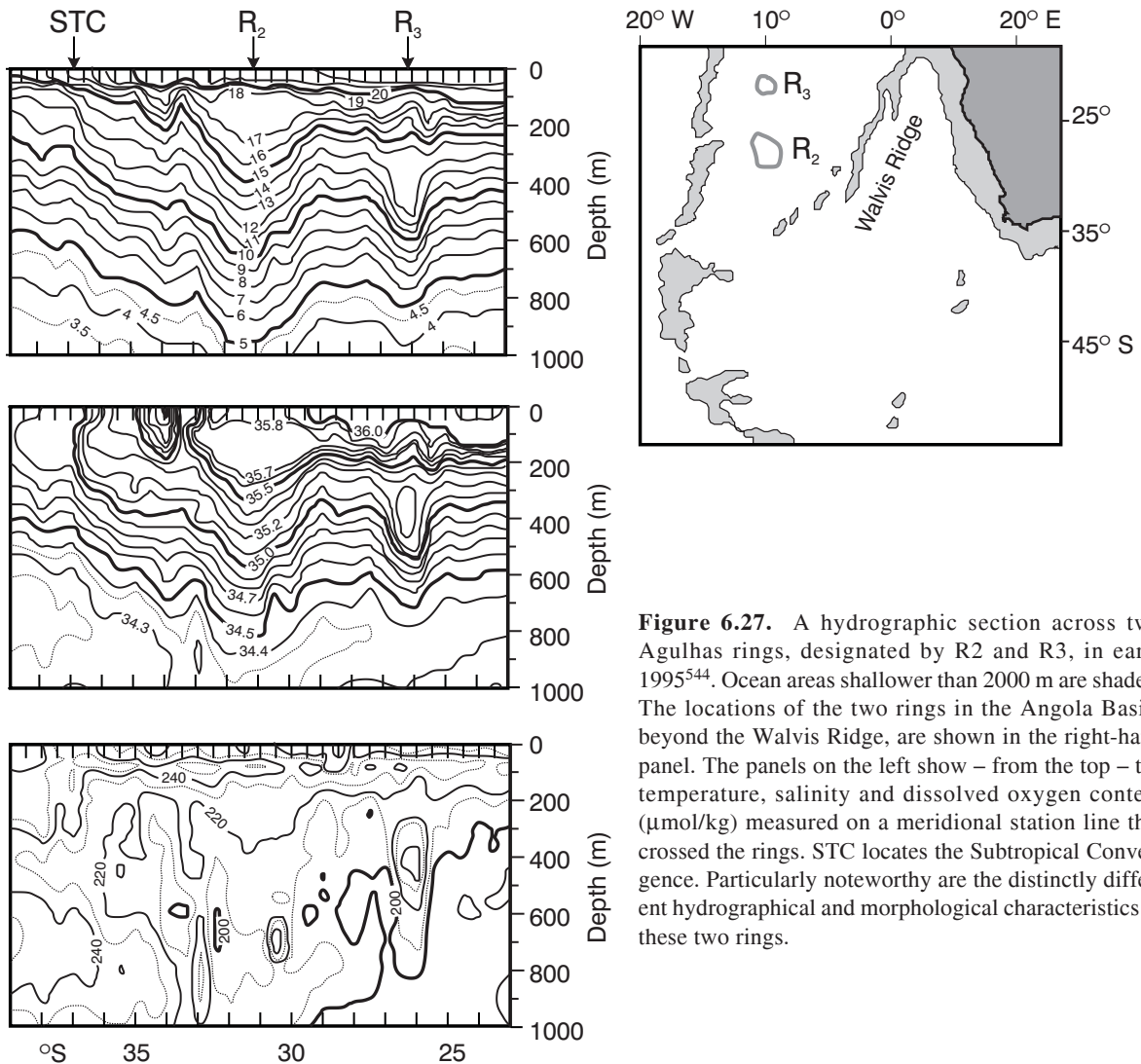


**Figure 6.27.** A hydrographic section across two Agulhas rings, designated by R2 and R3, in early 1995<sup>544</sup>. Ocean areas shallower than 2000 m are shaded. The locations of the two rings in the Angola Basin, beyond the Walvis Ridge, are shown in the right-hand panel. The panels on the left show – from the top – the temperature, salinity and dissolved oxygen content ( $\mu\text{mol/kg}$ ) measured on a meridional station line that crossed the rings. STC locates the Subtropical Convergence. Particularly noteworthy are the distinctly different hydrographical and morphological characteristics of these two rings.

### *Dissipation mechanisms at depth*

An analysis focused on low frequency variability in the southern Agulhas Current system<sup>545</sup> has found strong westward radiation of Rossby waves around  $32^\circ\text{S}$  to the west of South Africa. The energy for this radiation seems to come from Agulhas rings propagating in a north-westward direction in the south-eastern Atlantic Ocean. It has been claimed that there also is substantial local mixing through Stokes' drift between the water masses of the South Atlantic and the propagating disturbances<sup>545</sup>. These are but some of the mechanism that may be responsible for the local degeneration of Agulhas rings. Modelling Agulhas rings with a realistic two-layer representation suggests<sup>546</sup> that the decay scale for rings that make it across the Walvis Ridge agrees roughly with this numerical simulation.

As will emerge below, rings may also split, although this may not of necessity increase their rate of dissipation<sup>770</sup>. It has been assumed for some time that anticyclones cannot split of their own accord<sup>786</sup>. Using a numerical, multilayer, primitive equation model it has been shown<sup>768</sup> that they can indeed not split by barotropic mechanisms alone. However, barotropic instability is a necessary ingredient for splitting to occur. An extensive analysis of the linear stability of ocean rings<sup>767</sup> has found that they are remarkably robust with respect to changes in ring parameters, like diameter, far field stratification and momentum balance. Nevertheless, realistic rings in theory should be quite unstable based on a linear analysis whereas in reality they do survive for long periods. Investigating the mixing of Agulhas rings using an isopycnals ocean model<sup>770</sup> has shown that the leakage of tracers placed within a simulated

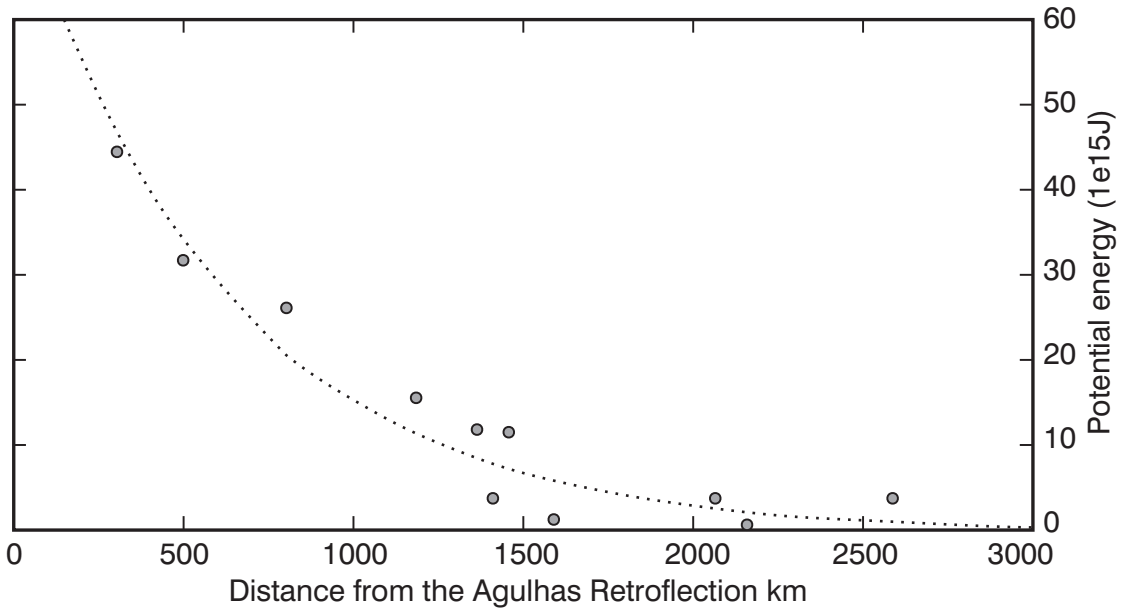


**Figure 6.28.** The available potential energy of eleven separate Agulhas rings related to their distance from the Agulhas retroflection. Potential energy has been estimated from hydrographic measurements across these features<sup>95</sup>.

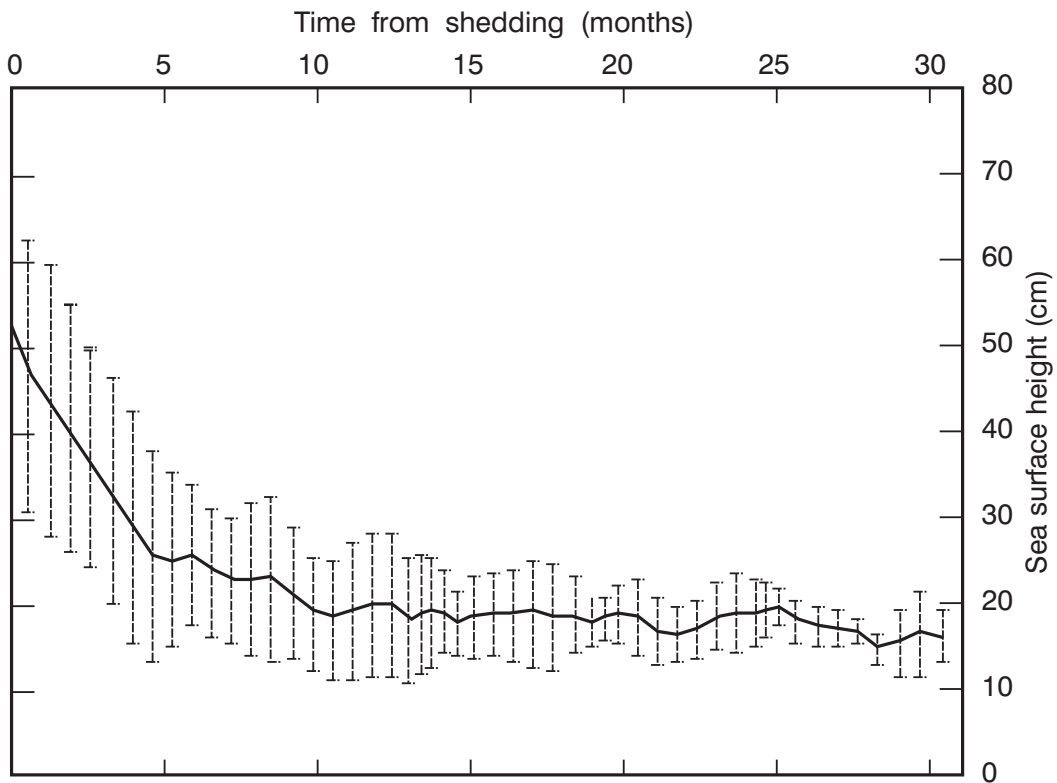


**Figure 6.29.** The mean sea surface height of all Agulhas rings identified by satellite altimetry between 1993 and 1996 that did not dissipate in the Cape Basin<sup>465</sup>. Error bars denote one standard deviation. More than half the value of surface elevations is lost within the first four months of the rings' existence. After ten months the rings seem to dwindle exceedingly slowly.

ring is associated with the formation of filaments (Figure 6.30). These tracers extend down to the permanent thermocline and therefore contain mostly water in the upper layers. Filaments arise largely because of the elongation of the ring. There are no marked differences between the leakage from one coherent ring and from the combined products of a ring that has split<sup>770</sup>. The main variables contributing to the mixing from this modeled ring are its initial deformation and self-advection. The loss of tracer from a ring shows that in the first months of its existence up to 40 per cent of the water in the ring can be mixed with the environment; in deeper layers up to 90 per cent. These theoretical results agree well with observations<sup>465</sup>.

However, as has been mentioned before, Agulhas rings undergo their greatest dissipation while they are in the southern Cape Basin<sup>465</sup>, close to their spawning region. This region has therefore been called the Cape Cauldron<sup>628</sup> since on many occasions it is densely populated by a large number of Agulhas rings and cyclones, both with a range of dimensions. This means that few Agulhas rings decay in isolation, at least not before they cross the Walvis Ridge. Comparing theory with actual observations of the decay of an Agulhas ring would therefore be very valuable (Figure 6.31). A ring, called Astrid, was observed hydrographically a number of times<sup>650</sup>, showing that its demise corresponded well with previous observations<sup>465</sup> using only sea surface

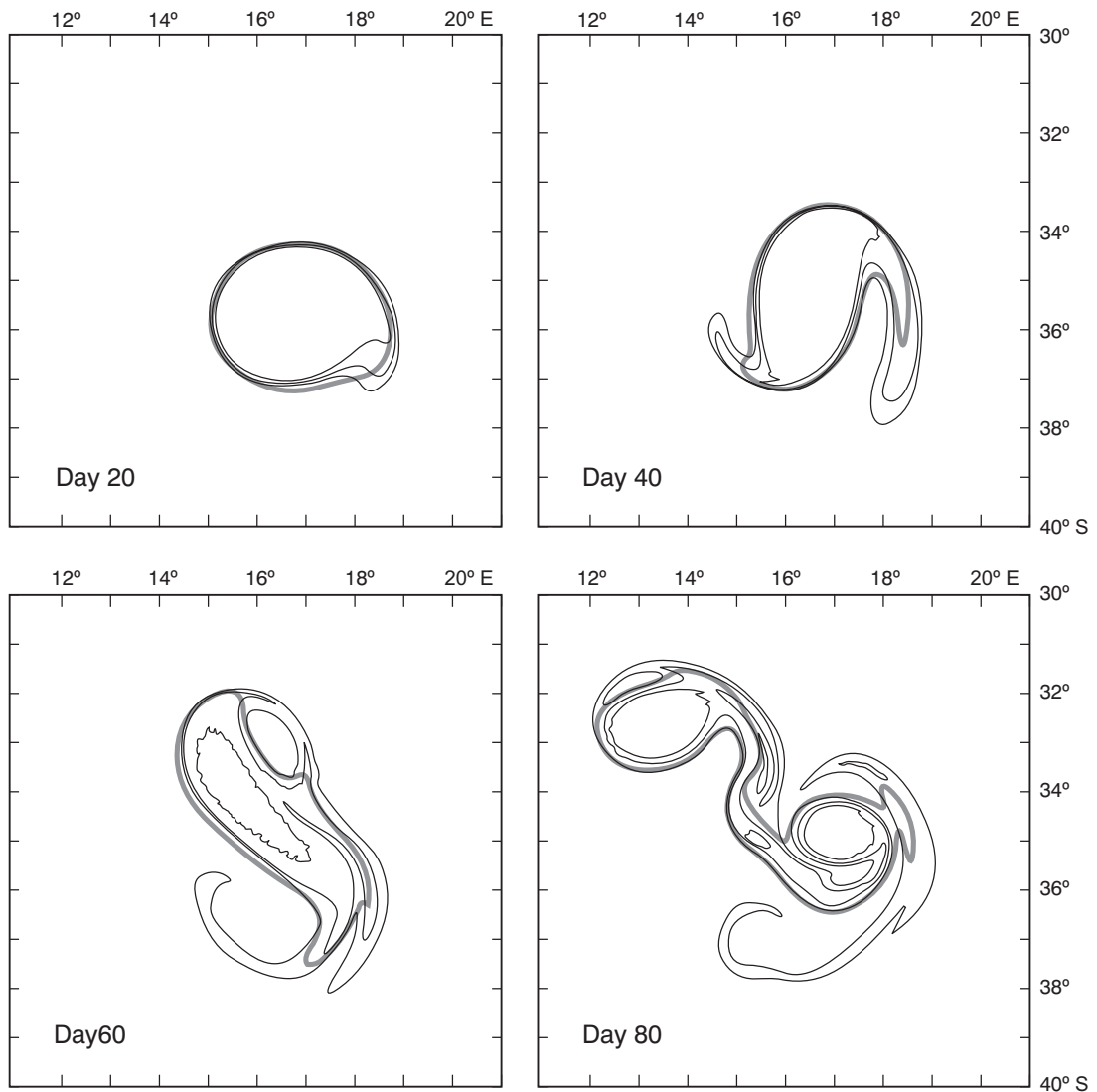


**Figure 6.30.** The development of the concentration of a tracer in a modelled Agulhas ring as well as the boundary of such a ring<sup>770</sup>. The ring boundary is shown by a thick line.

height anomalies. It decayed most rapidly shortly after being shed. The early evolution of this ring is well predicted by a linear stability analysis. The modelled ring features an energy conversion from its barotropic to its baroclinic components and may eventually split.

Following an individual ring over a period of seven months<sup>784</sup> has shown that its available heat and salt anomaly were reduced by about 30 per cent over this period; its available potential energy by about 70 per cent. It is significant to note that one third of this loss was due to changes at intermediate depth (i.e. between 800 m to 1600 m). This latter process was exemplified by the fact that RAFOS floats placed in this particular ring were detrained after two revolutions in the ring. The vigorous water exchanges at this depth were an underlying cause for the high variability of hydrographic characteristics inside and outside the ring. This is exemplified in Figure 6.32. The temperature and salinity fields at the edge of a well-surveyed Agulhas ring<sup>785</sup> show that inside the ring the distributions of both variables are fairly well-behaved, whereas at the borders there are a variety of disturbances including many boluses of warm water and lenses of saline water. These small scale perturbations to the thermohaline field indicate vigorous mixing at the ring edges. To date these mixing processes at depth have not been quantified. Processes in the upper layers are even more important.

#### *Dissipation mechanisms at the sea surface*

As mentioned elsewhere, the loss of heat from Agulhas rings to the atmosphere is an important consideration in the processes involved in their dissipation, particularly in newly formed rings. In the detailed study<sup>785</sup> of one ring in particular it was shown that the loss of heat to the atmosphere was even severe during summer ( $54 \text{ W/m}^2$ ), mainly due to the large mean turbulent flux of latent heat ( $180 \text{ W/m}^2$ ). Clearly the heat flux to the atmosphere will show considerable short term variations as different atmospheric systems pass overhead. This has been addressed in a preliminary way<sup>700</sup> by investigating the crossing of weather systems over components of the Agulhas system a number of times. Under an anti-cyclonic atmospheric circulation (i.e. easterly flow) the total turbulent heat flux to the atmosphere over the retroflexion was  $170 \text{ W/m}^2$  with a maximum at any one time of  $360 \text{ W/m}^2$ . The latent heat flux made the largest contribution. During the passage of a cold atmospheric front, the total turbulent heat flux remained more or less the same, but the maximum values increased to  $500 \text{ W/m}^2$ . The last synoptic atmospheric system studied was a cold air outbreak during a

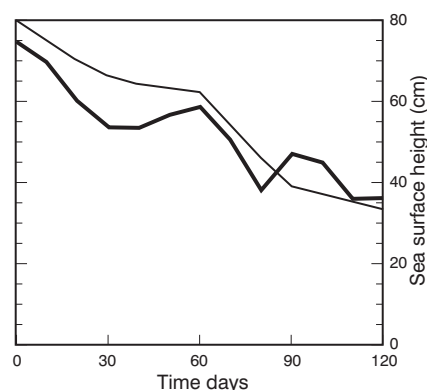


**Figure 6.31.** Decay of an Agulhas ring as a function of time<sup>766</sup>. The thick line shows the modelled decrease in sea surface height; the thin line the observed decrease.

post-frontal southerly flow. The mean heat flux increased to  $420 \text{ W/m}^2$  with maximum values reaching  $630 \text{ W/m}^2$ . In this case the effect on the atmospheric boundary layer was substantial<sup>700</sup>. It increased from a convective thermal, internal boundary layer of 500 m height to a well-mixed layer of 900 m. The effect of this heat loss on individual Agulhas rings naturally is substantial.

In the study of two Agulhas rings<sup>544</sup> discussed before, it was found that far from their spawning grounds they showed the disparate structure of a ring that had been formed in summer and that had moved rapidly equatorward, into warmer atmospheric conditions, compared to one that had been formed in winter and that had remained near to the point of formation. Their interaction with the atmosphere in early stages of their development therefore had been crucial. Both had substantial thermostads, but these thermostads had different temperatures and were found at distinctly different depths. (See Figure 6.27.) The effect of winter cooling on one particular ring over a period of seven months<sup>784</sup> has indicated the changes to the upper layers that can be expected. In March the temperatures at the sea surface exceeded  $19^\circ \text{C}$ , but after the winter there was no water warmer than  $17^\circ \text{C}$ . During the same period the thickness of the mixed layer had increased two-fold. It is clear that this increase in Agulhas rings is due to the convective motion induced by cooling at the sea surface, to increased turbulence induced by strong winter winds and due to increases in the salinity of the surface layers due to evaporation. The latter process has not been quantified in any reliable way. In the case of the ring observed seven months apart<sup>784</sup>, and discussed above, the salinity of the upper 300 m had in fact – unexpectedly – decreased. During this period, the depths of all isotherms had decreased, suggesting mixing with

the surrounding waters. An attempt to model<sup>757</sup> the impact of cooling on the water mass exchanges of Agulhas rings has produced some interesting results.

A bowl shaped ring was simulated with a diameter of 280 km. Below 800 m depth the Agulhas ring in this model rapidly loses its original water mass. This result agrees substantially with that found by studying the motion of RAFOS floats placed in such rings<sup>625</sup> and

with hydrographic observations<sup>785</sup> in rings. In this model strong surface cooling generates a shallow overturning cell with radially outward flow near the surface and a compensating flow at depth. As a result the surface water does not remain trapped in the core of the ring, but exchanges water with the surrounding waters. The overturning cell amplifies this water mass exchange by constantly bringing new water to the edge of the ring where it gets the opportunity to mix with ambient waters.

The question how rapidly rings undergoing all these mixing processes will be absorbed by the ambient water masses may to some extent depend on the trajectories they follow.

### Ring pathways

Drifting buoys have suggested an initial drift rate away from the inception region of 5 to 8 km/day<sup>94</sup>. However, it is now clear that Agulhas rings may stall, change direction, split or speed up during their progression across the South Atlantic Ocean, particularly in the Cape Basin. Whatever the initial drift rate, it has been observed that a number of rings tend to remain close to the retroflexion for a considerable time. They have, for instance, been observed to be quite persistent southwest of Cape Town<sup>444</sup> (e.g. Figure 6.26). The presence of Agulhas rings in this particular spot is of added importance because rings situated here will enhance the shelf-edge current as well as the rapid advection of Agulhas filaments into the South Atlantic<sup>92</sup>.

In both satellite imagery<sup>61</sup> as well as research cruises<sup>455</sup> up to nine rings and eddies have been observed at the same time clustered around the Agulhas retroflexion. Hydrographic data show their further movements (Figure 6.19), although to date only three rings has been visited more than once<sup>543,784-5</sup>. Other types of information therefore have to be employed to evaluate the movement of rings.

Satellite altimetry has proven to be an exceptionally useful tool<sup>70,354,543</sup> to track Agulhas rings, particularly since they have strong signals in sea level elevation<sup>95,464</sup> and drift through a comparatively quiescent region<sup>498</sup>. Comparison between altimetric observations and the measurements from moored current meters and inverted echo sounders has shown that in the southeastern Atlantic Ocean anomalies of the sea surface are significantly related to the thermocline depth and to the dynamic height of the sea surface<sup>547</sup>. Considerable work has been done to refine the analysis<sup>74</sup> and interpretation of altimetric data in the region, including data assimilation into quasi-geostrophic models<sup>548</sup>.

Initial investigations<sup>73</sup> using altimetric data have shown rates of translation of 4–8 cm/s, and even<sup>517</sup> up

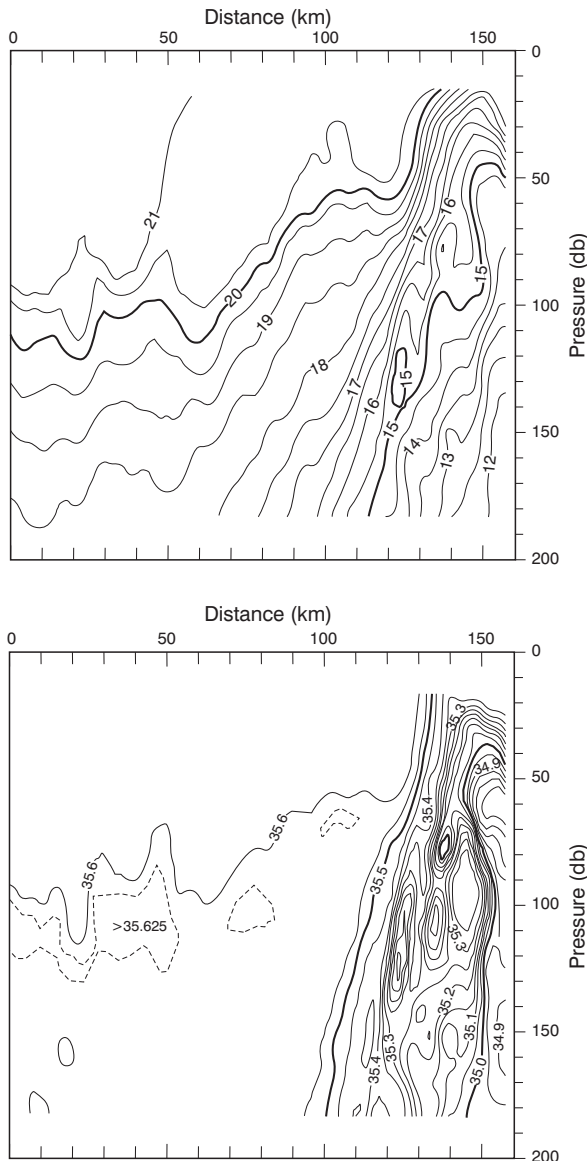


**Figure 6.32.** Hydrographic disturbances along the edge of a relatively new Agulhas ring<sup>785</sup>. These closely spaced observations were made with a Scanfish undulator resolving the structure to a lateral accuracy of 1.8 km. The upper panel shows the thermal structure; the lower the salinity distribution.

to 16 cm/s, in a general north-westerly direction for the anomalies assumed to be Agulhas rings. Other estimates<sup>362</sup> are 3–7 cm/s. Propagation rates based on RAFOS floats<sup>783</sup> give values of 5.5 to 6.5 cm/s. Modelling studies<sup>546</sup> suggest a rate of about 9 km/day and show that ring trajectories undergo a transition from a turbulent character in the Cape Basin to a much more steady propagation in the rest of the South Atlantic<sup>760</sup>, but that this is due to ring decay and not to the topography being crossed. The propagation speeds of those rings that are durable and those that eventually cross the Walvis Ridge show no systematic seasonal variations<sup>712</sup> in their speed of translation. A detailed study of one particular ring<sup>784</sup> for a period of seven months has shown that its north-westerly progression varied between 3 km/day to 20 km/day, possible due to its interaction with other rings and cyclones along its path.

Further studies using altimetry have been able to track anomalies of sea surface height over the greater width of the South Atlantic and were able to positively identify some of these anomalies as Agulhas rings at sea<sup>464,544</sup>. Van Ballegooyen et al.<sup>129</sup> have, for instance, been able to establish a very close correspondence between the hydrographic observations of individual Agulhas rings and their altimetric signatures. During the two-year period of their investigation rings migrated no farther than 1500 km from the Agulhas retroflection.

A similar study<sup>95</sup>, for a period of three years (Figure 6.33), has shown inferred Agulhas rings to advect across the South Atlantic Ocean slightly to the left of the mean flow. None crossed the South Atlantic Ocean north of a latitude of 25° S. In a few instances Agulhas rings have been tracked all the way to the coast of Brazil; in one instance<sup>754</sup> there is evidence that a ring was subsequently carried poleward by the Brazil Current over a distance of at least 10° of latitude. Rings probably are advected with the ambient water movement<sup>807</sup>, but also exhibit a substantial degree of self-steering due to their own internal dynamics. Calculations have shown that only about 15 per cent of the observed drift of rings is self-induced; advection by the background flow therefore dominating the rate at which they translate. Comparing the movement of floats placed in Agulhas rings, at intermediate depths, with those placed outside rings and therefore in the Benguela Current, Richardson et al.<sup>781</sup> have been able to establish the rate at which rings move through the background waters. The background speeds were about 2 km/day; those of Agulhas rings roughly 6 km/day. This means that rings have a self-induced movement at 750 m of about 4 km/day. The background speed may have its origin in the Benguela Current<sup>807</sup>.

Sea height anomalies south of 45° S in general migrate eastwards<sup>362</sup>. Anomalies that migrate eastwards originate at 40° S as far west as 20° W longitude<sup>95</sup>. In all probability these latter ones are not Agulhas rings, but mesoscale eddies shed at the Subtropical Convergence in the South Atlantic<sup>549</sup>, or by the South Atlantic Current<sup>83</sup>. The furthest westward Agulhas retroflection observed to date, or Agulhas ring at its inception, has been at 8° E longitude<sup>512</sup>. The other mesoscale features found in the Cape Basin, cyclones, have been shown to migrate roughly at right angles to the mean trajectory of Agulhas rings<sup>628</sup>, but since they seem to have a much shorter lifetime have not been followed farther than the confines of the Cape Basin. As mentioned in another context, this cross-traffic of anti-cyclones and cyclones seem to be a characteristic of a number of west coasts of continents, including North America and Australia<sup>780</sup>. In their subsequent journey across the southern Atlantic Ocean Agulhas rings have to cross a number of bottom ridges. Since the rings extend to great depths, it is valid to examine the influence of these bathymetric obstacles on their behaviour.

#### *Interaction with bottom ridges*

The influence that distinctive features of the bottom topography may have on the paths taken by Agulhas rings across the South Atlantic is not immediately obvious. In many models<sup>764,758</sup> the effect of the bathymetry is evident, but the magnitude of this effect differs substantially between individual models<sup>763</sup>. One of the major bottom features that rings will have to cross, in order to follow the streamlines of the subtropical gyre, is the Walvis Ridge that lies from about 20° S latitude at the west African coast in a south-westward direction (viz. Figure 6.27). It is interesting to note that of 30 RAFOS floats placed<sup>781</sup> at a depth of roughly 750 m in the Cape Basin, virtually all that crossed the Walvis Ridge did so associated with the passage of Agulhas rings or Cape Basin cyclones. The crossing of the Walvis Ridge by Agulhas rings has been shown to occur irregularly and aperiodically<sup>712</sup>. There is evidence that most rings slow down on traversing this feature<sup>95</sup>, but there are also some that show signs of drift acceleration<sup>73</sup>. Initial translational speeds of 12 km/day have been observed to decrease to 6 to 7 km/day over the ridge<sup>519</sup>.

Schouten et al.<sup>465</sup> have demonstrated that once Agulhas rings have been slowed down on crossing the Walvis Ridge, they never regain their previous propagational speed, but remain sluggish in their subsequent movement. There also is greater directional uniformity amongst rings that have successfully crossed this

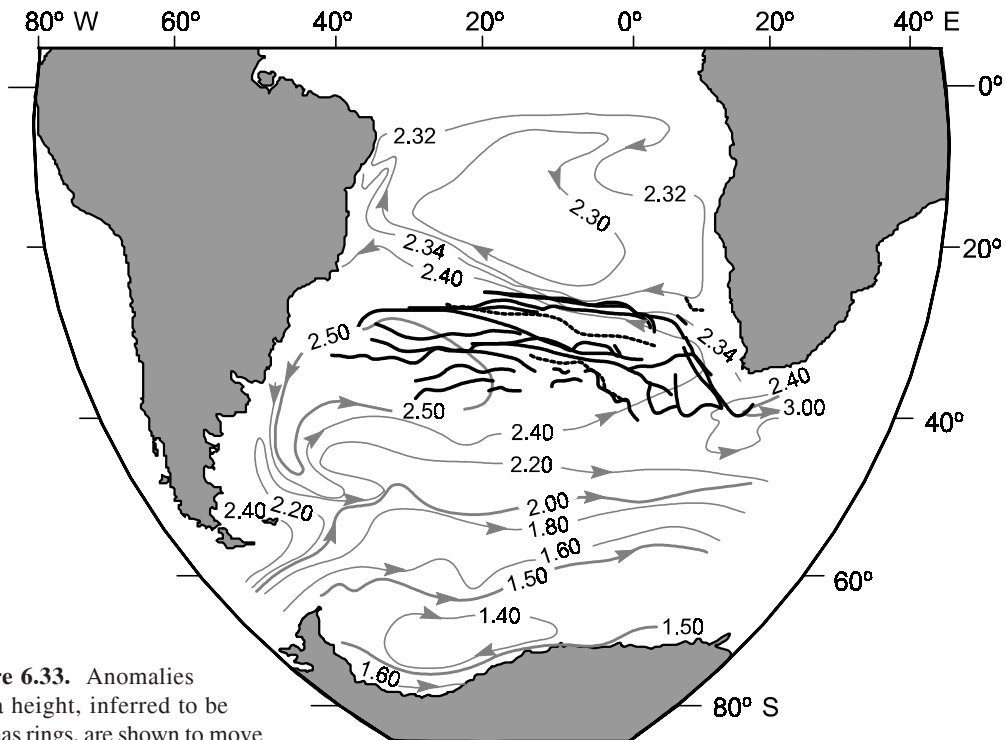


**Figure 6.33.** Anomalies of sea height, inferred to be Agulhas rings, are shown to move westwards. Data used for this study<sup>95</sup> were altimetric measurements from the Geosat exact repeat mission between 1986 to 1989. Drift tracks are superimposed on the general direction of movement from the steric anomaly at 500 dbar<sup>195</sup>. The rings exhibit a drift tendency slightly to the south of the averaged background flow.

hurdle. Their rate of decay moreover drops markedly on having crossed the Walvis Ridge, but this may be a function of their age (viz. Figure 6.29) and may not only be due to interaction with the ridge.

Modelling Agulhas rings with realistic dimensions and characteristics<sup>546</sup> shows that they may indeed slow down, stall or even be destroyed at the Walvis Ridge, depending on their configurations. Rings with sufficient initial vertical shear can cross the ridge, but ones that are nearly barotropic cannot. In general, baroclinic rings modelled in this manner all slow down to a translational speed of 4 km/day on crossing the ridge, adjusting their vertical structure and intensifying towards the same final, ridge-crossing state<sup>546</sup>. This particular model predicts that the surface elevation of rings will increase measurably on crossing the ridge. This has been observed in some, but not in all, rings in nature. According to this model, the Walvis Ridge may therefore act as a substantial filter, allowing only rings with vertical characteristics under a certain threshold to pass. Other models<sup>760</sup> do not indicate any such function for the Walvis Ridge. A different model<sup>550</sup>, using a two-layer ocean at rest and with Gaussian-shaped anoma-

lies, shows that the ridge in stead affects the drift direction of deep-reaching eddies.

On reaching the upslope of the ridge they are forced in a more equatorial direction. This has been seen in some, but again not in all, altimetric trajectories of such rings<sup>465</sup>. Eddy permitting numerical simulations have shown that the trajectories of Agulhas rings that are intensified in their upper layers are changed by the Walvis Ridge to a more westerly direction. The deep compensation generated by the ridge in the model causes an energy loss of about 30 per cent. However, only modelled eddies with a substantial dynamic signal in the lower layer are influenced by the bottom topography. In nature rings have been observed predominantly to cross the ridge where the water is deep<sup>95,465</sup>, but this may be the result of the general background advection (Figure 6.33) and not directly due to topographical steering. The waters of the extension of the Benguela Current may move predominantly through these gaps in the Walvis Ridge, carrying Agulhas rings with them. The transits of Agulhas rings cross not only bottom ridges, but seamounts as well.

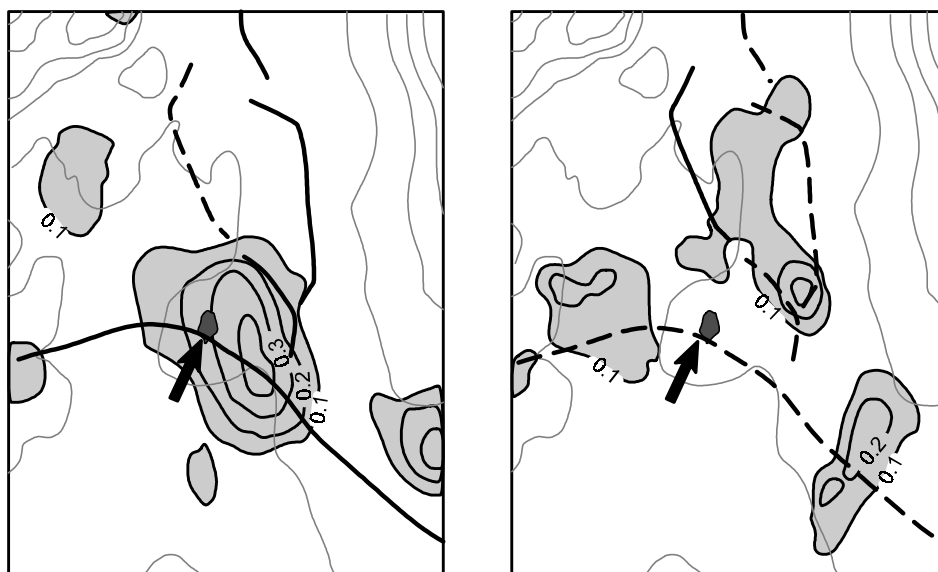


**Figure 6.34.** The splitting of an Agulhas ring on crossing the Vema Seamount in the Cape Basin of the south-eastern Atlantic Ocean<sup>465</sup> in October 1996. The time difference between the two portrayals is six weeks. The location of the seamount is indicated by an arrow; the sea surface heights are in metre and are derived from altimetric information. Background isobaths slope from left to right. Thick lines denote the trajectory of the single ring on approaching the Vema Seamount and the paths of the collision products subsequently.

#### *Ring interaction with seamounts*

A much less geographically prominent feature of the bottom topography in the Cape Basin is the Vema Seamount. This peak rises from an otherwise deep and unremarkable abyssal plain to a reported depth of less than 32 m below the sea surface and would, at first glance, not constitute an insurmountable obstacle to an Agulhas ring. Nonetheless, there is growing evidence from satellite altimetry<sup>465</sup> that rings that come into contact with this oceanic pinnacle have a tendency to split into two or more smaller rings (Figure 6.34). This is similar to the sequence of events that has been detected at the Erica Seamount<sup>544</sup>.

Theoretical investigations<sup>769,771</sup> have shown that the advection by a ring of deep fluid parcels generates deep anti-cyclonic and cyclonic circulations near the bathymetry. These circulations exert a strong shear on the upper layers which causes an erosion of the ring by filamentation or, sometimes, the subdivision of the ring. Under certain circumstances<sup>771</sup> an eddy, such as a ring, may be scattered by a topographic obstacle.

The products of a ring-seamount collision subsequently take different routes. Recent high-resolution modelling<sup>325</sup> has suggested a fork in the trajectories for Agulhas rings in the general vicinity of the Vema Seamount, with two distinctly different pathways downstream. This modelling result therefore is consistent

with what has been observed from the movement of positive anomalies of sea surface height in this ocean region<sup>465</sup>. It also clearly demarcates the wide-ranging influence that the passage of Agulhas rings may possibly have on the background current of the south-western Atlantic Ocean.

#### *The Benguela Current*

To recapitulate briefly what has been dealt with more thoroughly above, the Benguela Current forms the eastern and part of the northern component of the wind-driven, anti-cyclonic gyre of the South Atlantic Ocean<sup>779</sup>. It starts in the south-eastern corner of the Cape Basin and reaches the South American coast at about 18° S. The presence of Agulhas rings in the southern Benguela Current, south of 30° S latitude, has a profound influence on the nature of this current. Whereas the mean flow next to the African continent is more invariant, the western part is dominated by the transient effects of passing rings<sup>519</sup>. Observations of equatorward transport show strong correlations between increases in this transport and Agulhas water influx via rings. The primary inter-annual variability in the transport of the south-eastern part of the Benguela Current therefore derives almost totally from the passage of Agulhas rings and variations in the inflow from the South Atlantic subtropical gyre<sup>547</sup>. In the upper

1000 m the annual contribution to the volume flux of the Benguela by the Agulhas Current varies between 10 per cent and 50 per cent. Over a period of five years<sup>782</sup> the contribution from the South Atlantic Ocean to the Benguela is 58 per cent, that of the Indian Ocean about 30 per cent. However, at intermediate depths the greater part of the waters in the Cape Basin is supplied from the Indian Ocean<sup>628</sup> with minor direct inflow from the Atlantic Ocean. Red Sea Water contributes<sup>775</sup> about 6 per cent. More about this follows below.

An investigation<sup>772</sup> combining sea surface height and sea surface temperature measurements has suggested that a convoluted jet is found in the Benguela Current, probably separating the coastal upwelled water from the deep-sea waters. This jet shows seasonal behaviour, being stronger in summer. This strengthening is due to an increase in coastal upwelling, but also due to an increased injection of Agulhas ring water on the offshore side of the jet. One should at this stage perhaps remind oneself that the movement of these Agulhas rings is of course highly unusual. No other products of a western boundary current are known to move past such a well-developed coastal upwelling regime<sup>551-3</sup>.

#### *Agulhas rings and coastal upwelling*

The Benguela upwelling system of the South East Atlantic Ocean extends from about 15° S to 35° S latitude<sup>551</sup>. Its northern border is the Angola/Benguela front<sup>554</sup>, while the wind-driven upwelling on the Agulhas Bank<sup>473</sup> may be considered to be its southern extremity. This upwelling system has a central point where it is most intense and durable, at Lüderitz, and is otherwise concentrated in a number of relatively distinct upwelling cells<sup>470</sup>. The frequency of upwelling at these cells decreases both north- and southwards with distance from Lüderitz, while the southernmost cells are totally seasonally driven.

Notwithstanding this along-coast variability in upwelling intensity, the instantaneous upwelling expression along this coastline is one of a contiguous strip of cold water at the sea surface that overlies the continental shelf, and a zone about twice as wide that is populated by a range of wisps of cold surface water, upwelling filaments, vortex dipoles<sup>555</sup> and small eddies<sup>556-7</sup>. Some of these mesoscale frontal features seem to occur at random while others<sup>557</sup> seem to be locked to the morphology of the coastline. Some of the upwelling filaments can, probably by a combination of extreme offshore berg winds and entrainment in offshore eddies, be made to extend to distances of 1000 km offshore<sup>558</sup>. This may bring them into the path of passing Agulhas rings.

At least one such interaction between an Agulhas ring and an upwelling filament has been investigated in detail<sup>559-60</sup>. A pioneering investigation of an upwelling filament off the south-western coast of Africa by Shillington et al.<sup>561</sup> has suggested the presence of a warm eddy to the south of this particular filament at the time, the former possibly of Agulhas origin. A subsequent set of cruises, to follow an Agulhas ring in its northward movement along the coastline<sup>543</sup>, have established that on one occasion this particular ring was encircled by a filament of cold surface water (e.g. Figure 6.35). Temperature–salinity characteristics of the filament showed it to be nearly pure upwelling water<sup>559</sup>. It was about 50 km wide, 100 m deep and, when entrained around the full circumference of the ring, would have had a length of 1000 km.

It has been suggested<sup>560</sup> that removing this amount of water from the upwelling front could have a profound effect on the biota of the upwelling regime and could, on this particular occasion, have been partially responsible for depressing the anchovy year-class of that year and hence the recruit biomass available for the following year. An eddy-permitting, large-scale model of the whole upwelling system<sup>562</sup> has simulated cases of filament-ring interaction, demonstrating that under the appropriate conditions this may be an inherent part of the system. Subsequent hydrographic studies in the region<sup>563</sup> have produced circumstantial evidence that Agulhas rings draw upwelled water as well as tropical Atlantic Ocean water, found over the upper continental slope, into the ocean interior. It has in fact been suggested that Agulhas rings are the primary removal mechanism for the low oxygen water found on the slope<sup>563</sup>. This process can probably only come about if an Agulhas ring during its equatorward passage reaches the upwelling front itself.

Filaments of water blown offshore by extreme wind events would be lost to the upwelling system irrespective of whether they get entrained in Agulhas rings far offshore<sup>558</sup> or not. The frequency of Agulhas trajectories lying closer inshore would therefore be a prime factor in ascertaining how important Agulhas rings are in this exchange process compared to wind events. Altimetric studies of such trajectories<sup>95,362,465</sup> to date suggest that an Agulhas ring conjunction with the active upwelling front may be a very rare event. These unusual incidents may nonetheless have a significant local effect on a fragile fish recruitment process. The continuous creation of warm Agulhas rings and their steady movement into the South Atlantic, forming the basis of the inter-basin exchange of water south of Africa, has, by contrast, effects on a much larger scale.

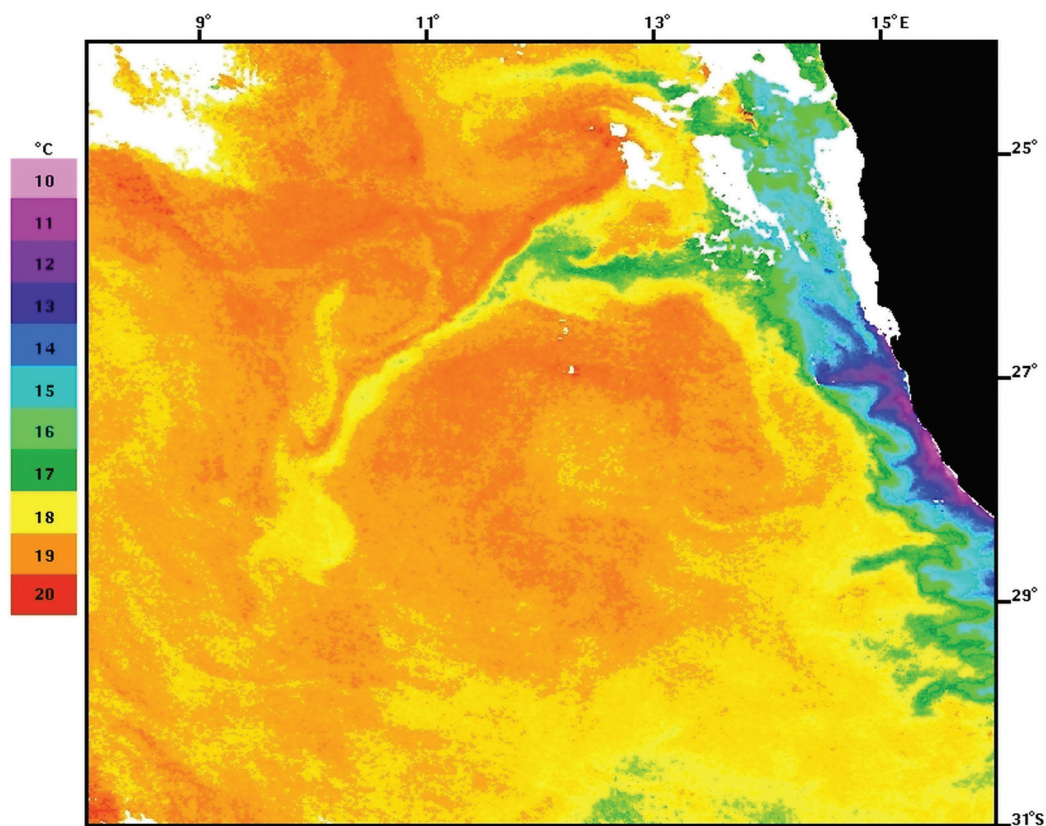


**Figure 6.35.** A satellite image showing a cold filament, from the coastal upwelling system, being wrapped around a passing Agulhas ring<sup>559</sup>. Note the low temperatures (blue-green) in the upwelling regime off the south-west coast of Africa. These sea surface temperatures are from the radiometer on board the NOAA 17 satellite for 4 December 2005.

### Inter-ocean exchange at the Agulhas retroflection

As discussed previously, the Agulhas Current may be a key link in the global thermohaline circulation cell<sup>65,68</sup>. Since leakage of its water into the South Atlantic is the mechanism by which this process is maintained here, it is vitally important to establish how much water is exchanged, how frequently and what the various factors are that may influence, or control, this process<sup>413</sup>.

As we have seen, the major process in this inter-ocean exchange south of Africa is the shedding of Agulhas rings<sup>66</sup>. There may also be some direct flux of Indian Ocean water into the Atlantic. Secondary processes are the northward advection of Agulhas filaments<sup>92</sup> (Figure 5.10), and the movement of Agulhas Bank water.

#### *Direct leakage*

The geostrophic estimates of the direct volume flux of water past the tip of Africa<sup>516</sup> is summarised in Table 6.4. The estimates vary from  $4 \times 10^6$  m<sup>3</sup>/s to  $10 \times 10^6$  m<sup>3</sup>/s.

Data sets on which these estimates are based are from separate cruises and therefore independent. The manner in which they have been calculated – and the reference depths used for the calculations – are not the same, making comparisons difficult. The contribution to the inter-ocean flux by water from the Agulhas Bank has been inadequately studied to make any substantive pronouncements at all. Gordon et al.<sup>230</sup> have estimated it to be about  $10 \times 10^6$  m<sup>3</sup>/s, relative to 1500 decibar, on one occasion. The geographic distribution of observations of water with a shallow oxygen minimum<sup>231</sup>, that is usually associated with water from the Agulhas Current core (viz. Figure 6.14), shows such water as extending as far as 32° S along the west coast of South Africa.

A number of studies<sup>773–5</sup> have been undertaken to try to establish how much water and of what water type is exchanged south of Africa. Using compendiums of hydrographic data, these studies do not differentiate between the mechanisms that may have caused the inter-ocean transfers, they only quantify the end results. You<sup>774</sup> has, for instance, investigated the origin of

Antarctic Intermediate Water in the South Atlantic Ocean and come to the conclusion that of this type the water originating from the Drake Passage is dominant. Antarctic Intermediate Water from the Indian Ocean comprises 30–60 per cent of that originating in the South Pacific Ocean in the subtropical latitudes of the South Atlantic Ocean. The meridional volume transport of Antarctic Intermediate Water in these subtropical latitudes consists of 64 per cent water from the Drake Passage, 36 per cent from south of Africa. The former extends to the south-western Indian Ocean in a continuous band<sup>775</sup> whereas the Indian Ocean source waters spread to the southeastern South Atlantic mostly in a patchy distribution, perhaps indicating the intermittency of their generation. The volume transport of Antarctic Intermediate Water south of Africa consists of water from the Drake Passage (63 per cent), from the South Indian Ocean (16 per cent), from the Indonesian Seas (10 per cent) and from the Red Sea (12 per cent). Only a small proportion of Antarctic Intermediate Water from the Drake Passage that moves into the Indian Ocean is eventually returned westward<sup>775</sup>.

One known mechanism for interocean exchange south of Africa, albeit it not the major one, is the movement of filaments drawn from the core of the Agulhas Current.

#### *Agulhas filaments*

Agulhas filaments are advected past the western edge of the Agulhas Bank (viz. Figure 5.10), carry only surface water from the upper 50 m of the Agulhas Current<sup>92</sup> and are often entrained in the perimeter of passing Agulhas rings. By being captured in the rim of Agulhas rings they may be replenishing the rapidly cooling surface layers of such features, increasing their surface salinity and enhancing convective overturning in these ageing rings. Agulhas filaments presumably carry little net heat into the South Atlantic Ocean, all

excess heat being rapidly lost to the colder overlying atmosphere<sup>121</sup>. This may be surmised from the occasional presence of cumulus cloud bands above these filaments<sup>143</sup>, suggesting substantial fluxes of heat and moisture to the atmosphere. Agulhas filaments are, nonetheless, estimated as contributing an annual net flux of 3 to  $9 \times 10^{12}$  kg salt, or 9 per cent of that due to Agulhas rings. The contribution to inter-ocean exchange by Agulhas filaments is therefore small, but not entirely negligible. Such surface water exchange may occasionally increase substantially<sup>439</sup> through interaction with Agulhas rings and under wind conditions conducive to northward advection<sup>564</sup>.

#### *Leakage by Agulhas rings*

Nevertheless, the major component of the inter-ocean exchange of heat and salt south of Africa, in the thermocline and surface waters, seems to be due to Agulhas rings<sup>413,516</sup>. Using a box model informed by measurements from an array of inverted echo sounders, Garzoli and Goñi<sup>782</sup> have demonstrated the sources of water crossing the Cape Basin at 30° S. A total of  $12 \times 10^6$  m<sup>3</sup>/s water in the upper 1000 m moves across this line. This is an average over five years. Of this  $6 \times 10^6$  m<sup>3</sup>/s comes from the South Atlantic, possibly largely from the South Atlantic Current,  $2 \times 10^6$  m<sup>3</sup>/s directly from the South Indian Ocean and the rest ( $3 \times 10^6$  m<sup>3</sup>/s) is a mixture of Agulhas water in filamentous form and tropical Atlantic water originating from the north. The ratios are very variable. During 1995 more than 50 per cent of the volume transport came from the Indian Ocean; in 1996 it was barely 10 per cent. This incorporation of water from the north has also been shown from the drift tracks of floats at intermediate depths<sup>781</sup>. Near 30° S floats placed east of the Walvis Ridge tended to move southward before turning northwestward to join the Benguela Current.

**Table 6.4.** Geostrophic estimates of the direct flux, i.e. excluding Agulhas rings or filaments, of Indian Ocean water into the South Atlantic<sup>516</sup> in  $10^6$  m<sup>3</sup>/s.

Authors	Flux	Reference	Date
Harris and Van Foreest (1978) <sup>92</sup>	5	1100 db	March 1969
Gordon et al. (1987) <sup>230</sup>	10	1500 db	November–December 1983
Bennett (1988) <sup>533</sup>	6.3	T > 8 °C	November–December 1983
	2.8	T > 8 °C	February–March 1985
Stramma and Peterson (1990) <sup>83</sup>	8	1000 m	November 1983
Gordon et al. (1992) <sup>67</sup>	10	T > 9 °C	December 1989–January 1990
	15	1500 db	December 1989–January 1990
Garzoli et al. (1997) <sup>547</sup>	4	1000 db	September 1992–December 1995

An estimate of the inter-ocean exchange brought about by Agulhas rings that is probably the most accurate to date, being based on the largest number of actual hydrographically measured rings<sup>129</sup>, gives a volume flux of  $6.2 \times 10^6 \text{ m}^3/\text{s}$  for water warmer than  $10^\circ\text{C}$  and  $7.3 \times 10^6 \text{ m}^3/\text{s}$  for water warmer than  $8^\circ\text{C}$ . A heat flux by Agulhas rings of 0.945 PW and a salt flux of  $78 \times 10^{12} \text{ kg/year}$  have thus been calculated. Estimates of the average excess of heat and salt contained in an Agulhas ring relative to the surrounding waters of the South Atlantic, based on the hydrographic surveys of a substantial number<sup>520</sup> of rings (Figure 6.21), give values of  $7.1 \times 10^{12} \text{ kg}$  salt and  $2.7 \times 10^{20} \text{ J}$  heat. This would lead to an inter-ocean heat flux of between 0.034 and 0.051 PW and a salt flux of between  $28.4$  and  $42.6 \times 10^{12} \text{ kg}$ . This heat flux has been substantially confirmed with independent altimetric estimates<sup>362</sup>.

Various other estimates have been made<sup>83,95</sup> of the mean volume flux achieved by these rings. These are all summarised in Table 6.5. The values in this table are for fluxes by individual rings only. They should therefore be viewed in concert with the estimated number of ring-shedding events, given in Table 6.6. By doing this it can be seen that the total fluxes achieved through the process of ring shedding lie between  $2 \times 10^6 \text{ m}^3/\text{s}$ <sup>464</sup> and  $15 \times 10^6 \text{ m}^3/\text{s}$ <sup>20,65</sup>. Some calculations<sup>517</sup> assign an average of  $1 \times 10^6 \text{ m}^3/\text{s}$  to each ring, a value that is in rough agreement with the average for all estimates to date (Table 6.5). It has accordingly been estimated<sup>94</sup> that the replacement time for water above  $10^\circ\text{C}$  in the South Atlantic Ocean by Agulhas rings alone would take only 70 years.

As could be expected, and been suggested above, these volume transports by Agulhas rings are by no means invariant. In fact, they exhibit large interannual

variations<sup>782</sup> (Figure 6.36). It is evident that the upper layer transport from the South Indian Ocean to the South Atlantic Ocean varies from  $0 \times 10^6 \text{ m}^3/\text{s}$  to nearly  $40 \times 10^6 \text{ m}^3/\text{s}$ , that the number of rings shed per year is not constant and that the volume of water in each ring is very different from individual ring to individual ring. For example, during 1997 only four rings were formed, but the volume content of each was much higher than the average for the years 1993 to 1998. As a result the average inter-ocean volume flux for 1997 was much higher than normal. The mean volume transport by rings in 1997 was  $2.4 \times 10^6 \text{ m}^3/\text{s}$  whereas it was  $0.8 \times 10^6 \text{ m}^3/\text{s}$  in 1993<sup>782</sup>. This high level of variability would also hold for other inter-ocean fluxes such as that of potential and kinetic energy.

An estimate of the mean, available potential energy flux per year due to Agulhas rings of  $20 \times 10^{16} \text{ J}$  has been made<sup>95</sup> with an average, concurrent kinetic energy flux of  $22 \times 10^{16} \text{ J}$ . These results depend directly on the properties of potential energy and kinetic energy found in individual rings. Values for these variables, as calculated from hydrographic measurements, are tabulated in Table 6.7. In these calculations, as for those for those of net salt and heat fluxes, the hydrographic values within rings are compared to those of unsullied South Atlantic water masses. The values accepted as representative for the ambient waters are therefore critical to an accurate estimate. Hydrographic stations so selected are usually chosen to be in the vicinity of the ring in question, but seemingly unaffected by foreign water masses. This selection process remains a hazardous one since all the waters of the south-eastern Atlantic Ocean probably exhibit some influence of Indian Ocean water or other. None would be pristine.

The net energy values calculated to date for transport

**Table 6.5.** Estimates of inter-ocean volume transports south of Africa by ring translation<sup>516</sup>. Sv is  $10^6 \text{ m}^3/\text{s}$ . Results obtained by Lutjeharms and Cooper (1996)<sup>93</sup> are for Agulhas filaments.

Authors	Flux/ring [Sv]	Reference	Date
Olson and Evans (1986) <sup>94</sup>	0.5–0.6	$T > 10^\circ\text{C}$	November–December 1983
Duncombe Rae et al. (1989) <sup>543</sup>	1.2	total	April–May 1989
Gordon and Haxby (1990) <sup>464</sup>	1.0–1.5	$T > 10^\circ\text{C}$	May 1987
	2.0–3.0	total	May 1987
McCartney and Woodgate-Jones (1991) <sup>395</sup>	0.4–1.1	total	February–March 1983
Van Ballegooyen et al. (1994) <sup>129</sup>	1.1	$T > 10^\circ\text{C}$	February–March 1987
Byrne et al. (1995) <sup>95</sup>	0.8–1.7	1000 db	10 cruises in the 1980s
Clement and Gordon (1995) <sup>537</sup>	0.45–0.90	1500 db	May 1993
Duncombe Rae et al. (1996) <sup>520</sup>	0.65	total	June 1992; May–October 1993
Lutjeharms and Cooper (1996) <sup>93</sup>	0.10	total	November 1983; December 1992
Goni et al. (1997) <sup>517</sup>	1.0	$T > 10^\circ\text{C}$	September 1992–December 1995

**Table 6.6.** The number of shedding events per annum for Agulhas rings as estimated by different authors<sup>516</sup>. Results obtained by Lutjeharms and Cooper (1996)<sup>93</sup> are for Agulhas filaments. Numbers in parentheses denote the average number of rings shed per year.

Authors	Number per year	Device	Period
Lutjeharms and Van Ballegooyen (1988) <sup>91</sup>	6–12 (9)	infrared	1978–1983
Gordon and Haxby (1990) <sup>464</sup>	5	altimeter	November 1986–November 1987
Feron et al. (1992) <sup>74</sup>	4–8 (6)	altimeter	November 1986–September 1989
Van Ballegooyen et al. (1994) <sup>129</sup>	6	altimeter	December 1986–December 1988
Byrne et al. (1995) <sup>95</sup>	6	altimeter	November 1986–August 1989
Duncombe Rae et al. (1996) <sup>520</sup>	4–6	echo sounder	June 1992–October 1993
Lutjeharms and Cooper (1996) <sup>93</sup>	6.5	infrared	1987–1991
Goni et al. (1997) <sup>517</sup>	4–7 (6)	altimeter	September 1992–December 1995

by Agulhas rings therefore may differ by more than just the variations in the characteristics of the rings themselves (Table 6.7). The potential energy calculated for Agulhas rings in this way varies between 2.8 to  $51.4 \times 10^{15}$  J; the kinetic energy lay between 2.01 to  $8.7 \times 10^{15}$  J. Notwithstanding the inherent variability to be expected in a collection of Agulhas rings, as well as the variability introduced by the different selection criteria for reference stations used, the level of energy in these features remains enormous. Olson and Evans<sup>94</sup> have consequently judged these rings to be the most energetic in the world ocean. Studies of annual and interannual variability in the South East Atlantic Ocean<sup>572</sup>, using sea surface temperatures for the past 80 years, show high correlations for the greater offshore part of this region. Interannual changes in heat input by Agulhas rings can therefore most probably not be resolved in this way. This may be possible using observations of sea surface height.

A study<sup>712</sup> of inter-annual variability<sup>754</sup> of the circu-

lation in the South Atlantic using satellite altimetry for a period of four years has demonstrated that there can be a transition from a state of high mean sea level to a state of lower sea level over a period of months (Figure 6.37) with the commensurate increase and decrease in circulation intensity in the Agulhas retroflection region. This was due to a basin-scale mode consisting of a broad, flat gyre replaced by a more zonally compact gyre, the latter with a stronger western boundary flow. The Agulhas ring corridor in the South Atlantic Ocean also widened when the average sea level was high and shrunk to a narrower one when the average sea level was lower<sup>712</sup>, suggesting that the basin-scale mode in the South Atlantic Ocean plays a role in the dispersal of Agulhas rings. The dominant mode of basin-scale, zonal wind forcing in the South Atlantic was in phase with these inter-annual changes in the Agulhas retroflection region<sup>712</sup>. This may well imply that the leakage of heat and salt to the South Atlantic Ocean by Agulhas rings are partially controlled by inter-annual

**Table 6.7.** Physical properties of Agulhas rings as presented by different authors<sup>516</sup>. Heat flux ( $F_Q$ ), salt flux ( $F_S$ ), available potential energy (APE) and kinetic energy (KE) have all been calculated with respect to the properties of the ambient waters in which the rings were found. Results obtained by Lutjeharms and Cooper (1996)<sup>93</sup> are for Agulhas filaments.

Authors	$F_Q$ [ $10^{-3}$ PW]	$F_S$ [ $10^5$ kg/s]	APE [ $10^{15}$ J]	KE [ $10^{15}$ J]
Olson and Evans (1986) <sup>94</sup>			30.5 51.4	6.2 8.7
Duncombe Rae et al. (1989) <sup>543</sup>	25	6.3		
Duncombe Rae et al. (1992) <sup>559</sup>			38.8	2.3
Van Ballegooyen et al. (1994) <sup>129</sup>	7.5	4.2		
Byrne et al. (1995) <sup>95</sup>			18	4.5
Clement and Gordon (1995) <sup>537</sup>			7.0	7.0
Duncombe Rae et al. (1996) <sup>520</sup>	1.74	1.1	11.3	2.01
Lutjeharms and Cooper (1996) <sup>93</sup>	1.1	0.15–0.46		
Goni et al. (1997) <sup>517</sup>			24	
Garzoli et al. (1996) <sup>519</sup>	1.0–1.6	0.7–1.0	2.8–3.8	

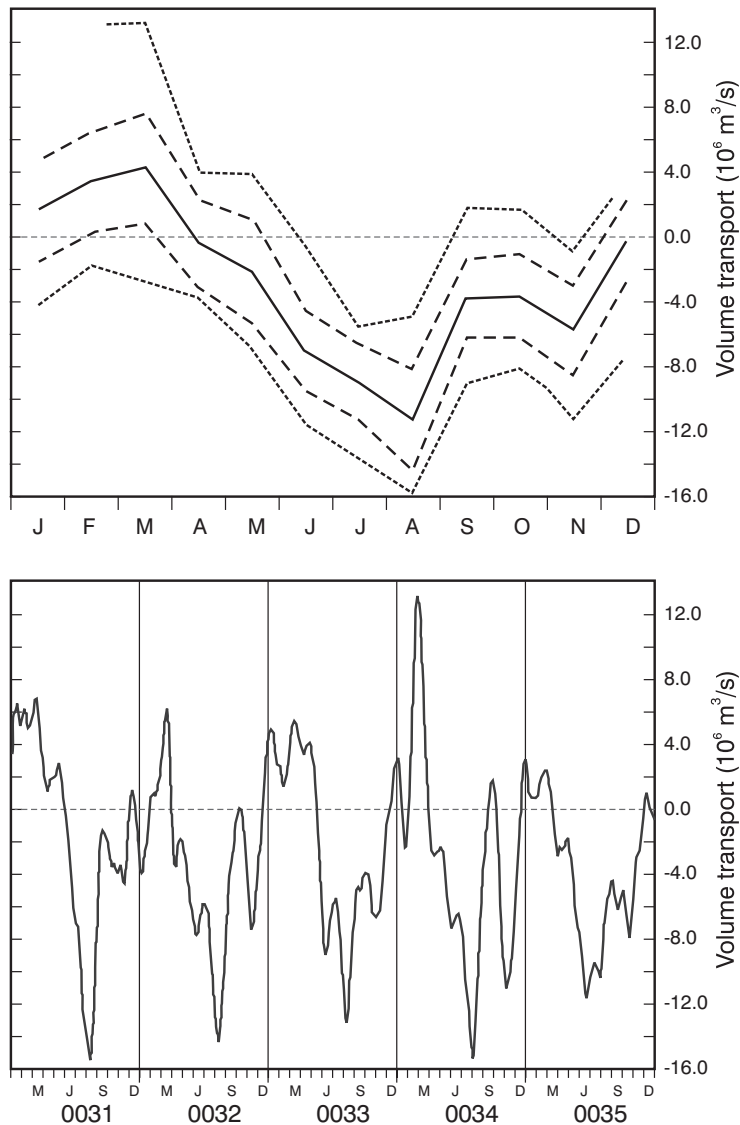


**Figure 6.36.** The volume transport across the 20° E meridian south of Africa as simulated by a numerical model<sup>777</sup> for a period of five years. The meridional extent from 35 to 45° S covers both the Agulhas Current as well as the Agulhas Return Current. The upper panel shows the mean value as a thick line with one standard deviation bordering the mean and the maximum and minimum values as final borders. The lower panel shows the a time series for these five years highlighting the variability in the flux. Positive values denote eastward transport.

variations of the wind-forced, large-scale circulation. Apart from inter-annual variations in the Agulhas Current retroflection region, there also is some evidence of a seasonal variability<sup>418</sup>. In fact, early results from satellite altimetry<sup>752</sup> suggest that in the South Atlantic Ocean, the strongest seasonality is found at the Agulhas retroflection.

In all this it is crucial to remember that just after spawning Agulhas rings find themselves in an extremely complex and varying environment<sup>628</sup>. Uncomplicated mechanistic visualizations of the subsequent behaviour

of Agulhas rings just will not do, as has been experienced in the planning of a number of research expeditions to the region<sup>650</sup>. The waters in the southern Cape Basin constitute a highly energetic field of rings that merge, split, deform and even reconnect to the Agulhas retroflection. To this veritable cauldron may further be added a field of cyclones that interact with the Agulhas rings as well as amongst themselves. An extra complication in estimating the inter-ocean leakage due to Agulhas rings may be the irregular occurrence of upstream retroflection in the Agulhas Current itself.

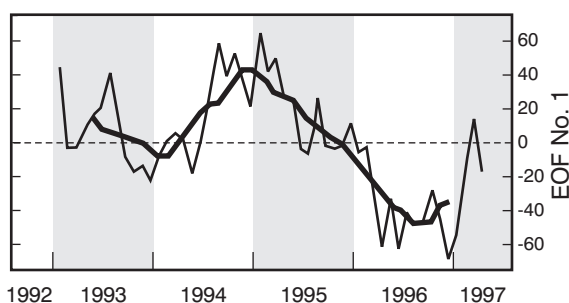


**Figure 6.37.** The intra-annual variability for the Agulhas retroflection and the Cape Basin for a period of five years<sup>712</sup> as expressed by a regional empirical orthogonal function. This mode 1 explains 45 per cent of the variance in the region. The thick line is a nine-month running mean for the amplitude.

#### *Upstream retroflection*

Whereas the normal location of the Agulhas retroflection loop lies west of  $20^{\circ}$  E<sup>91</sup>, there have been instances<sup>64</sup> in which the disposition of sea surface temperatures have suggested that part – if not all – of the Agulhas Current retroflected south of Port Elizabeth (viz. Figure 1.2). These suggestions of an upstream retroflection have been supported by the tracks of drifters. Such early retroflection has been assumed<sup>64</sup> to come about when an exceptionally well-developed Natal Pulse forces the core of the Agulhas Current sufficiently far offshore so that it intersects the shallow bathymetry of the Agulhas Plateau to the south and is thus forced eastward. Few such upstream short circuits in the normal trajectory of the current have been observed to date. On occasion a seemingly incomplete early retroflection has been noticed in thermal infrared imagery<sup>412</sup>. It can be assumed that such short-lived events do not contribute to a major change in the inter-ocean fluxes south of Africa. A long-lasting early retroflection, over the full depth of the current, would naturally have a substantial effect on the interchange south of Africa since Agulhas water would never reach the normal retroflection region. It would therefore not be available for inter-ocean exchange.

It has been assumed<sup>133</sup> that augmentations in the incidence of large Natal Pulses and concurrent increases in early retroflection events would be instrumental in substantial changes in the global thermohaline circulation. For this to be a robust mechanism, early retroflection events would have to be durable. An event lasting a number of months was observed from satellite remote sensing for the first time in 2000–2001<sup>670–1</sup>. This gives an indication of the limited frequency of these events that can be expected. One of the

main questions that remain would be the extent to which early retroflections succeed in siphoning off the greater part of the flux of the full Agulhas Current, i.e. how deep do they extend. During the 2000–2001 event fortuitous hydrographic measurements could be made<sup>672</sup> across the path of the current, proving that this particular upstream retroflection involved the greater part of the Agulhas Current. The significance of this finding is substantial.

#### *Global significance*

With the ever more accurate estimates of the inter-ocean exchanges by Agulhas rings, the role they play in the global thermohaline circulation cell would seem to be increasingly more reliably quantified. This is not yet the case. Nonetheless, establishing the effect of Agulhas rings remains critical to an understanding of the role in global climate of the one major ocean basin – the Atlantic Ocean – in which there is a substantial net heat flow across the equator in a northward direction. This flow has been estimated<sup>753</sup> to be about 0.29 PW.

Rintoul, using an inverse model, has concluded<sup>565</sup> that no input of warm Indian Ocean is required to account for the net northward heat flux in the South Atlantic Ocean, the flow being totally determined by differences in the water masses entering via the Drake Passage and leaving the South Atlantic sector of the Southern Ocean between Africa and Antarctica. A different model, using as constraint the historical hydrographic data, predicts that an inflow into the South Atlantic Ocean of  $4$  to  $7 \times 10^6$  m<sup>3</sup>/s can be accommodated, but no larger values<sup>247</sup>. A strong correlation is found between the meridional heat transport in this latter model, the strength of the global thermohaline cell and inflow from the Indian Ocean. The model has no Agulhas rings and may therefore be biased.

On the other hand, use of a primitive equation model of the southern hemisphere<sup>566</sup> has suggested that 85 per cent of the northward heat transport into the Atlantic originates in the Indian Ocean, only the remainder coming through the Drake Passage. Others<sup>67</sup> have shown that up to two-thirds of the Benguela Current of the South Atlantic, within and above the thermocline, has its origin in the South Indian Ocean. The total transport has been estimated<sup>759</sup> at  $28(\pm 4) \times 10^6$  m<sup>3</sup>/s. Another published value<sup>779</sup> is  $25 \times 10^6$  m<sup>3</sup>/s. The results of all inversion studies to date that have estimated the heat flux across  $30^{\circ}$  S latitude in the South Atlantic are given in Table 6.8; those for modelling studies in Table 6.9. From these tables it is clear that linkages of Atlantic and Indian Ocean waters continue into deep water and, as

**Table 6.8.** The heat fluxes ( $F_Q$ ) and the volume transports across 30° S latitude in the South Atlantic Ocean according to a number of inversion studies<sup>516</sup>. Values are given in  $10^6$  m<sup>3</sup>/s; positive values denoting equatorward transport. Values are given for different water masses: SW representing Surface Water; AAIW, Antarctic Intermediate Water; NADW, North Atlantic Deep Water and AABW, Antarctic Bottom Water. *Date* refers to the date on which a hydrographic section was carried out along 30° S latitude.

Authors	SW	AAIW	NADW	AABW	$F_Q$ [PW]	Date
Fu (1981) <sup>567</sup>	15	10	-24	-2	0.85	July–August 1925 METEOR
	9	6	-20	1	0.88	April–June 1959 IGY
Rintoul (1991) <sup>565</sup>	8	5	-17	4	0.25	April–May 1959 IGY
MacDonald (1993) <sup>568</sup>	6.1	7.9	-21.6	7.5	0.3	February 1988–February 1989
Schlitzer (1993) <sup>569</sup>	2.2	10.0	-15.8	3.1	-0.05	historical
Schlitzer (1996) <sup>570</sup>	2.0	11.9	-18.7	4.2	0.3	historical
Boddem and Schlitzer (1995) <sup>247</sup>	-1.9	9.8	-8.9	1.1	0.04	historical
Holfort et al. (1998) <sup>571</sup>					0.26	January 1993 WOCE

could be expected from the relative volumes of the water types<sup>363</sup>, are greatest by volume in deep water.

The set of historical hydrographic data in the Agulhas retroflection and in the South Atlantic Ocean show<sup>250</sup> the progression of Antarctic Intermediate Water to mirror that of the Agulhas Current and Agulhas rings, but cannot resolve their influence directly. Agulhas rings do not seem to have an adequately distinct hydrographic signal, or are not present in sufficient abundance, to leave behind a tell-tale record in the hydrographic data at depth to indicate their range of influence or average path<sup>195</sup>. Nevertheless, estimates of potential vorticity on the 27.3 isopycnal<sup>575</sup> shows clear evidence of leakage of Antarctic Intermediate Water from the Indian to the Atlantic Ocean and its penetration in a north-westerly direction across the South Atlantic Ocean.

Modelling of the impact of inter-ocean exchanges on the thermohaline overturning of the Atlantic Ocean<sup>68,668–9</sup> has been very suggestive. Weijer et al.<sup>68</sup> have, as mentioned above, shown that the heat and salt transports by the South Atlantic subtropical gyre play an essential role in the heat and salt budgets of the Atlantic as a whole. It has been shown that in this model the exported North Atlantic Deep Water is fresher than

the return flows and that the overturning circulation thus exports freshwater from the Atlantic Ocean. Even small changes in the composition of the return transports of the North Atlantic Deep Water may influence the overturning circulation in this ocean considerably. The model furthermore shows<sup>68</sup> that interocean fluxes of heat and salt are important for the strength and operation of the overturning circulation. Comparing the roles of the inter-ocean exchanges between the Atlantic, the Pacific through the Drake Passage, the Pacific through the Bering Sea and the South Indian Ocean<sup>668</sup> in a global circulation model, it can be shown that it is especially the Indian–Atlantic transfers of heat and salt by leakage from the Agulhas Current that contributes to the strength and the stability of the northern sinking circulation. When the stabilizing effect of the leakage from the Agulhas Current disappears, the destabilizing influence on the overturning circulation by freshwater from the Bering Strait becomes more effective. Of particular importance in these model studies has been an investigation on the influence of water from the Agulhas Current on the Atlantic overturning as a whole<sup>669</sup> (viz. Figure 6.38).

From Figure 6.38 it is clear that the model's overturning circulation is sensitive to changes in the inter-

**Table 6.9.** The heat fluxes (last column) and volume transports for different water masses across 30° S latitude in the South Atlantic Ocean, according to a few modelling studies<sup>516</sup>. Volume fluxes are given in  $10^6$  m<sup>3</sup>/s. Water masses are: SW: Surface Water; AAIW: Antarctic Intermediate Water; NADW: North Atlantic Deep Water and AABW: Antarctic Bottom Water.

Authors	SW	AAIW	NADW	AABW	$F_0$ (PW)
FRAM Group (1991) <sup>272</sup>	11	8	-22	3.2	0.56
Semtner and Chervin (1992) <sup>274</sup>	12	4.7	-18	1.3	0.60
Matano and Philander (1993) <sup>573</sup>	6.8	1.6	-10.9	2.5	0.19
Thompson et al. (1997) <sup>574</sup>	12.7	6.8	-20.9	1.4	0.56

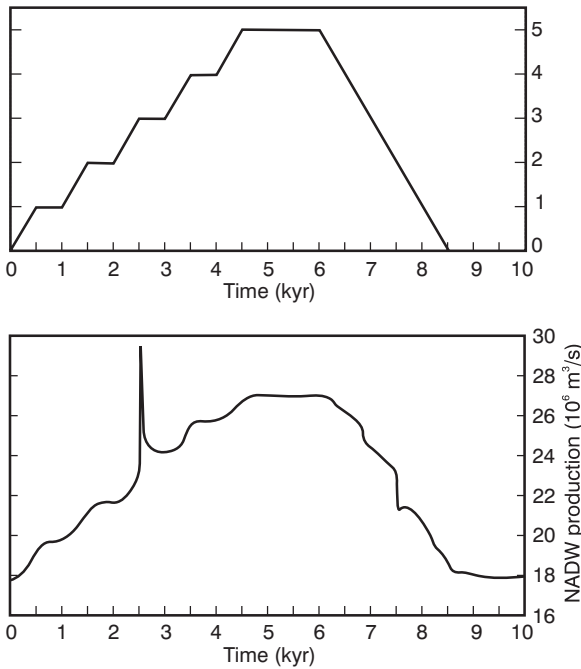


**Figure 6.38.** Response of the overturning circulation in the Atlantic Ocean to changes in volume flux from the Agulhas Current<sup>669</sup>. The upper panel shows the volume flux applied to a model, where a value of 1 is the value currently estimated by observations at sea<sup>129</sup>; 0.045 PW for heat and 2.52 Gg/s for salt. The lower panel shows the concurrent production of North Atlantic Deep Water. It closely reflects the source function in the upper panel, following each step in the increased volume flux as applied to the model. Stopping the throughflow entirely results in a remaining flux of about  $18 \times 10^6 \text{ m}^3/\text{s}$  in the production of North Atlantic Deep Water.

ocean leakage of water from the Indian Ocean. The response of the overturning strength to changes in the inter-ocean transfers is mainly linear. Changes in the transfers of buoyancy affect the strength of the Atlantic Ocean's overturning by the modification of the basin-scale meridional density and pressure gradients. This response takes place within a few years, being the time it takes for barotropic and baroclinic Kelvin waves to reach the northern Atlantic Ocean. The heat and salt anomalies inserted into the model's South Atlantic by contrast take three decades to be advected all the way to the northern North Atlantic. These model studies suggest the decisive influence alterations in the inter-ocean exchanges of heat and salt south of Africa may have on the global overturning circulation. The importance of this influence has been confirmed by palaeoceanographic results<sup>667</sup> discussed elsewhere. But how to quantify this importance?

Using Lagrangian path following techniques it has been shown<sup>756</sup> that 90 per cent of the upper branch of the overturning circulation in the Atlantic Ocean is derived from inflow of Indian Ocean water. One may wonder about this, since the inter-ocean leakage from the Agulhas Current takes place in the upper 2000 m of the water column, but it has been demonstrated that 95 per cent of all the volume transport that contributes to the upper branch of the thermohaline overturning circulation is found in the upper 1000 m. In contrast to other studies<sup>774-5</sup> this analysis indicates that almost all water from the Drake Passage moves eastward, past the tip of Africa.

Loss of water from the Indian Ocean by the formation of mesoscale eddies at the Agulhas retroflexion is not, however, restricted to Agulhas rings.

### Agulhas Current eddies

The portrayal of temperature fronts at the Agulhas Current retroflexion presented in Figure 6.2 shows a number of circular features to the south of the retroflexion. The first vortex of this region that has been hydrographically observed<sup>511</sup> may well have been one of these. This seems clear from the fact that it was well-imbedded in surface water colder than  $14^\circ\text{C}$ , the mean temperature for the front of the Subtropical Convergence in this region<sup>97</sup>. Eddies of this kind are continually being formed, carrying substantial amounts of heat poleward across the Subtropical Convergence<sup>458</sup> thus contributing to the global, meridional heat flux of the ocean. However, they may lose up to  $800 \text{ W}/\text{m}^2$  of heat to the atmosphere<sup>496</sup> under the cold and stormy conditions found in this region and thus exhibit considerable effects of convective overturning in their upper layers.

Those that have been observed hydrographically extend into deep water<sup>262,455</sup> and have azimuthal velocities similar to that of the parent current. How many are shed per year is not known. Very persistent cloud coverage over the region has limited the use of satellite observations in the thermal infrared, while altimetric measurements have not been able to resolve such features well<sup>362</sup>. This could possibly be explained by the features remaining virtually stationary. With a strong eastward current and substantial meridional shear in the flow, this is not what one would expect. Analyses of these features<sup>63</sup> have suggested that they populate only a restricted region, but this is perhaps best included in the discussion of the Agulhas Return Current and the South Indian Ocean Current that follows.

The important concept that needs to be kept in mind here is that the loss of water that occurs between the southern Agulhas Current and the Agulhas Return

Current – in other words, while the current passes through the retroflection – is not only lost to the South Atlantic Ocean, but also to the Southern Ocean. The processes in both cases might be much better quantified if the dynamics were better understood. To this end a fair degree of modelling, both analytical and numerical, has been carried out.

### The dynamics of the Agulhas retroflection

The forcing of the processes that occur at the Agulhas retroflection has been investigated by modelling using a wide range of approaches. These may, for ease of description, be grouped into four broad categories. First, there have been attempts to simulate the flow path of the Agulhas Current by using an inertial jet<sup>130,506</sup>. Secondly, a series of wind-driven models have been constructed specifically for the Agulhas System employing increasingly realistic coastal outlines and bottom topographies<sup>268,576–7</sup>. Thirdly, modelling the system incorporating data assimilation<sup>265,548,578–9</sup> – mostly satellite altimeter observations – has considerably increased the verisimilitude of modelling results and, fourthly, a number of global circulation models have simulated certain aspects of the Agulhas retroflection<sup>273,276</sup> fairly well, and therefore are instructive about the forcing involved. Modelling<sup>469,580</sup> of a more analytic nature, to address certain fundamental problems concerning the reasons for a retroflection<sup>741,778</sup>, have been discussed above.

#### *Inertial jet models*

Hydrographic investigations as well as satellite remote sensing in the thermal infrared have all shown that the Agulhas Current follows the edge of the continental shelf quite religiously and that downstream of the Agulhas retroflection the path of the Agulhas Return Current is noticeably affected by the presence of shallower regions. Early modelling efforts have therefore concentrated on the sensitivity of the current trajectory to the bottom topography and thus its role on the retroflection, and shown that in some model configurations the Agulhas Current is very sensitive to small changes in current speeds at the bottom<sup>506</sup>.

Using a more realistic polygonal velocity profile<sup>130</sup>, it has been demonstrated that penetration of the Agulhas Current into the Atlantic Ocean is a function of high current shear and high bottom velocities. Penetrations of the Agulhas retroflection loop are a function of volume transport in the current; the more westerly retroflections occurring, according to this model, with lower volume transports (Figure 6.39). Although the simu-

lated path resembles a retroflection loop, these loops are unstable, the jet trajectories crossing themselves further upstream. This problem has subsequently been addressed<sup>469</sup> by using a model in which the boundary current is confined to the upper layer.

The point at which the simulated boundary current in this specific model leaves the coastline is a function of the volume flux, upstream separation occurring with increased volume transport. This more sophisticated model furthermore suggests that both the inertial and the beta ( $\beta$ ) effect play an important role in the retroflection of the Agulhas Current. Using a transport model of the large-scale wind-driven ocean circulation in the subtropical region of the Atlantic and Indian Ocean<sup>580</sup> De Ruijter has demonstrated that inertia must be incorporated in model configurations in order to achieve a retroflection for the Agulhas Current.

#### *Wind-driven models*

In such a model the meridional gradient in the wind-stress curl over the Indian Ocean domain is a controlling factor for the Agulhas retroflection. If the wind-stress curl decreases substantially southward, most Agulhas Current water ends up in the South Indian Ocean Current. If not, a larger proportion of its transport will bend westward<sup>580</sup>. Increasing the spatial resolution of such wind-driven, barotropic models<sup>576</sup> has shown that the retroflection of the simulated Agulhas Current is largely due to the net accumulation of  $\beta$ -generated, anti-cyclonic, relative vorticity as the current follows an inertially driven southward path after having separated from the tip of Africa. The degree to which Agulhas water from the Agulhas retroflection penetrates into the South Atlantic has been shown primarily to be determined by the latitude of the zone of zero wind-stress curl<sup>576</sup>. Since this zone may wander with season, as well as interannually, the degree of isolation of the two anti-cyclonic gyres east and west of Africa may change commensurably.

By increasing the complexity of this particular model through the inclusion of baroclinicity<sup>581</sup>, Boudra and De Ruijter have successfully increased the intensity of the simulated retroflection loop, but decreased the inter-basin leakage of surface water (Figure 6.40). The process responsible for the Agulhas retroflection in this model remains an adjustment to the change in the vorticity balance as the current overshoots the continent. Along the coast the current gains relative vorticity by the  $\beta$ -effect, but loses this as friction to the shelf edge. After separation, however, gain in relative vorticity is accommodated by an eastward turn. Agulhas ring formation in the model may thus require inter-

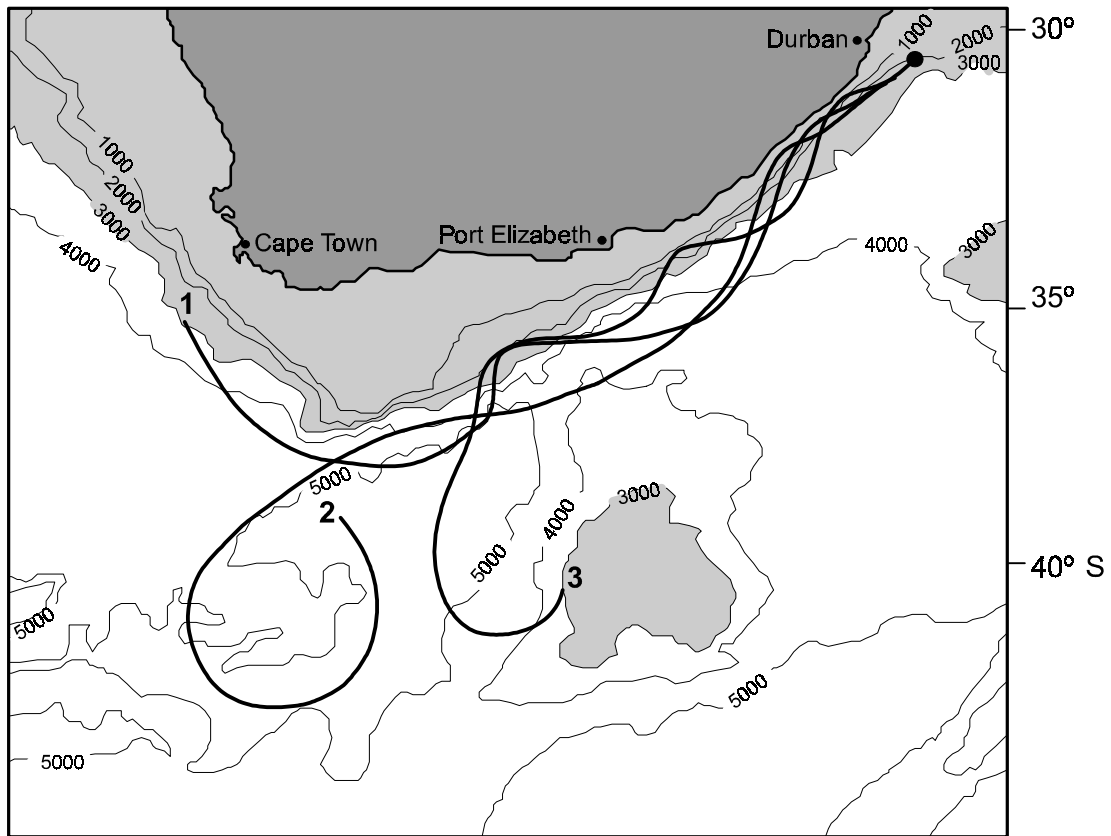


**Figure 6.39.** Trajectories of a free inertial jet used to simulate the flow path of the Agulhas Current in the retroflexion region<sup>130</sup>. Farther westward penetration of the retroflexion loop is achieved by decreasing the volume flux of the jet.

action with the eastward flow to the south<sup>581</sup>.

The importance of a substantial viscous stress curl along the coast of Africa in determining the nature of the Agulhas retroflexion has become evident in more advanced model simulations<sup>582</sup>. Whether rings will form in this model configuration has been shown to be primarily a factor of the southward inertia and the baroclinicity of the overshooting Agulhas Current<sup>132</sup>. Baroclinic–barotropic instabilities have been suggested by this model version as being associated with ring formation. No attempt has been made in these models to include thermodynamic forcing<sup>529</sup>, but allowing isopycnal outcropping has made this series of wind-driven models more realistic. The model results from these latter numerical experiments, shown in Figure 6.41, show the type of realism that has been achieved. These simulated rings have a coherent structure all the way to the ocean floor<sup>577</sup>. The model shows that rings that have drifted into the South Atlantic move westwards predominantly due to the large-scale ambient water movement in the gyre.

Pichevin et al.<sup>583</sup> have attempted to understand, from an analytical viewpoint, why rings are shed from the

Agulhas retroflexion at all. They come to some unconventional conclusions. Using a reduced gravity, one-and-a-half layer, primitive equation model they show that the generation of rings from a retroflexing current is inevitable. They conclude that the triggering of ring spawning is not necessarily due to instabilities but, rather, is due to the zonal momentum flux of an Agulhas jet that curves back on itself. To compensate for this momentum flux, rings have to be produced. Spawning rings exert a compensating momentum effect analogous to the backward push when a rifle is fired. The fact that the observed rings are considerably larger than what the local Rossby radius of deformation would suggest that they should be, is explained in a novel way. Vortices at the Rossby radius would come about due to normal flow instability; here the rings need to balance the momentum flux of a large retroflexing current, hence their size. In this model<sup>583</sup> a simulated Natal Pulse has no obvious relationship to ring occlusion.

The causes of the Agulhas retroflexion have also been investigated using the Princeton Ocean Model, a primitive equation model in sigma co-ordinates<sup>268</sup>. A series of process-oriented studies, using different wind-

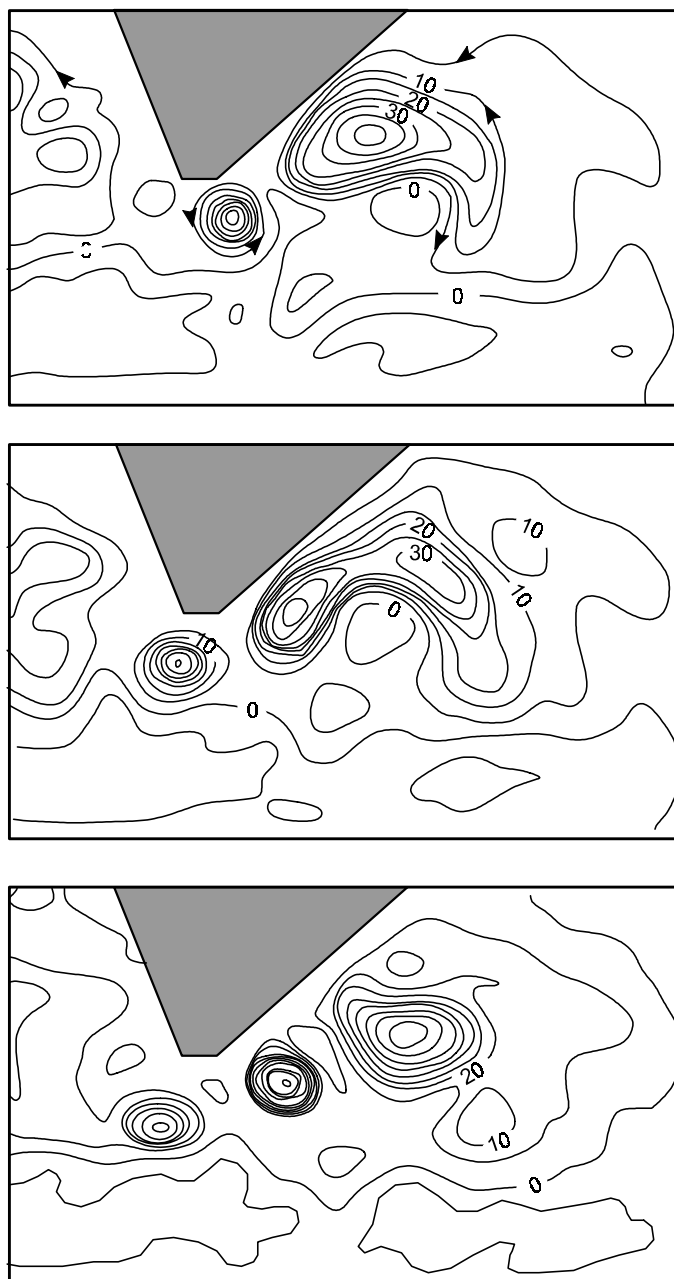


**Figure 6.40.** Modelling results that simulate the shedding of an Agulhas ring at the Agulhas retroflexion and the movement of a previously shed ring into the South Atlantic Ocean<sup>132</sup>. The mass transport stream function is shown for the upper layer of the model. Contour intervals are at  $7 \times 10^6 \text{ m}^3/\text{s}$ . The results are given, from top to bottom, for days 2950, 2990 and 3010.

stress distributions and different degrees of smoothing of the bathymetry, has produced some interesting results. It has been shown that in this model the simulated Agulhas retroflexion is more strongly affected by the torques exerted by the bottom topography than by the effect of  $\beta$ -accumulated vorticity or the effect of coastline curvature. An adaptation of the Princeton

Ocean Model, NORWECOM, has been used<sup>765</sup> to study biological aspects of the southern part of the Agulhas Current system as well as the Benguela upwelling regime. This includes primary production. The near oligotrophic nature of the south Agulhas Current is successfully simulated.

An eddy-permitting model that focuses on the Cape

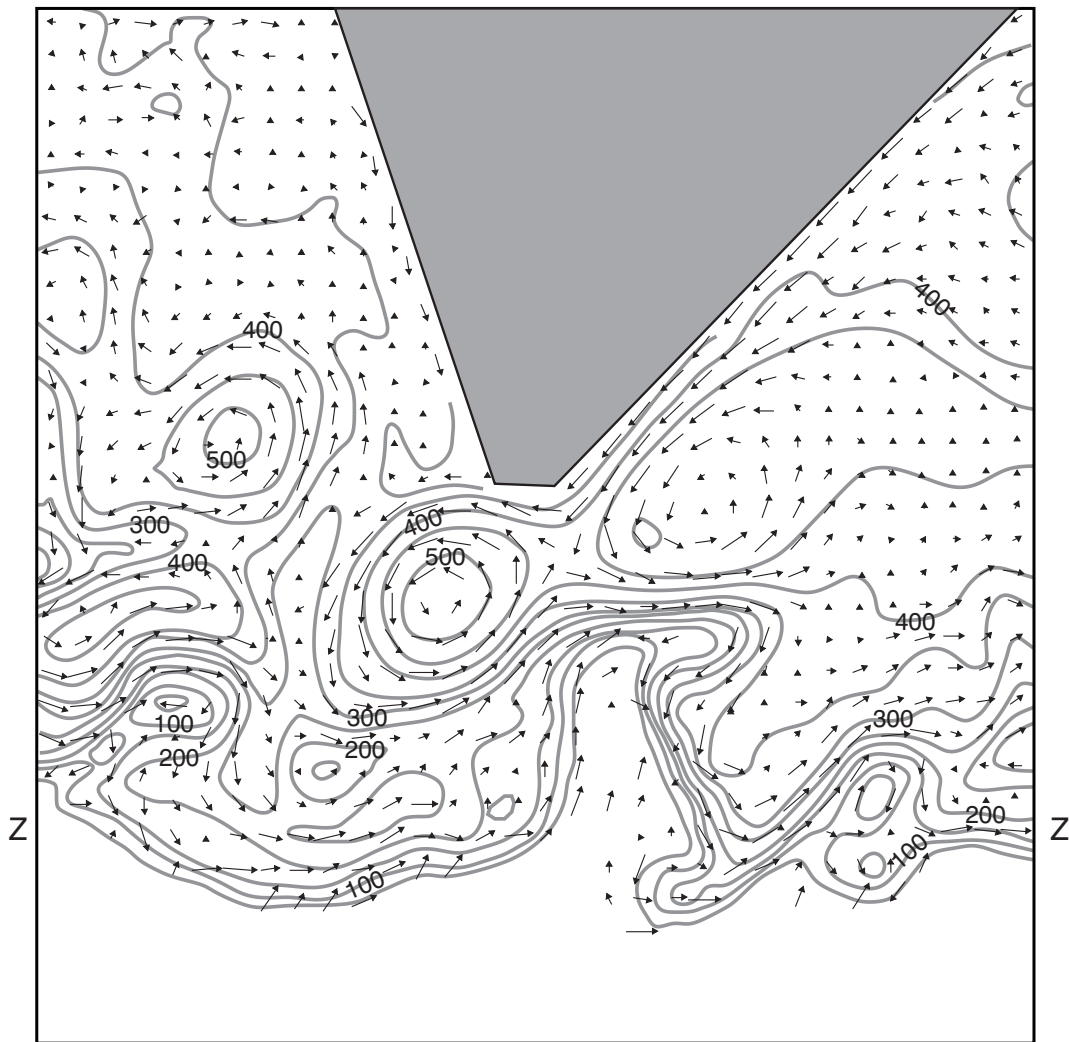


**Figure 6.41.** Detail of the Agulhas retroflexion loop, a ring-spawning event, progression of a previously spawned ring and meanders in the Subtropical Convergence and Agulhas Return Current, all as simulated by a pure-isopycnic, numerical model with three layers<sup>529</sup>. Shown is the velocity and thickness field of the intermediate layer. Flow vectors are given for every other grid point. The latitude where the wind stress curl is nil is shown by the letter Z along the borders of the figure. Note the substantial meander in the Agulhas Return Current over the Agulhas Plateau.

Basin<sup>776</sup>, but that includes a large part of the South West Indian Ocean and the South Atlantic Ocean, has successfully simulated the role that Agulhas rings play not only in the transients of the region, but also fluxes associated with the mean circulation. Modelled rings, correctly, indicate that most of the energy in the Benguela Current is supplied by themselves. This model shows the co-existence of anti-cyclonic rings and cyclones in firm dipole structures. This modeled configuration should not be confused with the freely moving cyclones derived from the west African coastline that were described in detail above<sup>628</sup>. The modelled cyclones<sup>776</sup> are bottom intensified vortices with baro-

tropic structures. Their passage is blocked by the Walvis Ridge and the Vema Seamount. Using such an eddy-permitting model to evaluate the variability in the inter-ocean fluxes south of Africa<sup>777</sup> has shown a seasonal variation of about 10 per cent across a section at 35° S in the South Atlantic Ocean and around 20 per cent through a section at 20° E. Simulated volume transports of the Agulhas Current through a section at 35° S are about  $58 \times 10^6 \text{ m}^3/\text{s}$  in summer/autumn and about  $64 \times 10^6 \text{ m}^3/\text{s}$  in winter/spring (viz. Figure 6.42). Short term variability in this model simulation is large and seems realistic.

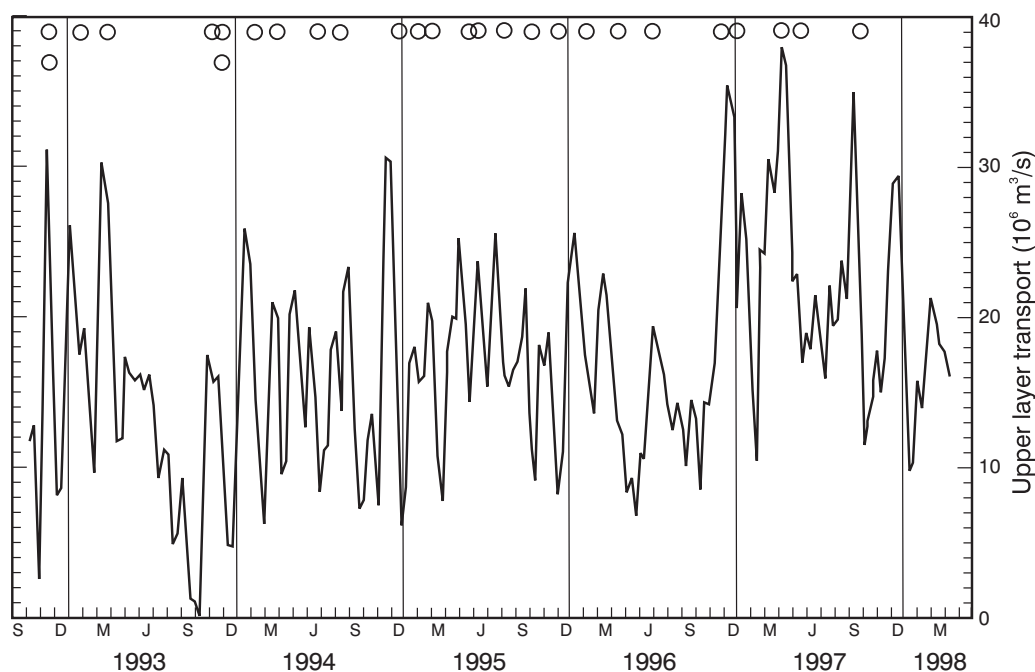


**Figure 6.42.** A time series of the upper layer volume transport of the Agulhas Current into the South Atlantic across the 19° E meridian<sup>782</sup>. The circles indicate the times when each Agulhas ring that contributed to the flux was first detected. Particularly noteworthy is the high level of temporal variability.

#### *Modelling with data assimilation*

One of the major limitations of most of these models of the Agulhas retroflection and of the ring shedding process is the inability of these models to predict events with sufficient accuracy that they may reliably be used prognostically. This could conceivably be achieved if real-time data of sufficient spatial resolution were to be assimilated on a regular basis. A first attempt to do this for the region around southern Africa has been carried out<sup>265</sup> with promising results. A next attempt<sup>548</sup> has used an ensemble Kalman filter to assimilate Geosat altimeter data into a two-layer quasi-geostrophic ocean model.

This method has increased the frequency of ring shedding which in most other quasi-geostrophic models is too low. It has therefore been concluded that this type of data assimilation system accommodates ageostrophic effects that cannot be accounted for in other models of this kind. This procedure has been further developed<sup>578</sup> by combining the time-varying part of altimetric data with a two-layer, quasi-geostrophic model, imposing the time-mean circulation as an unknown. This data assimilation experiment has been successful in reducing errors in the time-mean, sea surface topography from about 10 cm to 3 cm. Van Leeuwen has subsequently shown<sup>584</sup> that in such data assimila-

tion models designed to study Agulhas Current processes a smoother will give superior results to a filter.

The most successful of the data assimilation models for the Agulhas retroflection region to date has a  $1/6^\circ$  grid, with four layers, is quasi-geostrophic and incorporates altimetric data from both the TOPEX/Poseidon and the ERS 1 satellites<sup>579</sup>. Not only the large-scale, time-mean circulation is simulated well by this model; the meso-scale processes also are very realistic (Figure 6.43). In the Agulhas Current proper a surface speed of 1.3 m/s is simulated; the volume flux above 1200 m is  $75 \times 10^6 \text{ m}^3/\text{s}$  and the general disposition of the retroflection in the model agrees closely with what has been observed. The model suggests an interesting decrease in the core speed of the Agulhas Current from 130 cm/s to 80 cm/s along the Agulhas Bank. This needs to be confirmed by appropriate measurements in this region. The ring-shedding process is simulated well, as are the subsequent drifts of Agulhas rings across the South Atlantic, even including the dissipation of three rings in the Cape Basin<sup>579</sup>. This is not particularly remarkable, however, since information on these rings is assimilated from altimetric anomalies. All the above-mentioned models either have a relatively coarse horizontal resolution or a small number of layers in the vertical. In most of the global circulation models this is very different.

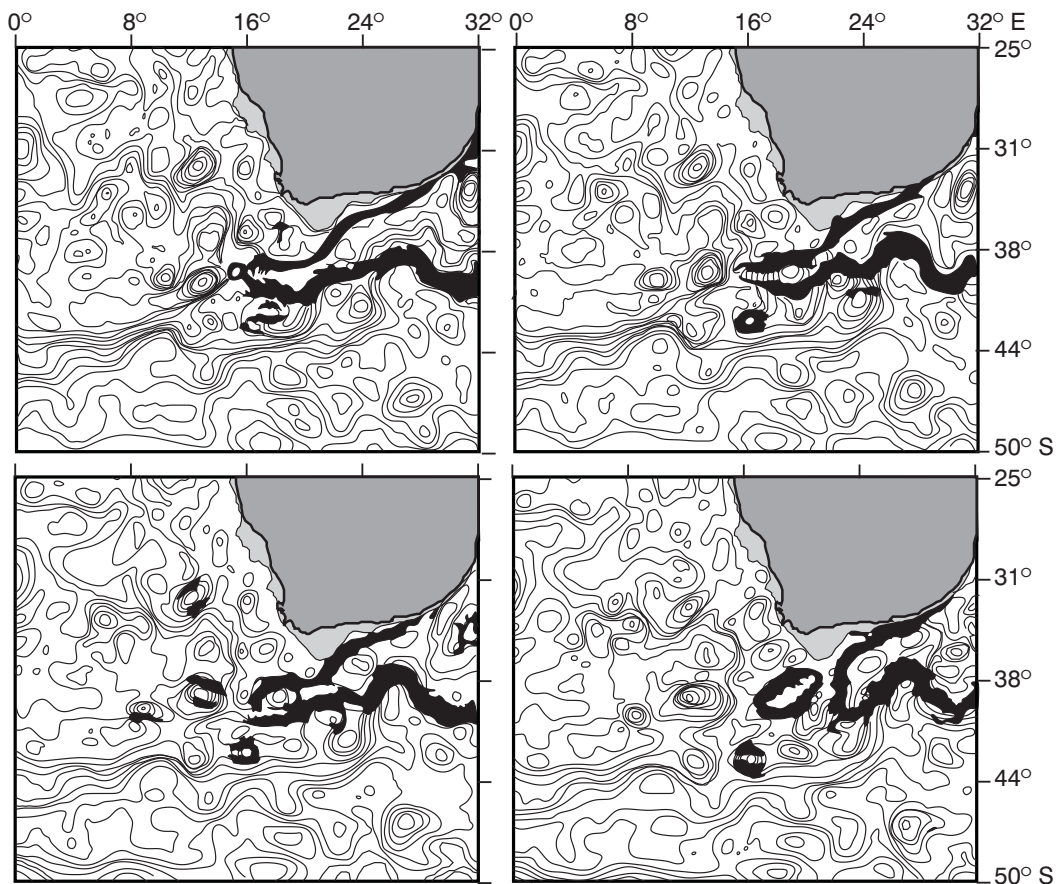


**Figure 6.43.** Ring shedding at the Agulhas Current retroflexion as simulated by a four-layer, quasi-geostrophic numerical model with data assimilation<sup>776</sup>. The panels are representations of the instantaneous stream function at ten-day intervals, starting on 4 August 1994. The northward penetration of a meander in the Agulhas Return Current and its role in the occlusion of an Agulhas ring is evident. This corresponds well with what has been observed for this process using satellite thermal infrared observations<sup>91</sup>.

#### *Global circulation models*

With a  $\frac{1}{2}^\circ$  latitude by  $\frac{1}{2}^\circ$  longitude spatial grid, 20 vertical levels, a realistic geometry and annual mean wind forcing, the eddy resolving model by Semtner and Chervin<sup>273</sup> has simulated the spawning of warm-core rings which enter the South Atlantic Ocean and move off in a northwest direction. The spawning of both anti-cyclonic and cyclonic disturbances has been produced by this model. These dipoles have not been unambiguously observed in most of the hydrographic data to date, but there are some suggestions of their presence in satellite altimetry<sup>362</sup>. An important result of this particular model has been its simulation of the global thermohaline circulation cell and, particularly, the warm water path due to Agulhas rings.

Changing the wind forcing to climatological monthly forcing<sup>274</sup> in this global model does not change this re-

sult substantially. The geographic distribution of eddy-variability produced in the model resembles closely that for the Agulhas retroflexion region found from altimetric data<sup>73</sup>. This is also reflected in further studies<sup>275</sup> that have compared the eddy kinetic energy in a model simulation of the southern Agulhas Current, Agulhas Retroflexion and Agulhas Return Current with altimeter, drifter and current-meter data. More advanced forms of the Semtner model<sup>325</sup>, driven by very realistic atmospheric forcing, have simulated the shedding of Agulhas rings even more realistically. In this global, eddy-resolving model 3.6 rings are shed per year and they take about three years to cross the South Atlantic Ocean. It is of interest to note that the rings take two preferred paths in this version of the model<sup>325</sup> and that the split seems to coincide with the location of the Vema Seamount.

The FRAM (*Fine Resolution Antarctic Model*)<sup>272</sup> is,

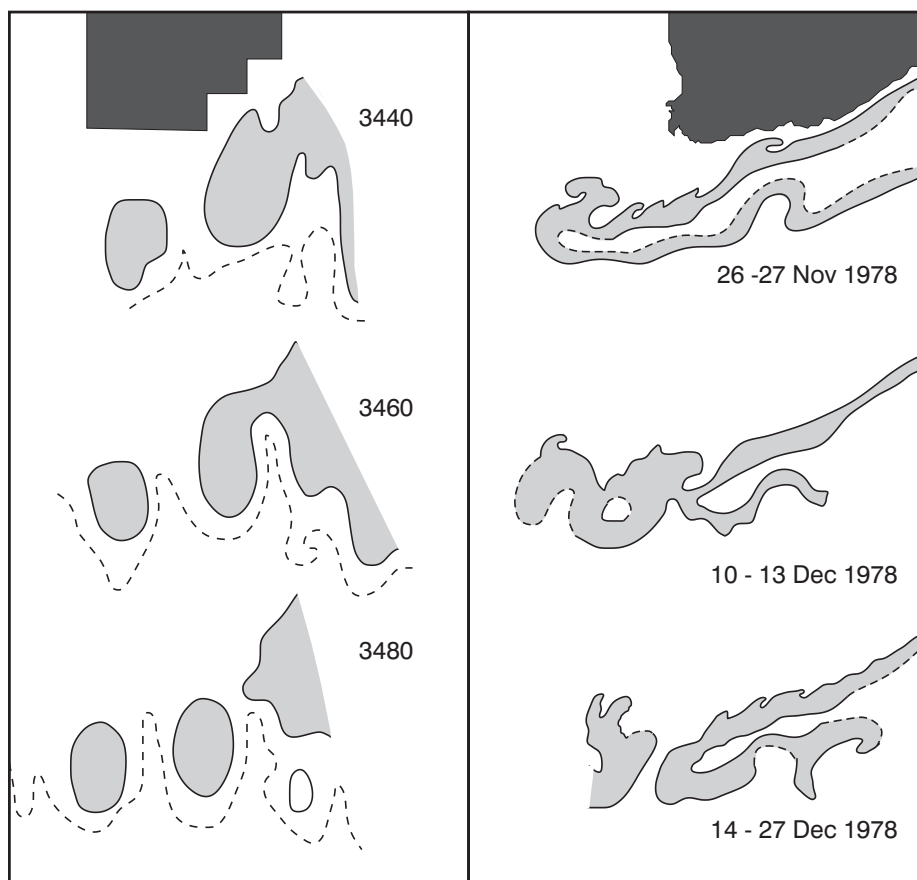


**Figure 6.44.** The ring shedding process at the Agulhas Current retroflexion as observed from satellite infrared imagery<sup>60</sup> (right-hand panel) and simulated by the FRAM (Fine Resolution Antarctic Model; left-hand panel)<sup>277</sup>. Broken lines denote the Subtropical Convergence; dotted lines regions where temperatures were poorly resolved. A comparison between actual dates (right) and model days (left) shows that the process occurs too slowly in this model.

by contrast, restricted to the region south of  $24^{\circ}$  S latitude, with a  $\frac{1}{4}^{\circ}$  north–south spatial resolution;  $\frac{1}{2}^{\circ}$  in the east–west direction. It has 32 horizontal levels, spaced at increasing intervals with depth. It was run with a weak relaxation to the mean values produced by Levitus<sup>348</sup> and allowed to run freely after that. It models the creation of Agulhas rings very convincingly<sup>276</sup> (Figure 6.44). They start with an internal volume transport of  $140 \times 10^6 \text{ m}^3/\text{s}$ , and are shed at 160 day intervals. Both these values are too large when compared to observation<sup>74,91</sup>. Fortunately these values partially compensate each other so that the net heat flux is realistic<sup>585</sup>.

The rings modelled by the FRAM drift off into the South Atlantic slowly losing their kinematic and hydrographic characteristics, but do not stray from a singular track followed by all rings<sup>277</sup> (Figure 6.45). This is clearly at odds with observation (e.g. Figures 6.19, 6.33). Rings in the model are also shed too far upstream.

The regular cycles of wind-stress and the simplified bottom topography may be the respective culprits. The FRAM shows no direct interaction of Agulhas rings with the coastal upwelling system of the South East Atlantic<sup>562</sup>, possibly due to the invariant, offshore tracks of all simulated rings. The model does indicate that the thermal structure of the South Atlantic Ocean, and in consequence the meridional heat transport, depends heavily on the input of heat via Agulhas rings<sup>574</sup>. Models that do not include this inter-ocean exchange south of Africa<sup>544,565</sup> exhibit a much lower equatorward transfer of heat.

Clearly, even the most sophisticated numerical models are at present incapable of simulating the Agulhas retroflexion and the ring-shedding process with a verisimilitude that makes them reliable tools for prediction or even experimentation. Nevertheless, the realism with which these processes are already represented by models suggests that most of the underlying physics of

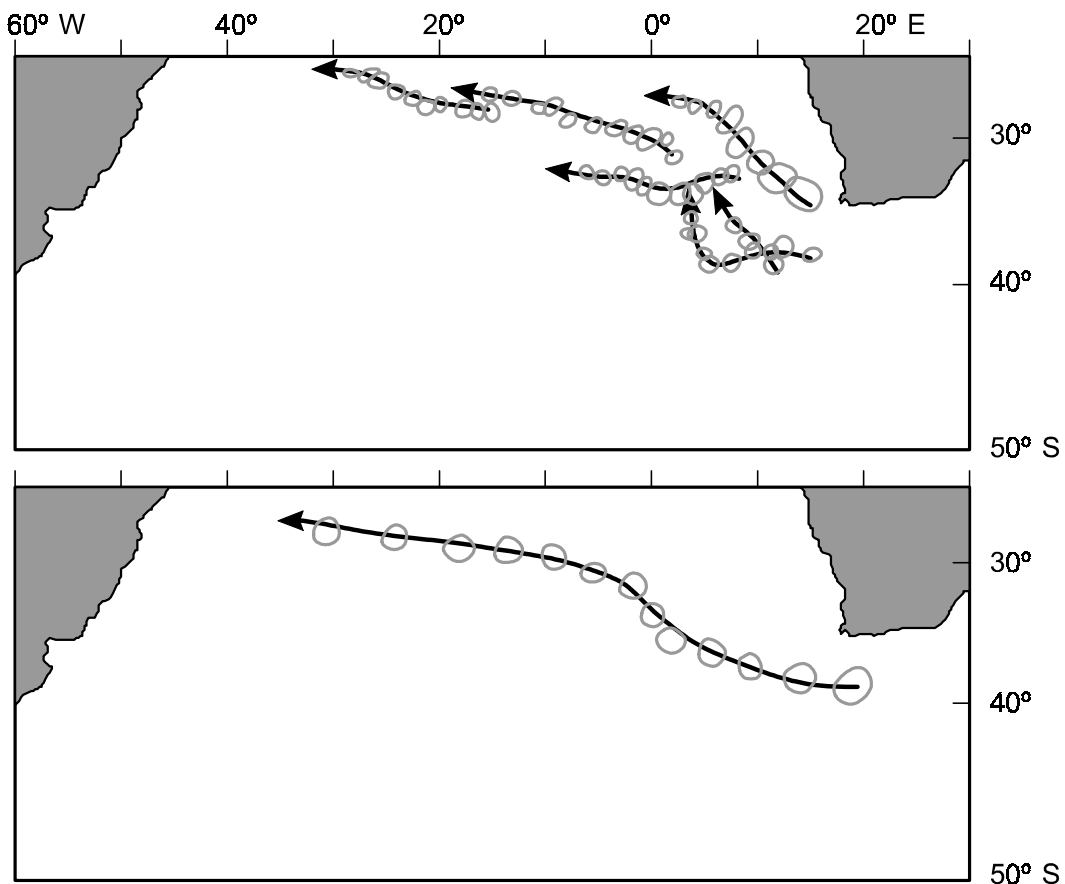


**Figure 6.45.** Trajectories of Agulhas rings in the South Atlantic Ocean from satellite altimetry<sup>464</sup> and as represented by a streamline field for model-year 8 in the FRAM (Fine Resolution Antarctic Model)<sup>277</sup>. Rings in this model follow the path shown without exception, whereas rings in nature move over a wide range.

these processes is adequately understood. With an increase in spatial and temporal resolution for the models, with more realistic bottom configurations and wind-stress forcing, an Agulhas retroflection simulation closer to that available to date can be expected from numerical models in the near future.

One of the smaller-scale processes that may have a decided effect on the rate and timing of ring shedding at the Agulhas retroflection is the downstream movement of the Natal Pulse<sup>62</sup>. As discussed previously, it has been shown that a well-developed Natal Pulse may cause upstream retroflection between Port Elizabeth and the Agulhas Plateau<sup>64</sup> (viz. Figure 1.2). The logical question would then be<sup>131</sup> whether the downstream progress by an average Natal Pulse all the way to the retroflection would precipitate ring shedding in an already far-prograded retroflection loop. Some numerical models suggest this, and recent results from satellite altimetry<sup>401</sup> have largely substantiated this process (viz. Figure 6.8).

### Overview

The development, spatial scales and temporal behaviour of the Agulhas Current retroflection are now fairly well known. Forced mainly by a balance between inertia, planetary vorticity and bottom topography, the retroflective behaviour is thus increasingly well-modelled by a range of numerical models. This suggests that the underlying physics may be adequately understood. However, accurate predictive capability has not been reached yet. This might occur sooner for the ring shedding events at the retroflection.

The process of Agulhas ring spawning seems to be partially, but not totally, due to an imbalance in momentum. The timing of shedding events seems to be a result of the arrival of Natal Pulses. The downstream translation of these triggering features seems highly predictable so that there may be a great deal of prognostic potential in monitoring the onset of Natal Pulses at the Natal Bight.

The behaviour of Agulhas rings subsequent to spawning has been intensively studied. Their observed drift behaviour across the South Atlantic Ocean has nonetheless raised a number of key questions. A large number seem totally to disintegrate in the Cape Basin. This raises questions about the mixing processes involved in their decay. A large observational programme has been undertaken to investigate these. A substantial number split into smaller eddies that may, conceivably, mix out faster. This splitting process may be strongly influenced by the presence of seamounts. The physics of such processes needs to be investigated. There is no clear-cut indication of how rings are affected by the Walvis Ridge. All disparate model predictions are accommodated by the behaviour of at least some observed rings on crossing this ridge. On having passed this obstacle, the behaviour of the remaining rings seems more uniform, suggesting the filtering

behaviour of the Walvis Ridge. From the diverse behaviours of Agulhas rings in the Cape Basin it is clear that there is a wide spectrum of natural histories for Agulhas rings once shed, substantially affecting the interbasin exchanges south of Africa.

Models currently in use for studying the global thermohaline cell show the decisive influence of the leakage of water from the South Indian Ocean into the South Atlantic Ocean on the overturning behaviour. The fluxes at depth are still poorly understood, but are being investigated. The fluxes in the upper layers are dominated by the shedding of the huge Agulhas rings. Direct exchanges and Agulhas filaments play minor roles. In this region of extreme mesoscale flow variability there is also a substantial exchange between the subtropics and the subantarctic, mostly by the shedding of Agulhas eddies from the Agulhas Return Current.

---

